The medfate reference book

true

2019-06-01

Contents

Preface

This is a reference book for the models implemented in the R package **medfate**. This package provides functions for the simulation of functioning and dynamics of Mediterranean forests.

How to use this book

This is a *reference book* for simulation and static models included in package **medfate** (ver. **0.8.3**). Hands-on user guides to run simulation functions and static functions can be found as *package vignettes* within the package. Our aim is to continuously update the reference book along with package developments, so that users have detailed information about the models at the time functions are run. As the manual will follow package updates, after a given model application users should store a **PDF version** of the reference manual to be sure it matches the version the package reported in their application report or article.

The first part of the book present the main functions of the package and describes the soil, vegetation and meteorology inputs that apply to all models. After that, the book presents each simulation model using a set of chapters. The first of them provides an overview of the model and the remaining ones describe the details of formulations by processes. Those process formulations that are common to more than one model (like hydrology) are described only once. Static models and their functions are presented grouped at the end of the book, before the appendices, which include parametrization information and a list of all symbols for reference.

In this book we use `objectname` or `variablename` to indicate R code or to refer to an R objects or a variable within data frames, and `functionname()` to refer to a package function. When relevant, we indicate the correspondence between mathematical symbols, their units and names within R.

Acknowledgements

Part I

Preliminaries

Chapter 1

Introduction

1.1   Purpose

Being able to anticipate the impact of global change on ecosystems is one of
the major environmental challenges in contemporary societies. However, uncer-
tainties in how ecological systems function and practical constraints in how to
integrate available information prevent the development of robust and reliable
predictive models. Despite the amount of knowledge accumulated about the
functioning and dynamics of Mediterranean forests, scientists should make co-
ordinate their efforts to address the challenge of integrating the different global
change drivers in a modelling framework useful for research and applications.

The R package **medfate** has been designed to simulate the functioning and
dynamics of Mediterranean forest stands at temporal scales from days to years.
Fire and drought impacts are the main subjects covered by the package. Eco-
hydrological processes are fundamental for the simulation models included in
the package. In particular, the package allows the simulation of water balance
of soils and plants within forest stands. It also allows simulating plant growth
of a set of cohorts competing for light and water within a forest stand. Finally,
the package also includes functions to relate the amount of plant biomass and
the relative water content of plant tissues to live fuel moisture content, hence,
fire hazard.

The version of the reference manual that you are reading is intended to reflect
version 0.8.3 of the package.

1.2   Package installation

Package **medfate** can be found at CRAN, where it is updated every few months. Hence, it can be installed using:

```
install.packages("medfate")
```

Users can also download and install the latest stable versions GitHub as follows (required package `devtools` should be installed/updated first):

```
devtools::install_github("miquelcaceres/medfate")
```

When installing from GitHub, may need to force the installation of package vignettes, by using:

```
devtools::install_github("miquelcaceres/medfate",
                         build_opts = c("--no-resave-data", "--no-manual"))
```

1.3   Package functions

1.3.1   Dynamic simulation functions

Soil water balance can be studied for a given forest stand using function `spwb()`, with the following purposes:

1. Monitor or forecast temporal variation in soil water content in particular stands (for example to estimate mushroom yield).
2. Monitor or forecast temporal variation of plant drought stress in particular stands (for example to anticipate mortality events).
3. Monitor or forecast temporal variation of fuel moisture in particular stands (for example to monitor wildfire risk).

Changes in leaf area and plant growth are key to evaluate the influence of climatic conditions on forest structure and function. Function `growth()` allows simulating growth of a set of plant cohorts competing for light and water in a given forest stand, with the following purposes:

1. Monitor or forecast temporal variation in water fluxes and soil water content in forest stands (for example to estimate regulation ecosystem services) taking into account processes determining leaf area changes and plant growth.
2. Monitor or forecast temporal variation of plant size (i.e. growth) in forest stands.
3. Monitor or forecast temporal variation of live fuel moisture and the amount of standing dead and live fuels in forest stands (for example to monitor wildfire risk).

1.3.2 Sub-model functions

Many of the functions included in **medfate** are internally called by simulation functions. Some of them are made available to the user, to facilitate understanding the different sub-models and to facilitate a more creative use of the package. Sub-model functions are grouped by *subject*, which is included in the name of the function. The different sub-model functions are (by subject):

- `biophysics_*`: Physical and biophysical utility functions.
- `hydraulics_*`: Plant hydraulics.
- `hydrology_*`: Canopy and soil hydrology (rainfall interception, soil evaporation, soil infiltration).
- `light_*`: Light extinction and absortion.
- `moisture_*`: Live tissue moisture.
- `pheno_*`: Leaf phenology.
- `photo_*`: Leaf photosynthesis.
- `root_*`: Root distribution and conductance calculations.
- `soil_*`: Soil hydraulics and thermodynamics.
- `spwb_*`: Soil water balance parameter optimization/calibration routines.
- `transp_*`: Stomatal regulation and resulting transpiration/photosynthesis.

1.3.3 Static functions

Package **medfate** include a number of functions to examine properties of the plants conforming forests, summary functions at the stand level or vertical profiles of several physical properties:

- `plant_*`: Cohort-level information (species name, id, leaf area, height…).
- `species_*`: Cohort-level attributes aggregated by species (e.g. basal area).
- `forest_*`: Forest-level attributes (e.g. basal area).
- `vprofile_*`: Vertical profiles (light, wind, fuel density, leaf area density).

Vegetation functioning and dynamics have strong, but complex, effects on fire hazard. On one hand, growth and death of organs and individuals changes the amount of standing live and dead fuels, as well as downed dead fuels. On the other, day-to-day changes in soil and plant water content changes the physical properties of fuel, notably fuel moisture content. Package **medfate** provides functions to estimate fuel properties and potential fire behaviour in forest inventory plots. Specifically, function `fuel_stratification()` provides a stratification of the stand into understory and canopy strata; and `fuel_FCCS()` calculates fuel characteristics. Function `fuel_cohortFineFMC()` allows obtaining daily fuel moisture content estimates corresponding to the water status of plants, as returned by function `spwb()`. A fire behaviour model is implemented in function `fire_FCCS()` to calculate the intensity of surface fire reaction and the rate of fire spread of surface fires assuming a steady-state fire. Fuel and fire behaviour functions allow obtaining the following:

1. Fuel characteristics by stratum.
2. Surface fire behavior (i.e. reaction intensity, rate of spread, fireline intensity and flame length).
3. Crown fire behavior.
4. Fire potential ratings of surface fire behavior and crown fire behavior.

Chapter 2

Model inputs

Data input for process-based models of forest functioning and dynamics can be described using three broad categories. First, a description of the target **vegetation** is needed, at a level of detail appropriate for the model design. This includes not only species composition and/or structure, but also functional parameters of the plants. Second, most often **soil** information is required, specially if underground resources (i.e. water and/or nutrients) are important for the processes included in the model. While soil and vegetation features are sometimes considered static parameters in model simulations, **meteorology** is most often a dynamic input which defines the temporal variation of environmental conditions in which biological processes occur. This chapter describes the requirements of **medfate** package with respect to each of these three kinds of input. The last section describes additional parameters that are used to control the behaviour of simulation functions.

2.1 Soil description

Soils can be described in **medfate** using between 1 and 5 soil layers. The number and size of layers may reflect changes in soil properties, but also can be chosen to reflect different plant rooting depths. The physical properties of the soil are needed to estimate its hydraulic properties. Most soil properties are considered static parameters in simulations, except those that depend on soil water balance (e.g. soil moisture content, soil water potential and soil conductivity) and soil temperature, if the soil energy balance is considered in simulations.

2.1.1   Physical properties

Physical soil properties, like soil texture (i.e. percent of sand, silt and clay), bulk density or rock fragment content, can differ between soil layers, and this has important consequences for water retention capacity and soil hydraulics. In addition, specifying a deep rocky layer may be important in some biomes like the Mediterranean one, because plants often extend their roots into cracks existing in the parent rock (Ruffault et al., 2013). For each soil layer s the following physical parameters are needed:

Symbol	Units	R	Description
d_s	mm	widths	Soil layer width
$P_{clay,s}$	%	clay	Percent of clay (within soil particles)
$P_{sand,s}$	%	sand	Percent of sand (within soil particles)
OM	%	om	Percentage of organic mater per dry weight (can be missing)
BD_s	$g \cdot cm^{-3}$	bd	Bulk density
$P_{rocks,s}$	%	rfc	Rock fragment content as percent per soil volume

Soil depth is defined as the sum of soil layer widths. If possible, soil physical properties should be measured in soil profiles conducted at the target forest plot. Soil input data should be arranged in a `data.frame` with soil layers in rows and physical variables in columns (see function `defaultSoilParams()`). The package includes function `soilgridsParams()` to fetch soil information from SoilGrids.org, a global soil database currently providing soil data at 250m scale. This can be helpful to users lacking local soil measurements, but the uncertainty of SoilGrids estimates can be high for some areas and soil properties, especially soil depth and rock fragment content.

2.1.2   Water retention curves

The water retention curve of a soil is the relationship between volumetric soil moisture (θ, in $m^3 \cdot m^{-3}$ of soil, excluding rock fragments) and the soil water potential (Ψ, in MPa). This curve is characteristic for different types of soil, and is also called the *soil moisture characteristic curve*. Two water retention curve models are available in **medfate** (fig. 2.1):

1. *Saxton model*: In this model, volumetric soil moisture $\theta(\Psi)$ corresponding to a given water potential Ψ (in MPa) below Ψ_{fc} is calculated using:

$$\theta(\Psi) = (\Psi/A)^{(1/B)} \tag{2.1}$$

   where A and B depend on the texture and, if available, organic matter in the soil. If organic matter is available, A and B are calculated from P_{clay}, P_{sand} and OM following Saxton and Rawls (2006). Otherwise, they
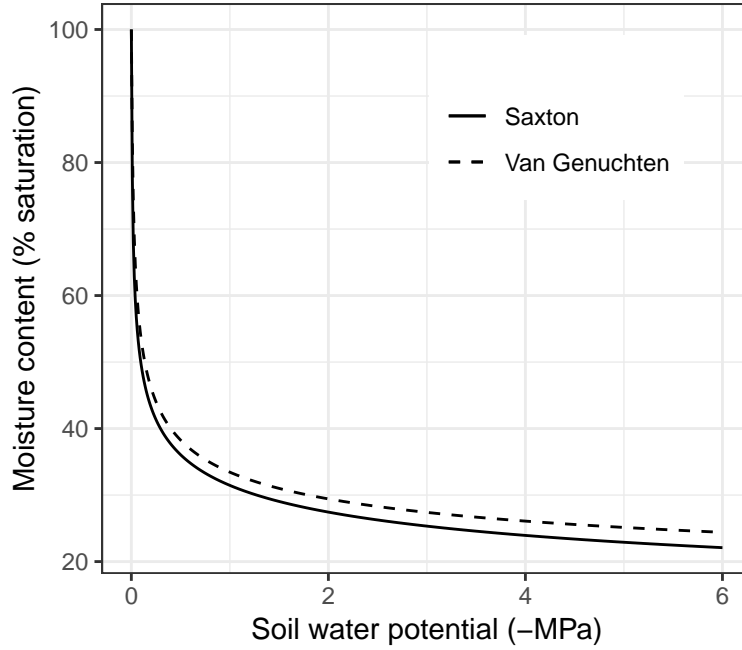
Figure 2.1: Water retention curves under the Saxton and Van Genuchten models, for the same physical attributes (25% sand, 25% clay, 50% silt and bulk density of $1.5g \cdot cm^{-3}$).

    are calculated from P_{clay} and P_{sand} as indicated in Saxton et al. (1986). Volumetric changes between field capacity and saturation are estimated using a linear function.

2. *Van Genuchten model*: The well known van Genuchten (1980) model is:

$$\theta(\Psi) = \theta_{res} + \frac{\theta_{sat} - \theta_{res}}{[1 + (\alpha \cdot \Psi)^n]^{1-1/n}} \tag{2.2}$$

where $\theta(\psi)$ is the water retention, θ_{sat} is the saturated water content, θ_{res} is the residual water content, α is related to the inverse of the air entry pressure, and n is a measure of the pore-size distribution.

2.1.3 Soil initialization

Soil initialization is needed to estimate soil hydrological parameters for each soil layer s from their physical attributes. Initialization is done using function `soil()`, which returns an object of a class with the same name. Function `soil()` adds the following information to the physical soil description:

Symbol	Units	R	Description
$P_{macro,s}$	%	`macro`	Percentage of macroporosity corresponding to each soil layers
γ_{soil}	$mm \cdot day^{-1}$	`Gsoil`	The maximum daily evaporation rate from soil
κ_{soil}		`Ksoil`	Extinction parameter to regulate the amount of water extracted from each soil layer when simulating evaporation from bare soil
$\theta_{sat,s}$	$m^3 \cdot m^{-3}$	`VG_theta_sat`	Volumetric moisture at saturation
$\theta_{res,s}$	$m^3 \cdot m^{-3}$	`VG_theta_res`	Residual volumetric moisture
n_s		`VG_n`	Parameter of the Van Genuchten (1980) model
α_s	MPa^{-1}	`VG_alpha`	Parameter of the Van Genuchten (1980) model

Macroporosity values are calculated using the equations given in Stolf et al. (2011), while γ_{soil} and κ_{soil} are derived from texture. Parameters of the van Genuchten model (including are estimated from the physical description of the soil using one of two pedotransfer functions (see help for `soil()`):

1. Using the USDA texture classification and the average texture class parameters given by Carsel and Parrish (1988).
2. Directly from the soil texture, organic matter and bulk density, using the pedotransfer functions in Tóth et al. (2015).

All simulation functions need an object of class `soil` to be run. Users can edit the `soil` object manually (it is actually a list), for example to provide specific parameters of the Van Genuchten retention curve calibrated from soil samples.

2.1.4   Water content and water table depth

The *water content* (V_s in mm) of a soil layer s is calculated from its water potential and water retention curve using:

$$V_s(\Psi) = d_s \cdot ((100 - P_{rocks,s})/100) \cdot \theta_s(\Psi) \qquad (2.3)$$

where d_s is the depth of the soil layer (in mm) and $P_{rocks,s}$ is the percentage of rock fragments. Besides this general formula, a number of contents are important to remember.

- *Water holding capacity* ($V_{fc,s}$, in mm) of the soil layer s is defined as the volumetric water content at field capacity, i.e. -0.033 MPa:

$$V_{fc,s} = V_s(-0.033) = d_s \cdot ((100 - P_{rocks,s})/100) \cdot \theta_{fc,s} \qquad (2.4)$$

  where $\theta_{fc,s} = \theta_s(-0.033)$.
- *Water content at saturation* is calculated anagolously, but replacing $\theta_{fc,s}$ by $\theta_{sat,s} = \theta_s(0)$.
- *Water content at wilting point* (-1.5 MPa) is calculated replacing $\theta_{fc,s}$ by $\theta_{wp,s} = \theta_s(-1.5)$.
- The *amount of extractable water* is the difference between water content at field capacity and a the water content at a conventional minimum water potential, which can be set at wilting point or lower values (by default at -5 MPa in **medfate**).

The depth of water table is the depth of saturated soil. In medfate, *water table depth* (WT, in mm) equals soil depth when all soil layers are below field capacity. When some layers are between field capacity and saturation, water table depth is calculated as:

$$WT = \sum_s d_s \cdot \min\left[1, (\theta_{sat,s} - \theta(\Psi_s))/(\theta_{sat,s} - \theta_{fc,s})\right] \qquad (2.5)$$

2.2 Vegetation description

The representation of plants within a target plot is done in **medfate** by means of **cohorts** of woody plants (i.e. trees and shrubs). A plant cohort respresents plants that belong to the same species (or functional group) and are more or less of the same *size*. For example, trees in a stand may be grouped by species and diameter class. This representation is chosen so that package functions can be easily applied to forest plot data, for example from national forest inventories. The description of plant cohorts includes a measure of *abundance* of the cohort in the stand, which in the case of trees is density as stems per hectare and for shrubs is percent cover. In fact this (and the fact that shrubs are multi-stemmed) is the only motivation for distinguishing between tree cohorts and shrub cohorts.

Note that one limitation of the representation of vegetation using plant cohorts is that it is not spatially-explicit (i.e. plants cannot have explicit coordinates within forest stands) and hence spatial (horizontal) interactions cannot be taken into account.

2.2.1 Attributes of plant cohorts

A plant cohort i is either a *tree cohort* or a *shrub cohort*, and is defined using a set attributes shown in the following table, where columns **spwb** and **growth** indicate whether attributes are required by functions `spwb()` and `growth()`, respectively:

Symbol	Units	R	Description	spwb	growth
SP_i		`Species`	Species identity	Y	Y
H_i	cm	`Height`	Average tree or shrub height	Y	Y
CR_i		`CR`	Crown ratio (i.e. ratio between crown length and plant height)	Y	Y
N_i	$ind \mathring{u} ha^{-1}$	`N`	Density of tree individuals	N	Y
DBH_i	cm	`DBH`	Tree diameter at breast height	N	Y
$Cover_i$	$\%$	`Cover`	Shrub percent cover	N	Y
LAI_i^{live}	$m^2 \cdot m^{-2}$	`LAI_live`	(Maximum) leaf area index	Y	Y
LAI_i^{dead}	$m^2 \cdot m^{-2}$	`LAI_dead`	Dead leaf area index	Y	Y
LAI_i^{ϕ}	$m^2 \cdot m^{-2}$	`LAI_expanded`	Current expanded leaf area index	Y	Y
$Z_{50,i}$	mm	`Z50`	Depth above which 50% of the fine root mass is located	Y	Y
$Z_{95,i}$	mm	`Z95`	Depth above which 95% of the fine root mass is located	Y	Y

Height values refer to average height of individuals included in the cohort, and the same for crown ratio and DBH. LAI variables refer to one-side leaf area of plants in the cohort per surface area of the stand. While plant height is relatively easy to measure, it is normally quite hard to estimate leaf area indices for stands and species. Package **medfate** provides some utilities to provide estimates crown ratio and LAI from forest inventory data (e.g. heights, DBH and density for measured trees), using allometric relationships calibrated for catalonia (see chapter 18).

Trees and shrubs do not need to be distinguished in soil water balance calculations, since both kinds of cohort have a LAI value. Vegetation characteristics stay constant during simulations using function `spwb()`, although the actual expanded leaf area and dead leaf area may vary is the species is winter deciduous.

In contrast, growth simulation requires updating the structure of vegetation, i.e. heights, tree diameters and shrub cover. Function `growth()` can modify any of the vegetation attributes.
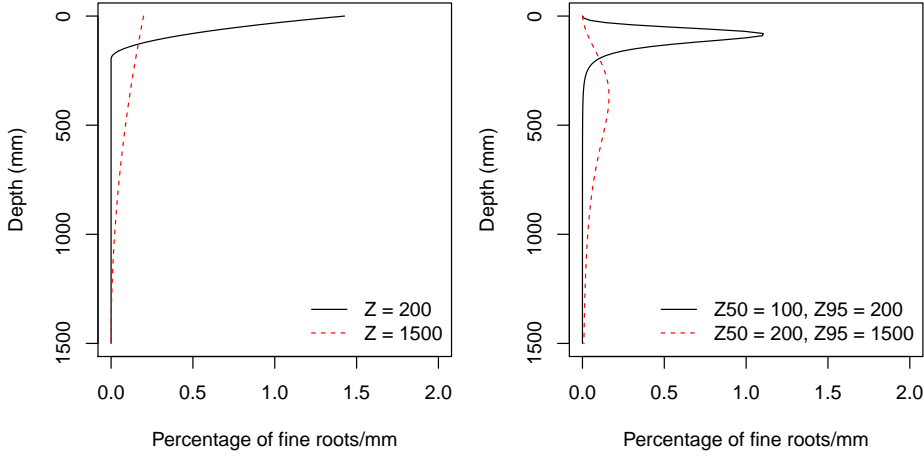
Figure 2.2: Examples of root density profile according to a conic distribution (left) and the linear dose response model (right).

2.2.2 Vertical root distribution

The root system of each plant cohort i is described using the proportion of fine roots in each soil layer s: $v_{i,s}$. The proportions $v_{i,s}$ are normally defined using the linear dose response model (Schenk and Jackson, 2002; Collins and Bras, 2007):

$$Y_i(z) = \frac{1}{1 + (z/Z_{50,i})^{c_i}} \tag{2.6}$$

where $Y_i(z)$ is the cumulative fraction of fine root mass located between surface and depth z; $Z_{50,i}$ is the depth above which 50% of the root mass is located; and c_i is a shape parameter related to $Z_{50,i}$ and $Z_{95,i}$ as $c_i = 2.94/\ln(Z_{50,i}/Z_{95,i})$ (see `root_ldrDistribution()`).

Note, however, that the actual input to simulation functions is the matrix of $v_{i,s}$ values - not $Z_{50,i}$ and $Z_{95,i}$ -, which means that the proportions of fine roots can be modified manually or be defined by another model. In fact, **medfate** also allows calculating $v_{i,s}$ values assuming a conic distribution of fine roots (see `root_conicDistribution()`), as shown in fig. 2.2 above.

2.2.3 Plant (species) traits and vegetation initialization

Besides the physical representation of vegetation, forest ecosystem models require information regarding vegetation functioning, because this influences the

outcome of biophysical, physiological and hydrological processes. In the following chapters, we will indicate for each simulated process its required trait parameters. Normally, plant traits are described at the species level because infra-specific parameters are hard to get. Even at the species level, many hard (e.g. physiological) traits are hard to obtain, so in **medfate** we provide a default species parameter table for woody species found in Catalonia, with many of them occurring elsewhere in the Mediterranean Basin (`SpParamsMED`).

The package provides functions `spwbInput()` and `growthInput()` that prepare the vegetation input for simulation functions `spwb()` and `growth()`, respectively. This preparation mostly consists in compiling the necessary functional traits from the species parameter table, following the species (or species group) attribute of plant cohorts. User can modify the output of these preparing functions to account for intra-specific trait variation (see function `modifySpParams()`).

2.3   Metereological input

Weather input data must include variables calculated at the **daily** scale. Data should be arranged in a data frame with days in rows and variables in columns. The following table indicates the symbols, units, definitions and the variable name in R.

Symbol	Units	R param	Description
T_{mean}	$^\circ$C	`MeanTemperature`	Mean temperature
T_{min}	$^\circ$C	`MinTemperature`	Minimum temperature
T_{max}	$^\circ$C	`MaxTemperature`	Maximum temperature
RH_{min}	%	`MinRelativeHumidity`	Minimum relative humidity
RH_{max}	%	`MaxRelativeHumidity`	Maximum relative humidity
P	$L \cdot m^{-2} = mm$	`Precipitation`	Precipitation
PET	$L \cdot m^{-2} = mm$	`PET`	Potential evapotranspiration, preferably calculated using Penman's equation
Rad	$MJ \cdot m^{-2}$	`Radiation`	Solar radiation after accounting for clouds
u	$m \cdot s^{-1}$	`WindSpeed`	Wind speed

Not all simulation models require all weather variables. In particular, basic water balance modelling requires much less information than advance water balance modelling. The meteorological variables required in each case will be indicated in the corresponding model chapters. Since it allows producing data frames with appropiate variable units and column names, we recommend mete-

orological input to be generated using package **meteoland** (De Cáceres et al., 2018).

2.4   Control parameters

Control parameters are a list of global parameter values, initialized using function `defaultControl()`, that the user can modify to change the general behavior of simulation functions. Here is the set of global control parameters currently accepted in **medfate**:

```
names(defaultControl())
```

```
##  [1] "verbose"                        "subdailyResults"
##  [3] "soilFunctions"                  "snowpack"
##  [5] "drainage"                       "leafPhenology"
##  [7] "transpirationMode"              "hydraulicCostFunction"
##  [9] "verticalLayerSize"              "nStemSegments"
## [11] "capacitance"                    "cavitationRefill"
## [13] "klat"                           "taper"
## [15] "numericParams"                  "fracRootResistance"
## [17] "averageFracRhizosphereResistance" "Catm"
## [19] "ndailysteps"                    "thermalCapacityLAI"
## [21] "defaultWindSpeed"               "storagePool"
```

Not all control parameters are relevant to all simulation functions (this will be indicated in the following chapters), but there is an important control parameter called `transpirationMode`, because it allows the user to switch between the basic and advanced water balance models (chapters 3 and 7).

Control parameters are employed when initializing vegetation information using functions `spwbInput()` and `growthInput()`, since they are needed also to make decisions at the point of initialization. Control parameters are also stored in the result of this functions, so the user does not need to specify again control parameters when calling simulation functions `spwb()` or `growth()`.

Part II

Basic water balance modelling

Chapter 3

Basic water balance model

This chapter provides an overview of the water balance model described in De Cáceres et al. (2015), which allows simulating the temporal variation in soil moisture on a daily step basis for a given forest stand and for the period corresponding to input weather data. While the information provided in this chapter should be enough to understand what the model does and when it can be useful, the following ones provide a deeper understanding on how the different processes are formulated.

3.1 Design principles

The model considers only the vertical spatial dimension of the stand and not the horizontal distribution of plants within it. In other words, the model is not spatially explicit (i.e., plants do not interact for space explicitly). Still, the stand is divided into groups of plants, here referred to as *plant cohorts* of different species, height and leaf area index (LAI). Height and LAI values determine competition for light. LAI values also drive competition for water, along with root distribution. The soil water balance follows the design principles of SIERRA (Mouillot et al., 2001; Ruffault et al., 2014, 2013) and BILJOU (Granier et al., 1999; 2007), although some features are taken from other models (Kergoat, 1998). Potential evapotranspiration (PET) is a required input and the model determines maximum canopy transpiration ($Tr_{\max}$) using an empirical relationship between the LAI of the stand and the ratio $Tr_{\max}/PET$ (Granier et al., 1999). Actual plant transpiration is estimated using a function that depends on current soil moisture levels, cohort-specific drought resistance, fine root distribution and the degree of shading of the target plant cohort.

27

3.2   State variables

The following are state variables in the model:

- Cumulative growth degree days, GDD, are tracked by the model and determine leaf phenological status of winter deciduous species.
- Daily soil moisture content dynamics on each layer s are tracked using $W_s = \theta_s(\Psi)/\theta_{fc,s}$, the **proportion of volumetric soil moisture in relation to field capacity**, where field capacity, $\theta_{fc,s}$, is assumed to correspond to $\Psi_{fc} = -0.033$ MPa. Note that W_s values larger than one are possible if the soil is between field capacity and saturation (which can happen if deep drainage is not allowed).
- If snow accumulation/melting is considered, the model tracks S_{snow}, the snow water equivalent (in mm) of the snow pack storage over the surface.
- If irreversible cavitation is activated, the model tracks $P_{embolized,i}$, the maximum value of daily drought stress so far experienced.

3.3   Water balance

Daily variations in soil water content (ΔV_{soil} in mm) can be summarized as:

$$\Delta V_{soil} = Pr + Sm - In - Ru - Dd - Es - Tr \qquad (3.1)$$

where Pr is precipitation as rainfall, Sm is water from melting the snow pack (if considered), In is the interception loss (i.e., water evaporated after being intercepted by the canopy), Ru is surface runoff, Dd is deep drainage (i.e. water percolated to layers beyond soil depth), Es is evaporation from soil and Tr is plant transpiration. If snow dynamics are considered, the water balance of the snow pack (ΔS_{snow} in mm of snow water equivalents) is defined as:

$$\Delta S_{snow} = Ps - Sm \qquad (3.2)$$

where Ps is precipitation as snowfall and Sm is snow melt.

3.4   Process scheduling

Every day, water balance is simulated in the following several steps:

- Update leaf area values according to the phenology of species and recalculate light extinction (sections 4.1 and 4.3).
- If snow dynamics are included, increase snow pack from snow precipitation (Ps) and decreases it from snow melting (Sm) (section 5.2).

- Determine rainfall interception loss (In) and net rainfall (Pr_{net}) (section 5.3)
- Increase soil water content due to net rainfall (Pr_{net}), surface runon (Ro) and snow melting (Sm), after accounting for surface runoff (Ru) and deep drainage (Dd) (section 5.4).
- Decrease soil water content due to bare soil evaporation (Es) (section 5.5).
- Determine transpiration, photosynthesis and drought stress for each plant cohort and decrease water content due to plant transpiration (Tr) (chapter 6).

Details of the formulation of each of these processes are provided within the referred chapters and sections.

3.5 Model input

3.5.1 Metereological input

The minimum weather variables required to run the model are mean temperature (T_{mean}), precipitation (P) and potential evapotranspiration (PET). Solar radiation (Rad) is required if snow pack dynamics have to be simulated. Additionally, the user may also specify values of wind speed (u) that are used to control leaf fall in autumn. Definitions and units of these variables are given in section 2.3.

3.5.2 Control parameters

The control values relevant for the simple water balance model are:

- `verbose [=TRUE]`: Whether extra console output is desired during simulations.
- `soilFunctions [= "SX"]`: Water retention curve model, either "SX" (for Saxton) or "VG" (for Van Genuchten).
- `leafPhenology [= TRUE]`: Whether leaf phenology is simulated.
- `snowpack [= TRUE]`: Whether dynamics of snow pack are included.
- `drainage [= TRUE]`: Whether water exceeding the field capacity of the bottom layer is lost by deep drainage into a non-reachable compartment.
- `transpirationMode [= "Granier"]`: Transpiration model, in this case "Granier".
- `defaultWindSpeed [= 2.5]`: Default value for wind speed (in $m \cdot s^{-1}$) when this is missing (only used for leaf fall).
- `cavitationRefill [= TRUE]`: If `FALSE` the model operates in a irreversible cavitation mode.

3.6   Model output

Function `spwb` returns a list object whose elements are data tables. Each table has dates as rows and has different output variables:

- `WaterBalance`: Components of the climatic and soil daily water balance (i.e. net precipitation, infiltration, runoff, plant transpiration…).
- `Soil`: Daily variation of soil variables (volume, moisture relative to field capacity, water potential) for each soil layer.
- `PlantLAI`: Daily values leaf area index for each plant cohort.
- `PlantTranspiration`: Daily transpiration (in mm) for each plant cohort.
- `PlantPhotosynthesis`: Daily net photosynthesis (in $gC \cdot m^{-2}$) for each plant cohort.
- `PlantPsi`: Daily water potential of each plant (in MPa).
- `PlantStress`: Daily stress level suffered by each plant cohort (relative whole-plant conductance).

The output of simulations can be inspected using specific `plot` and `summary` functions (see the corresponding package *vignette*).

Chapter 4

Leaf phenology and light extinction

4.1 Leaf phenology and leaf fall

Given a base temperature ($T_{base} = 5°$C), the growth degree days (GDD) are zero for all those days where mean temperature T_{mean} is below T_{base} and start increasing when temperatures become warmer than this threshold. In other words, the GDD function accumulates $\max(0.0, T_{mean} - T_{base})$ for all days previous to the current one. At the end of a year the cummulative value is set again to zero. Plant species can have either *evergreen* or *winter-deciduous* phenology. Evergreen plants maintain constant leaf area over the year, whereas in deciduous plants leaf-phenological status is updated daily, represented by ϕ_i, the fraction of maximum leaf area. Leaf area index (LAI) values of deciduous plants are adjusted for leaf phenology following (Prentice et al., 1993; Sitch et al., 2003):

$$LAI_i^{\phi} = LAI_i^{live} \cdot \phi_i \tag{4.1}$$

whereas for evergreen species $LAI_i^{\phi} = LAI_i^{live}$. Budburst in deciduous species occurs when daily temperature exceeds T_{base} and ϕ_i increases linearly from 0 to 1 as function of the degree days above T_{base}, until a the value $S_{GDD,i}$ is reached (i.e. until $GDD > S_{GDD,i}$). In autumn, ϕ_i drops to 0 when average daily temperature falls again below T_{base} (Sitch et al., 2003). The drop of ϕ_i causes live expanded leaves to become dead leaves. To avoid a sudden decrease of leaf area, dead leaves are kept in the canopy and they are reduced daily using a negative exponential function of wind speed:

$$LAI_i^{dead} = LAI_i^{dead} \cdot e^{-u/10} \tag{4.2}$$

where u is wind speed in $(m \cdot s^{-1})$.

We will call total leaf area of a plant cohort i (LAI_i^{all}) to the sum of dead and live expanded leaves of the cohort:

$$LAI_i^{all} = LAI_i^{\phi} + LAI_i^{dead} \tag{4.3}$$

If there are c plant cohorts, the leaf area index of the whole stand can be calculated for living leaves, expanded leaves, dead leaves and total leaf area as:

$$LAI_{stand}^{live} \;\;=\;\; \sum_{i=1}^{c} LAI_i^{live} \tag{4.4}$$

$$LAI_{stand}^{\phi} \;\;=\;\; \sum_{i=1}^{c} LAI_i^{\phi} \tag{4.5}$$

$$LAI_{stand}^{dead} \;\;=\;\; \sum_{i=1}^{c} LAI_i^{dead} \tag{4.6}$$

$$LAI_{stand}^{all} \;\;=\;\; \sum_{i=1}^{c} LAI_i^{all} = LAI_{stand}^{\phi} + LAI_{stand}^{dead} \tag{4.7}$$

Although simulations will normally start in winter and GDD will be zero at the beginning, the user can specify a starting non-zero value for GDD in the object created by function `spwbInput()`.

4.2   Leaf vertical distribution

Crown base height $(H_{b,i};$ in $cm)$ of cohort i is defined as the height corresponding to the first living branch. It is calculated from the crown ratio of the cohort $(CR_i;$ a proportion between 0 and 1), i.e. the ratio between crown length and total height:

$$H_{b,i} = H_i \cdot (1 - CR_i) \tag{4.8}$$

Leaf area of any plant cohort is assumed to be distributed vertically following a **truncated Gaussian function** whose standardized values -1.5 and 1.5 correspond to crown base height (CR_i) and total plant height (H_i), respectively. The model divides the vertical dimension into vertical layers (by default, each layer is 50 cm in width). Let us define $LAI_{i,j}^{all} = LAI_{i,j}^{\phi} + LAI_{i,j}^{dead}$ as the leaf area index of cohort i in layer j. The truncated Gaussian distribution defines the $LAI_{i,j}^{\phi}$ and $LAI_{i,j}^{dead}$ for all plant cohorts and vertical layers.
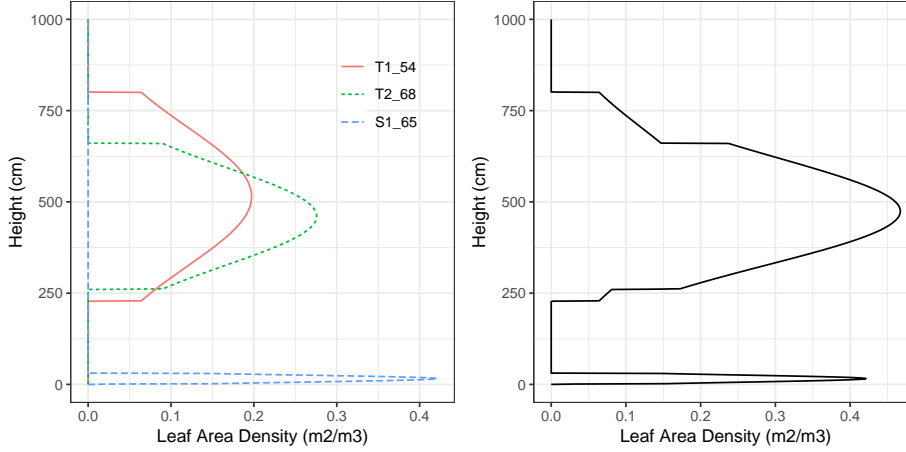
Figure 4.1: Leaf area density distribution in a forest stand. The left panel shows the distribution for each plant cohort separately, whereas the right panel shows the overall density distribution.

Dividing the leaf area of a given layer by its width, one obtains the *leaf area density* (LAD in $m^2 \cdot m^{-3}$). Figure 4.1 illustrates the leaf area density profile for an example forest stand (see function `vprofile_leafAreaDensity()`).

The leaf area density profile determines the extinction rates of light through the forest canopy. The same truncated Gaussian distribution is used to distribute leaf and small branch biomass in the vertical dimension.

4.3 Light extinction

The proportion of photosynthetic active radiation (PAR) and short-wave radiation (SWR; 400-3000 nm) decreases through the canopy following thee Beer-Lambert's light extinction equation. L_{ground}^{PAR}, the proportion of PAR that reaches the ground, is calculated as:

$$L_{ground}^{PAR} = e^{-\sum_{i=1}^{c} k_{PAR,i} \cdot LAI_i^{all}} \tag{4.9}$$

where $k_{PAR,i}$ is the PAR extinction coefficient of cohort i.

The proportion of shortwave radiation (SWR) energy absorbed by each plant cohort needs to be calculated to divide the transpiration of the stand among cohorts (chapter 6), and the radiation absorbed by the soil is needed to calculate soil evaporation (section 5.5). Foliage absorbs a higher proportion of PAR than SWR; thus, the extinction coefficient is higher for PAR than for
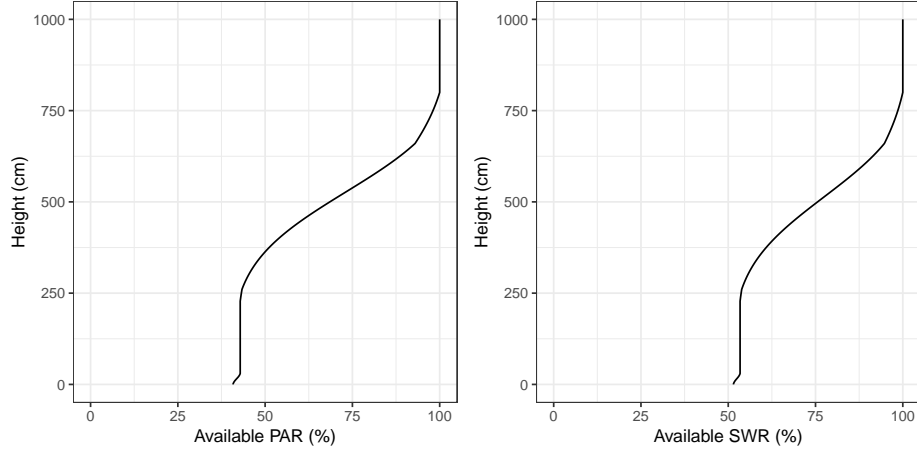
Figure 4.2: Light extinction in a forest stand. Note the sharper decrease of PAR (left panel) in comparison to SWR (right panel)

SWR. However, values for the ratio of extinction coefficients are rather constant. Following Friend et al. (1997) it is assumed that the extinction coefficient for PAR is 1.35 times larger than that for SWR (i.e. $k_{SWR,i} = k_{PAR,i}/1.35$). Figure 4.2 shows the PAR and SWR extinction profiles (see functions `vprofile_PARExtinction()` and `vprofile_SWRExtinction()`) corresponding to the leaf area density distribution of Fig. 4.1.

To calculate radiation absorption, where the vertical dimension of the plot is divided into layers (as explained for leaf area distribution), and the SWR absorbed is calculated for each plant cohort in each layer. Let n be the number of canopy layers. The fraction of radiation incident on layer j that is absorbed in the same layer is:

$$f_j = 1 - e^{-\sum_{i=1}^{c} k_{SWR,i} \cdot LAI_{i,j}^{all}} \tag{4.10}$$

where $LAI_{i,j}$ is the leaf area index of cohort i in layer j. Hence, the fraction transmitted is $(1 - f_j)$. The fraction of radiation incident on layer j that is absorbed by expanded leaves of plant cohort i in that layer (f_{ij}) is calculated from the relative contribution of these leaves to the total absorption in the layer:

$$f_{ij} = f_j \cdot \frac{k_{SWR,i} \cdot LAI_{i,j}^{\phi}}{\sum_{h=1}^{c} k_{SWR,h} \cdot LAI_{h,j}^{all}} \tag{4.11}$$

The fraction of canopy radiation absorbed by a plant cohort i across all layers is found by adding the fraction absorbed in each layer:

$$f_i = \sum_{j=1}^{n} f_{ij} \cdot \prod_{h>j}^{n} (1 - f_h) \tag{4.12}$$

where for each layer the fraction of the radiation incident in the canopy that reaches the layer is found by multiplying the transmitted fractions across the layers above it. For example, the fraction of SWR absorbed by each of the three cohorts of the example in Fig. 4.1 would be (see function `light_cohortAbsorbedSWRFraction()`):

```
##       T1_54       T2_68       S1_65
## 0.23371749 0.23236269 0.01904071
```

The proportion of (shortwave) net radiation absorbed by the ground is simply:

$$L_{ground}^{SWR} = 1 - \sum_{j}^{n} f_j \tag{4.13}$$

which in our example would be:

```
## [1] 0.5148791
```

as also shown in Fig. 4.2.

Chapter 5

Hydrology

5.1 Precipitation

Precipitation (P) is considered be snow precipitation (Ps) when $T_{mean} < 0$, and is considered rainfall (Pr) otherwise. Thus, we have:

$$P = Pr + Ps \tag{5.1}$$

Interception of snow by the canopy is neglected, and all snow is assumed to accumulate in a single storage compartment S_{snow} over the soil (i.e. canopy snow storage capacity is neglected). Rainfall interception is described in section 5.3.

5.2 Snow pack dynamics

A very simple snow submodel is used for snow pack dynamics (accumulation and melt), taken from Kergoat (1998). When mean air temperature is above 0 Celsius $T_{mean} > 0$, a simple energy budget relates snow melt, Sm (mm), to air temperature and soil-level radiation (see function `hydrology_snowMelt`):

$$Sm = \frac{Rad \cdot L_{ground}^{SWR} \cdot (1 - \alpha_{ice}) + \tau_{day} \cdot T_{mean} \cdot \rho \cdot C_p / r_s}{\lambda_{ice}} \tag{5.2}$$

where Rad is solar radiation ($MJ \cdot m^{-2}$), L_{ground}^{SWR} is the fraction of (short-wave) radiation reaching the ground, $\alpha_{ice} = 0.9$ is the albedo of snow, $\tau_{day} = 86400$ is the day duration in s, ρ is the air density (depending on temperature and elevation), $C_p = 1013.86 \cdot 10^{-6} MJ \cdot kg^{-1} \cdot C^{-1}$ is the specific heat capacity of

the air and $r_s = 100s \cdot m^{-1}$ is the snow aerodynamic resistance and $\lambda_{ice} = 0.33355MJ \cdot kg$ is the (latent) heat of fusion of snow.

5.3   Rainfall interception loss

As mentioned above, interception loss is only modelled for liquid precipitation (i.e. snow interception is not modelled). Rainfall interception loss, In, is estimated using the Gash et al. (1995) analytical interception model for sparse canopies, where rain is assumed to fall in a single event during the day. First, the amount of rainfall needed to saturate the canopy is calculated:

$$P_G = -\frac{S_{canopy}/C_{canopy}}{(E/R)} \cdot \ln(1 - (E/R)) \tag{5.3}$$

where S_{canopy} is the canopy water storage capacity (in mm) – i.e. the minimum amount of water needed to saturate the canopy –, C_{canopy} is the canopy cover and (E/R) is the ratio of evaporation rate to rainfall rate during the rainfall event. Simplifying assumptions are made to determine (E/R). Values of the Evaporation-to-rainfall ratio are calculated from daily potential evapotranspiration and rainfall, while accounting for seasonal variation in rainfall intensity ($mm \cdot h^{-1}$). Minimum values for rainfall intensity are assumed for convective storms (5.6 $mm \cdot h^{-1}$) and synoptic storms (1.5 $mm \cdot h^{-1}$) from Miralles et al. (2010). Synoptic storms are assumed between December and June, and convective storms are assumed for the remaining months, as typical in the Mediterranean Basin.

The amount of water evaporated from interception (In, in mm), is calculated as:

$$In = C \cdot P_G + C \cdot (E/R) \cdot (Pr - P_G) \, if \, Pr > P_G \tag{5.4}$$
$$In = C \cdot Pr \, if \, Pr \leq P_G \tag{5.5}$$

where Pr is the daily gross rainfall (in mm). Net rainfall (Pr_{net}, also in mm) includes throughfall and stemflow, and is calculated as the difference between gross rainfall and interception loss.

Although interception models are normally applied to single-canopy stands, we apply the sparse Gash model to the whole stand (including shrubs). Moreover, in our implementation stem interception is lumped with canopy interception, so that S_{canopy} represents both. Following Watanabe and Mizutani (1996) we estimate S_{canopy}, the canopy water storage capacity, from adjusted LAI values:

$$S_{canopy} = \sum_i s_{water,i} \cdot LAI_i^\phi \tag{5.6}$$
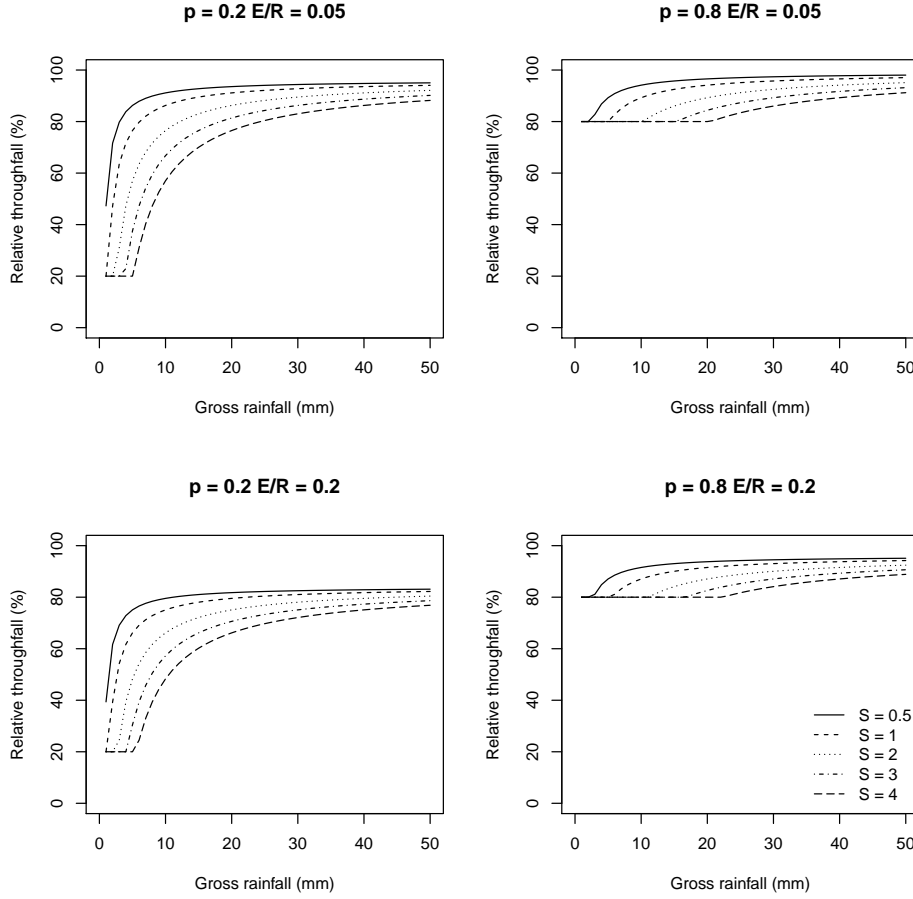
Figure 5.1: Examples of canopy interception with different S_{canopy} (canopy water storage capacity), E/R (ratio between evaporation and rainfall rates) and p (throughfall coefficient; $p = 1 - C_{canopy}$).

where $s_{water,i}$ is the depth of water that can be retained by leaves, branches and stems of cohort i per unit of leaf area index ($mm \cdot LAI^{-1}$). To estimate the stand cover, C_{canopy}, we use the complement of the percentage of PAR that reaches the ground, i.e. $C_{canopy} = 1 - L_{ground}^{PAR}$ (Deguchi et al., 2006). Fig. 5.1 below shows examples of relative throughfall (including stemflow), calculated according to the Gash et al (1995) interception model, under different situations (see function `hydrology_rainInterception()`).
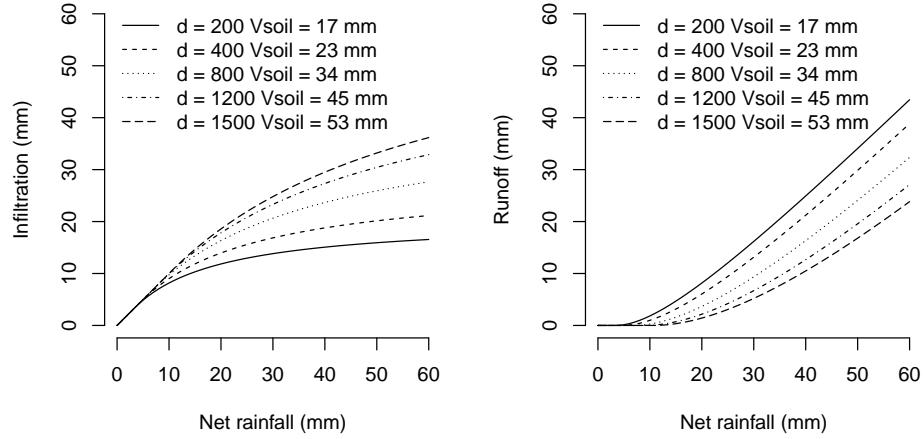
Figure 5.2: Examples of infiltration/runoff calculation for different values of net rainfall and overall retention capacity, V_{soil}, calculated from different soil depths (topsoil+subsoil) and assuming that soil texture is 15% clay and 25% sand. Rock fragment content was 25% and 40% for the topsoil and subsoil, respectively.

5.4   Runoff, infiltration and percolation

The water that reaches the soil is the sum of net rainfall (Pr_{net}), runon (Ro, in mm) and melted snow (Sm). The amount of water infiltrating into the soil is $Pr_{net} + Sm + Ro - Ru$, where Ru (in mm) is the water lost by surface runoff (see function `hydrology_infiltrationAmount()`).

Surface runoff, is calculated using the USDA SCS curve number method, as in Boughton (1989):

$$Ru = \frac{(Pr_{net} + Ro + Sm - 0.2 \cdot V_{fc,soil})^2}{(Pr_{net} + Ro + Sm - 0.8 \cdot V_{fc,soil})} \tag{5.7}$$

where V_{soil} (in mm) is the overall soil water retention capacity.

Following Granier et al. (1999), part of the water reaching one soil layer percolates quickly through the macropores. The amount of water reaching each layer through macropores is modelled using an extinction function (see function `hydrology_infiltrationRepartition`). The remaining water is retained by the micropores refilling the current soil layer. When this soil layer reaches its field capacity the excess of water also percolates to the soil layer below.

If `drainage = TRUE`, the water percolating from the lowest layer is considered deep drainage, Dd, and soil layers are never above field capacity. If `drainage = FALSE`, the excess of water in the lowest soil layer is not lost via drainage, so

that this layer (and those above) can be filled up to saturation. This additional filling is done starting from below, and when a given layer reaches saturation, the model adds the remaining water to the layer above. If all layers are filled to saturation, the remaining water is assumed to be infiltration excess and is added to the surface runoff.

5.5 Bare soil evaporation

Evaporation from the soil surface is the last component of the soil water balance to be calculated before calculating plant transpiration. Potential evaporation from the soil (PE_{soil}; in $mm \cdot day^{-1}$) is defined as the product between PET and L_{ground}^{SWR}, the proportion of SWR absorbed by the ground:

$$PE_{soil} = PET \cdot L_{ground}^{SWR} \tag{5.8}$$

Actual evaporation from the soil surface is modeled as in Mouillot et al. (2001), who in turn followed Ritchie (1972). First, the model determines the time needed to evaporate the current water deficit (difference between field capacity and current moisture) in the surface soil layer:

$$t = \left\{ \frac{V_{fc,1} \cdot (1 - W_1)}{\gamma_{soil}} \right\} \tag{5.9}$$

where $V_{fc,1}$ is the water retention capacity of layer 1, W_1 is the current proportion of volumetric moisture in relation to field capacity and γ_{soil} is the maximum daily evaporation ($mm \cdot day^{-1}$). The calculated time is used to determine the 'supplied' evaporation, SE_{soil}:

$$SE_{soil} = \gamma_{soil} \cdot (\sqrt{t+1} - \sqrt{1}) \tag{5.10}$$

The amount of water evaporated from the soil, Es, is then calculated as the minimum between supply and demand (Federer, 1982), the latter being the product of PET and the proportion of light that reaches the ground (see function `hydrology_soilEvaporationAmount`):

$$Es = \min(PE_{soil}, SE_{soil}) \tag{5.11}$$

Finally, Es is distributed along the soil profile according to an exponential decay function with an extinction coefficient κ_{soil} (Mouillot et al., 2001). Figure 5.3 shows the cumulative evaporation from soils for different values of maximum evaporation rate and extinction coefficient. When the extinction coefficient is smaller a higher proportion of the evaporated water is removed from the subsoil
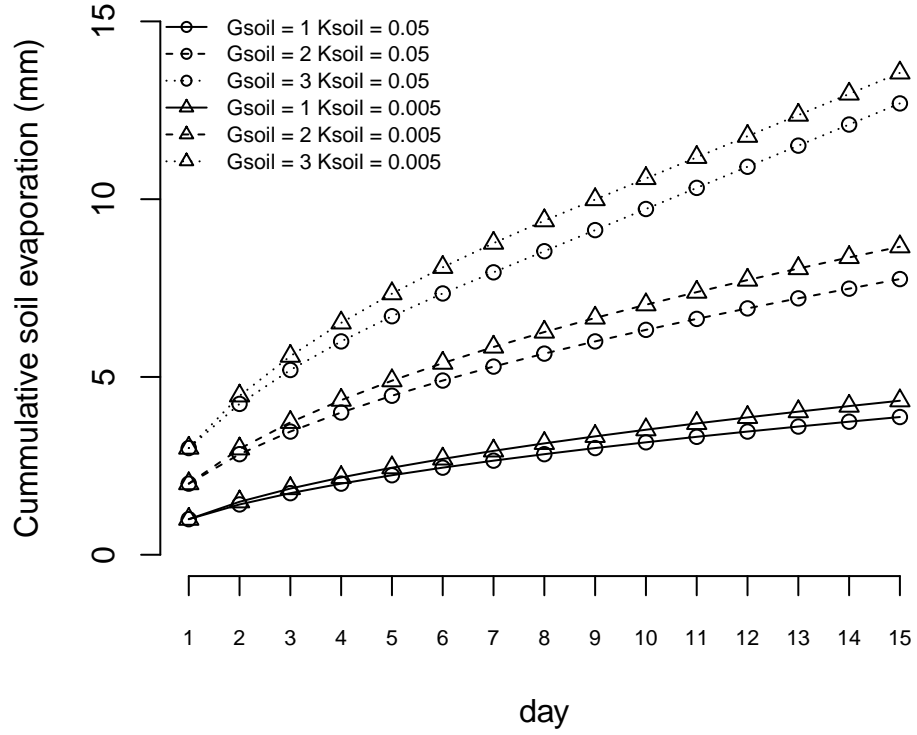
Figure 5.3: Cumulative bare soil evaporation for different values of maximum evaporation rate (γ_{soil}) and extinction coefficient (κ_{soil}). Three soil layers (0 – 30 cm; 30 – 150 cm; 150 – 400 cm) are initialized at field capacity ($V_1 = 50mm$; $V_2 = 201mm$; $V_3 = 35mm$). PE_{soil} was assumed not to be limiting.

and less from the topsoil. This causes more water being available to calculate t in the next step.

Chapter 6

Transpiration, photosynthesis and drought stress under Granier's model

6.1 Plant transpiration and photosynthesis

6.1.1 Maximum transpiration

Potential evapotranspiration (PET, in mm) is assumed to represent open water evaporation potential. Maximum canopy transpiration $Tr_{\max}$ depends on both PET and the amount of transpiring surface, i.e. the current cumulative LAI of the stand, LAI_{stand}^{ϕ}. To estimate $Tr_{\max}$ the model uses the empirical equation of Granier et al. (1999), where $Tr_{\max}/PET$ is a function of LAI_{stand}^{ϕ}:

$$\frac{Tr_{\max}}{PET} = -0.006 \cdot (LAI_{stand}^{\phi})^2 + 0.134 \cdot LAI_{stand}^{\phi} + 0.036 \qquad (6.1)$$

This equation has already been adopted for Mediterranean biomes (?Ruffault et al., 2013).

The maximum transpiration for a given plant cohort i is calculated as the portion of $Tr_{\max}$ defined by f_i the fraction of total absorbed SWR that is due to cohort i (see section 4.3):
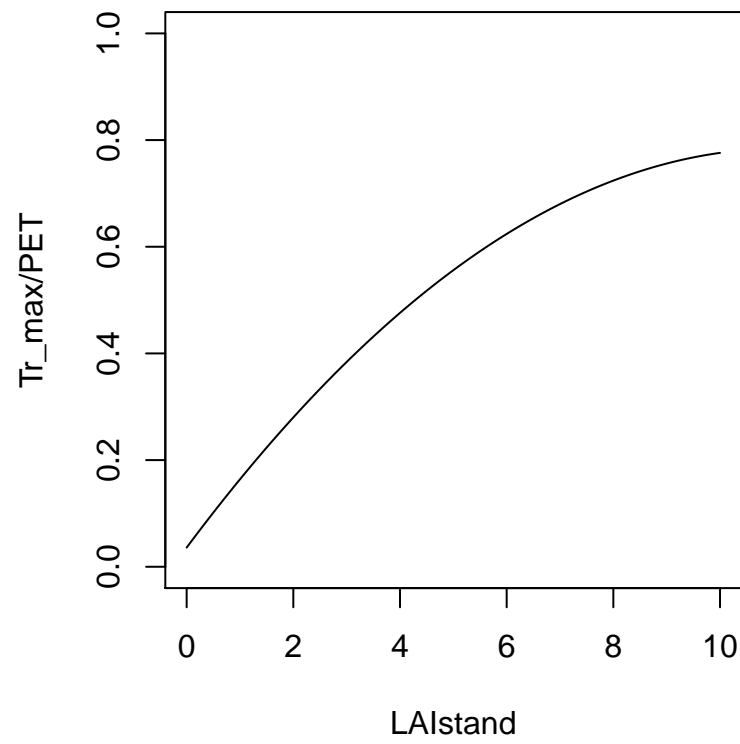
Figure 6.1: Empirical relationship between $Tr_{\max}/PET$ and LAI_{stand}^{ϕ}

$$Tr_{\max,i} = Tr_{\max} \cdot \frac{f_i}{\sum_j f_j} \tag{6.2}$$

6.1.2 Actual plant transpiration

Actual plant transpiration depends on soil moisture and is calculated for each plant cohort and each soil layer separately. $Tr_{i,s}$ (in mm) represents the transpiration made by cohort i from layer s. Actual plant transpiration from a given layer is regulated by soil moisture and the resistance to water flow through the plant. For each plant cohort i and soil layer s, the model first estimates the a whole-plant relative water conductance, $K_{i,s}$, which varies between 0 and 1 depending on $\Psi_{extract,i}$, the potential at which conductance is 50% of maximum, and Ψ_s, the water potential in layer s. This relationship is modelled using a Weibull function (see function `hydraulics_psi2K()`):

$$K_{i,s} = K_i(\Psi_s) = \exp\left\{\ln(0.5) \cdot \left[\frac{\Psi_s}{\Psi_{extract,i}}\right]^r\right\} \tag{6.3}$$

where r is an exponent that modulates the steepness of the decrease in relative conductance when soil potential becomes negative (by default, $r = 3$) and $\ln(0.5)$ is used to ensure that $K_i(\Psi_{extract,i}) = 0.5$ (Fig. 6.2).

Actual transpiration of plant cohort i from a given soil layer s, $Tr_{i,s}$, is defined as the product of (Mouillot et al., 2001): the maximum transpiration of the plant cohort ($Tr_{\max,i}$), the relative whole-plant conductance ($K_{i,s}$) corresponding to the species and water potential in layer s, and the proportion of plant fine roots in layer s, $v_{i,s}$:

$$Tr_{i,s} = Tr_{\max,i} \cdot K_{i,s} \cdot v_{i,s} \tag{6.4}$$

The total amount of water transpired by plants, Tr (in mm), is the sum of $Tr_{i,s}$ values over all plant cohorts and soil layers:

$$Tr = \sum_s \sum_i Tr_{i,s} \tag{6.5}$$

Assuming no water limitations (i.e. $K_{i,s} = 1$), we have that $Tr = Tr_{\max}$. Total stand transpiration will be lower than $Tr_{\max}$ if soil water potential in any layer is negative enough to cause a significant reduction in whole-plant conductance. At the plant level, the transpiration of a given plant cohort will be lower than that of others if:

a. The cohort is under the shade (it reduces f_i and hence $Tr_{\max,i}$)
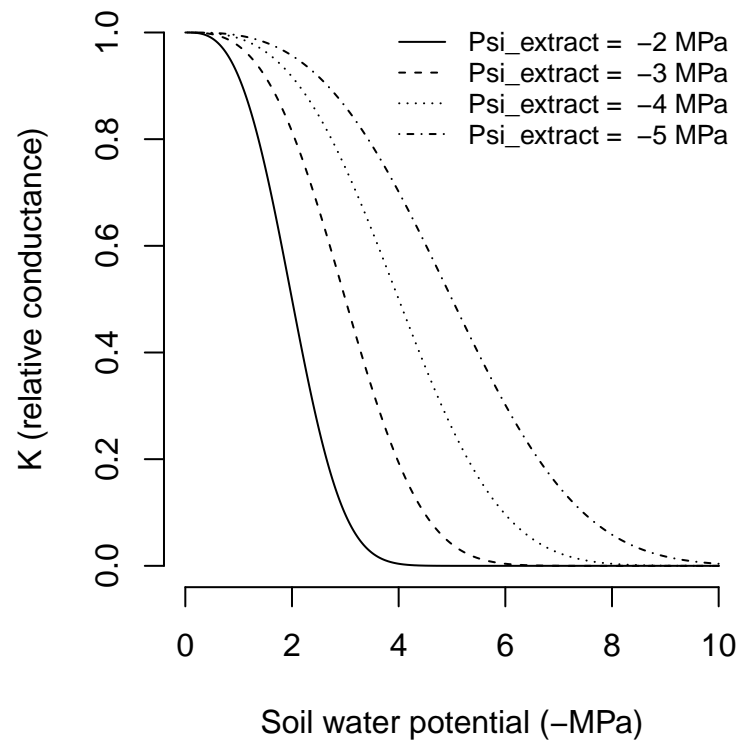
Figure 6.2: Whole-plant relative water conductance functions for different water potential values ($r = 3$ in all cases)

b. The cohort has a lower amount of leaf area (it reduces f_i and hence $Tr_{\max,i}$)

c. The soil layers exploited by the cohort have more negative water potentials (it reduces $K_{i,s}$).

6.1.3 Plant photosynthesis

Because it is useful for growth, and for compatibility with the 'Sperry' transpiration mode (chapter 7), the water balance model using 'Granier' transpiration mode also calculates net assimilated carbon. Assuming a constant maximum water use efficiency (WUE), photosynthesis for a given plant cohort i (in $gC \cdot m^{-2}$) is estimated as a function of transpiration (Mouillot et al., 2001):

$$A_n = \alpha \cdot WUE_{\max} \cdot Tr_i \tag{6.6}$$

where Tr_i is the transpiration of plant cohort i, $WUE_{\max}$ is the maximum water use efficiency of the corresponding species (in $gC \cdot mm^{-1}$) and $\alpha = T_{mean}/20$ is bounded between 0 and 1.

6.2 Plant drought stress

6.2.1 Daily drought stress and plant water potential

Similarly to Mouillot et al. (2002), daily drought stress of a given plant cohort i, DDS_i, is defined as the complement of relative whole-plant conductance and is aggregated across soil layers using the proportion of fine roots in each layer as weights:

$$DDS_i = \phi_i \cdot \sum_s \left(1 - K_{i,s}\right) \cdot v_{i,s} \tag{6.7}$$

Leaf-phenological status is included to prevent winter deciduous plants from suffering drought stress during winter. Daily drought stress values can be later used to define drought stress indices for larger temporal scales, as presented in the main text.

Granier's transpiration model does not allow estimating a water potential drop from soil to the leaf. Moreover, in a multilayered soil it is difficult to know what would be the water potential of the plant. Despite these limitations, a gross surrogate of (pre-dawn) 'leaf water potential' ($\Psi_{leaf,i}$; in MPa) may be obtained averaging whole-plant relative conductance values and inverting the conductance function:

$$\Psi_{leaf,i} = K_i^{-1} \left(\sum_s K_{i,s} \cdot v_{i,s} \right) \tag{6.8}$$

where K_i^{-1} is the inverse of the relative whole-plant conductance eq. (6.3) (see function `hydraulics_K2Psi()`).

6.2.2 Irreversible cavitation and hydraulic disconnection

The water balance model is normally run assuming that although soil drought may reduce transpiration, embolized xylem conduits are automatically refilled when soil moisture recovers (in other words, cavitation is reversible). It is possible to simulate irreversible cavitation by setting `cavitationRefill = FALSE` in the control parameters. This option causes the model to keep track of the maximum value of drought stress so far experienced:

$$P_{embolized,i} = \max\{P_{embolized,i}, DDS_i\} \tag{6.9}$$

and then $K_{i,s}$ cannot be larger than the complement of this maximum drought stress:

$$K_{i,s} = \min\{K_i(\Psi_s), 1.0 - P_{embolized,i}\} \tag{6.10}$$

Note that, even if cavitation can be considered irreversible, $P_{embolized,i}$ values are set to zero at the beginning of each year, assuming that embolized plants overcome the conductance loss by creating new xylem tissue.

Another optional behavior consists in allowing the plant to disconnect from the soil when its potential becomes too negative. This may be advantageous for a cavitation-sensitive plant that is competing for water with another plant with higher extraction capacity. Parameter $K_{rootdisc,i}$ can be used to specify the minimum relative conductance value that the plant will tolerate without disconnecting hydraulically from the soil (by default $K_{rootdisc,i} = 0$). If, after possibly accounting for irreversible cavitation, $K_{i,s} < K_{rootdisc,i}$ for a given soil layer, then the model assumes that transpiration from this soil layer is absent. Moreover, $K_{i,s}$ is assumed equal to $K_{rootdisc,i}$ for the sake of determining plant water potential.

Part III

Advanced water balance modelling

Chapter 7

Advanced water balance model

7.1 Design principles

The model performs soil water balance and energy balance for the input forest stand and for the period corresponding to input weather data. Soil water balance is calculated on a daily step basis for the input forest stand and for the period corresponding to input weather data. The model considers only the vertical spatial dimension of the stand, and not the horizontal distribution of plants within it. Still, the stand is divided into groups of plants (here referred to as 'plant cohorts') of different species, height and leaf area index (LAI). As hydrological processes, the model includes water interception loss (Gash et al., 1995), plant transpiration and hydraulic redistribution, evaporation from soil (Ritchie, 1972) and the partition between infiltration and runoff (Boughton, 1989). Water exceeding soil water holding capacity is lost via deep drainage. For plant transpiration, the model determines subdaily regulation of leaf water conductance and actual transpiration involving detailed calculations of hydraulics and photosynthesis (Sperry et al., 2016a). This level of complexity allows a precise estimation of photosynthesis and hydraulic redistribution of water among soil layers.

Radiation and energy balances are conducted subdaily at two levels: canopy/soil and leaf. One one hand the model keeps track of temperature variation of the air in the canopy (i.e. canopy energy balance) and in the soil (i.e. soil energy balance) as the result of energy exchanges between them and with the atmosphere. These energy balance equations are very similar to those of Best et al. (2011) for model JULES. On the other, the model performs the energy balance at the leaf level to determine transpiration (Sperry et al., 2016a). At this scale, radiation

inputs include shortwave radiation from the atmosphere absorbed by the leaf and absorbed longwave radiation coming from both the atmosphere and the canopy itself. Leaf temperature is determined assuming that the temperature of the air is that of the canopy. After performing stomatal regulation, the model upscales the transpiration flux at the canopy level and the corresponding latent heat is used to complete the calculation of the energy balance at the canopy level. Note that the latent heat fluxes from evaporation from the soil and of intercepted water are not currently included in the energy balance.

7.2 State variables

The model has the following state variables: + Cumulative growth degree days, GDD, are tracked by the model and determine leaf phenological status of winter deciduous species. + Daily soil moisture content dynamics on each layer s are tracked using $W = \theta(\Psi_s)/\theta_{fc,s}$, the **proportion of volumetric soil moisture in relation to field capacity**, where field capacity, $\theta_{fc,s}$, is assumed to correspond to $\Psi_{fc} = -0.033$ MPa. Soils are not allowed to contain more water than dictated by their field capacity. + The temperature of the canopy and of each soil layer (T_c and T_s; both in ºC) are tracked for every subdaily step. + If irreversible cavitation is activated, the model also tracks $P_{embolized,i}$, the maximum value of daily drought stress so far experienced.

7.3 Water and energy balances

7.3.1 Water balance

Daily variations in soil water content (ΔV_{soil} in mm) can be summarized as:

$$\Delta V_{soil} = Pr + Sm - In - Ru - Dd - Es - Tr \tag{7.1}$$

where Pr is precipitation as rainfall, Sm is water from melting the snow pack (if considered), In is the interception loss (i.e., water evaporated after being intercepted by the canopy), Ru is surface runoff, Dd is deep drainage (i.e. water percolated to layers beyond soil depth), Es is evaporation from soil and Tr is plant transpiration. If snow dynamics are considered, the water balance of the snow pack is defined as:

$$\Delta S_{snow} = Ps - Sm \tag{7.2}$$

where Ps is precipitation as snowfall and Sm is snow melt.

7.3.2 Energy balance

The canopy absorbs shortwave radiation from the atmosphere ($K_{abs,ca}$). It also absorbs longwave counterradiation from the atmosphere ($L_{abs,ca}$) and longwave radiation emmited from the soil ($L_{abs,cs}$). These inputs are counterbalanced by the longwave radiation emmited by the canopy ($L_{em,c}$) in both cases. Other energy fluxes considered are convective exchanges between the canopy and atmosphere (H_{ca}) and between the canopy and the soil (H_{cs}). Finally, energy is released to the atmosphere through latent heat (LE_c) produced via transpiration (so far, interception and soil evaporation are not included). The instantaneous energy balance equation for the canopy is thus:

$$C_c \cdot \frac{\delta T_c}{\delta t} = K_{abs,ca} + (L_{abs,ca} - L_{em,c}) + (L_{abs,cs} - L_{em,c}) - LE_c - H_{ca} - H_{cs} \quad (7.3)$$

where C_c is the canopy thermal capacitance. Like the canopy, the soil absorbs short- and longwave radiation from the atmosphere ($K_{abs,sa}$ and $L_{abs,sa}$). It also absorbs longwave radiation released by the canopy ($L_{abs,sc} = L_{em,c}$) and emmits longwave radiation ($L_{em,s}$). Note that $L_{abs,cs} \leq L_{em,s}$ because part of the radiation emmitted by the soil is sent to the atmosphere without being intercepted by the canopy. Finally, it also exchanges convective energy with the canopy (H_{cs}). The energy balance equation for the soil is:

$$C_s \cdot \frac{\delta T_s}{\delta t} = K_{abs,sa} + L_{abs,sa} - L_{em,s} + L_{abs,sc} + H_{cs} \quad (7.4)$$

where C_s is the soil thermal capacitance.

7.4 Process scheduling

Every day the model performs the following actions:

- Update leaf area values according to the phenology of species.
- Increase soil moisture due to precipitation after accounting for canopy interception loss, surface runoff and deep drainage.
- Determine subdaily temperature and direct/diffuse irradiance variations.
- Determine short- and longwave radiation absorved by the canopy and the soil at subdaily steps.
- Determine plant transpiration, photosynthesis and close soil/canopy energy balance at subdaily steps. This involves the following sub-actions:
  - Determine longwave radiation emmited by soil and canopy, according to their temperature.
  - Update the water supply function of each plant cohort, according to the hydraulic model and the current soil water potential.

- Calculate leaf temperature and photosynthesis, for shade and sunlit leaves of each plant cohort, corresponding to each transpiration value of the supply function.
- Determine stomatal conductance, transpiration and photosynthesis on shade and sunlit leaves of each plant cohort according to a profit maximization strategy.
- Update soil moisture after scaling transpiration from leaf to canopy level.
- Complete energy balance of the canopy and the soil (after translating plant transpiration to latent heat and calculating convective heat exchange for both the canopy and the soil).
- Determine drought stress index for each plant cohort.
- Decrease water content due to bare soil evaporation, closing the water balance.

7.5 Model input

7.5.1 Meteorological input

The minimum weather variables required to run the model are min/max temperatures (T_{min} and T_{max}), min/max relative humidity (RH_{min} and RH_{max}), precipitation (P) and solar radiation (Rad). Wind speed (u) is also needed for the model, but the user ma introduce missing values if not available (then, a default value will be used). Definitions and units of these variables are given in section 2.3.

7.5.2 Control parameters

The control values relevant for the advanced water balance model are:

- `verbose [=TRUE]`: Whether extra console output is desired during simulations.
- `soilFunctions [= "SX"]`: Water retention curve model, either "SX" (for Saxton) or "VG" (for Van Genuchten).
- `leafPhenology [= TRUE]`: Whether leaf phenology is simulated.
- `snowpack [= TRUE]`: Whether dynamics of snow pack are included.
- `drainage [= TRUE]`: Whether water exceeding the field capacity of the bottom layer is lost by deep drainage into a non-reachable compartment.
- `transpirationMode [= "Granier"]`: Transpiration model, in this case should be "Sperry".
- `defaultWindSpeed [= 2.5]`: Default value for wind speed (in $m \cdot s^{-1}$) when this is missing (only used for leaf fall).

- `hydraulicCostFunction [= 1]`: Variant of the hydraulic cost function used in the stomatal regulation model of Sperry et al. (2016a). Values accepted are 1 (original cost function based on the derivative of supply function), 2 (leaf vulnerability curve).
- `ndailysteps [=24]`: Number of daily substeps.
- `thermalCapacityLAI [= 1000000]`: Canopy thermal capacitance per LAI unit.
- `verticalLayerSize [= 100]`: The size of vertical layers (in cm) for photosynthesis calculation.
- `cavitationRefill [= TRUE]`: If `FALSE` the model operates in a irreversible cavitation mode.
- `taper [= TRUE]`: Whether taper of xylem conduits is accounted for when calculating aboveground stem conductance from xylem conductivity.
- `averageFracRhizosphereResistance [= 0.15]`: Fraction to total continuum (stem+root+rhizosphere) resistance that corresponds to rhizosphere (averaged across soil water potential values).
- `numericParams`: A list with params for numerical approximation routines.
- `Catm [=386]`: Atmospheric CO2 concentration (in micromol $CO_2 \cdot mol^{-1}$ = ppm).

7.5.3 Species parameters

Vegetation functional attributes are normally filled for each cohort by function `spwbInput()` from species identity. However, different parameters can be specified for different cohort of the same species if desired. Basic functional parameters relate to light extinction, water interception and leaf phenology:

- $k_{PAR,i}$ [`k`]: PAR extinction coefficient.
- $s_{water,i}$ [`g`]: Crown water storage capacity (i.e. depth of water that can be retained by leaves and branches) per LAI unit (in $mmH_2O \, \mathring{u} LAI^{-1}$).
- $S_{GDD,i}$ [`Sgdd`]: Growth degree days corresponding to leave budburst (in degrees Celsius).

A second set of plant functional parameters are related to plant transpiration and photosynthesis:

- $g_{wmin,i}$ [`Gwmin`]: Minimum leaf water conductance (in $mol \, \mathring{u} s^{-1} \mathring{u} m^{-2}$).
- $g_{wmax,i}$ [`Gwmax`]: Maximum leaf water conductance (in $mol \, \mathring{u} s^{-1} \mathring{u} m^{-2}$).
- $k_{rhizo,i,s}$ [`VGrhizo_kmax`]: Maximum hydraulic conductance of the rhizosphere for each soil layer.
- $k_{\max root,i,s}$ [`VCroot_kmax`]: Maximum hydraulic conductance of the root xylem for each soil layer.
- $c_{root,i}$ and $d_{root,i}$ [`VCroot_c` and `VCroot_c`]: Parameters of the root xylem vulnerability curve.
- $k_{\max stem,i}$ [`VCstem_kmax`]: Maximum hydraulic conductance of the stem xylem.

- $c_{stem,i}$ and $d_{stem,i}$ [`VCstem_c` and `VCstem_c`]: Parameters of the stem xylem vulnerability curve.
- $V298_{max,i}$ [`Vmax298`]: Maximum Rubisco carboxylation rate at 25ºC (in $\mu mol CO_2 \mathring{u} s^{-1} \mathring{u} m^{-2}$).
- $J298_{max,i}$ [`Jmax298`]: Maximum rate of electron transport at 25ºC (in $\mu mole \mathring{u} s^{-1} \mathring{u} m^{-2}$).}
- $P_{rootdisc,i}$ [`pRootDisc`]: Relative conductance of roots that leads to hydraulic disconnection from soil.
- $k_{rhizo,i,s}$ [`VGrhizo_kmax`]: Maximum rhizosphere conductance values for each soil layer.
- $k_{root,i,s}$ [`VCroot_kmax`]: Maximum root xylem conductance values for each soil layer.

7.6   Model output

Function `spwb` with `transpirationMode = "Sperry"` returns a list object whose elements are data tables. Each table has dates as rows and has different output variables:

- `WaterBalance`: Components of the climatic and soil daily water balance (i.e. net precipitation, infiltration, runoff, plant transpiration…).
- `Soil`: Daily variation of soil variables (volume, moisture relative to field capacity, water potential) for soil layers.
- `EnergyBalance`: Components of the atmosphere-canopy-soil energy balance, including latent heat, convective heat, conduction heat and radiation exchanges.
- `PlantLAI`: Daily leaf area index for each plant cohort.
- `PlantTranspiration`: Daily transpiration (in mm) for each plant cohort.
- `PlantPhotosynthesis`: Daily net photosynthesis (in g C · m-2) for each plant cohort.
- `PlantPsi`: Daily water potential of each plant (in MPa).
- `PlantStress`: Daily stress level suffered by each plant cohort (relative whole-plant conductance).

Chapter 8

Subdaily temperature and light variations

8.1 Air temperature

Diurnal above-canopy air temperature (T_a) variations are modeled assuming a sinusoidal pattern with $T_a = T_{\min}$ at sunrise and $T_a = (T_{\min} + T_{\max})/2$ at sunset. Air temperature varies linearly between sunset and sunrise (McMurtrie et al., 1990).

8.2 Diffuse and direct radiation

Daily global radiation (in $MJ \cdot m^{-2}$) is assumed to include both direct and diffuse shortwave radiation (SWR). Using latitude information and whether is a rainy day, this quantity is partitioned into instantaneous direct and diffuse SWR and PAR for different daily substeps. Values of instantaneous direct and diffuse SWR and PAR above the canopy (i.e. I_{beam} and I_{dif}) are calculated using the methods described in Spitters et al. (1986), which involve comparing daily global radiation with daily potential radiation.

8.3 Longwave radiation

Longwave radiation (LWR) coming from the atmosphere is calculated following Campbell and Norman (1998):

$$L_a = \epsilon_a \cdot \sigma \cdot (T_a + 273.16)^{4.0} \tag{8.1}$$

where T_a is air temperature, $\sigma = 5.67 \cdot 10^{-8.0} \text{ W} \cdot \text{K}^{-4} \cdot \text{m}^{-2}$ is the Stephan-Boltzmann constant and ϵ_a is the emmissivity of the atmosphere, calculated using:

$$\epsilon_a = (1 - 0.84 \cdot c) \cdot \epsilon_{ac} + 0.84 \cdot c \tag{8.2}$$

$$\epsilon_{ac} = 1.72 \cdot \left(\frac{vp_{day}}{T_a + 273.16} \right)^{1/7} \tag{8.3}$$

where vp_{day} is the average daily vapor pressure (in kPa) and c is the proportion of clouds.

Chapter 9

Radiation balance

The following subsection detail the calculation of radiation components of the energy balance equations.

9.1 Shortwave radiation absorbed by the canopy

The canopy is divided into vertical layers (whose size is determined by the control parameter `verticalLayerSize`), and the expanded and dead leaf area index of each cohort within each layer is determined. Let n be the number of canopy layers. And let $LAI_{i,j}^{all} = LAI_{i,j}^{\phi} + LAI_{i,j}^{dead}$ be the leaf area index of cohort i in layer j. Furthermore, it is generally accepted that sunlit and shade leaves need to be treated separately (De Pury and Farquhar, 1997). This separation is necessary because photosynthesis of shade leaves has an essentially linear response to irradiance, while photosynthesis of leaves in sunflecks is often light saturated and independent of irradiance.

The average irradiance reaching the top of each canopy layer j is calculated separately for direct beam and diffuse radiation:

$$I_{beam,j} = (1 - \gamma) \cdot I_{beam} \cdot \exp\left[\sum_{h=j+1}^{n} \sum_{i}^{c} -k_{b,i} \cdot \alpha_i^{0.5} \cdot LAI_{i,h}^{all} \right] \quad (9.1)$$

$$I_{dif,j} = (1 - \gamma) \cdot I_{dif} \cdot \exp\left[\sum_{h=j+1}^{n} \sum_{i}^{c} -k_{d,i} \cdot \alpha_i^{0.5} \cdot LAI_{i,h}^{all} \right] \quad (9.2)$$

where I_{beam} and I_{dif} are the direct and diffuse irradiance at the top of the canopy, γ is the leaf reflectance ($\gamma_{PAR} = 0.04$, $\gamma_{SWR} = 0.05$), $k_{b,i}$ is the ex-

tinction coefficient of cohort i for direct light ($k_{b,i} = 0.8$), $k_{d,i}$ is the extinction coefficient of cohort i for diffuse light (i.e. k_{PAR} or k_{SWR}) and α_i is the absorbance coefficient ($\alpha_{i,PAR} = 0.9$, $\alpha_{i,SWR} = 0.7$).

The proportion of sunlit leaves, i.e. leaves in a canopy layer that the direct light beams (sunflecks) reach is:

$$f_{SL,j} = \exp\left(\sum_{k>j}^{n}\sum_{i}^{c} -k_{b,i} \cdot LAI_{i,k}^{all}\right) \cdot \exp\left(\sum_{i}^{c} -k_{b,i} \cdot 0.5 \cdot LAI_{i,j}^{all}\right) \quad (9.3)$$

As an example we will consider a canopy of one species of LAI $= 2$, divided into ten layers with constant leaf density.

This canopy definition leads to a percentage of the above-canopy irradiance reaching each layer (Anten and Bastiaans, 2016). Extinction of direct radiation also defines the proportion of leaves of each layer that are affected by sunflecks (i.e. the proportion of sunlit leaves).
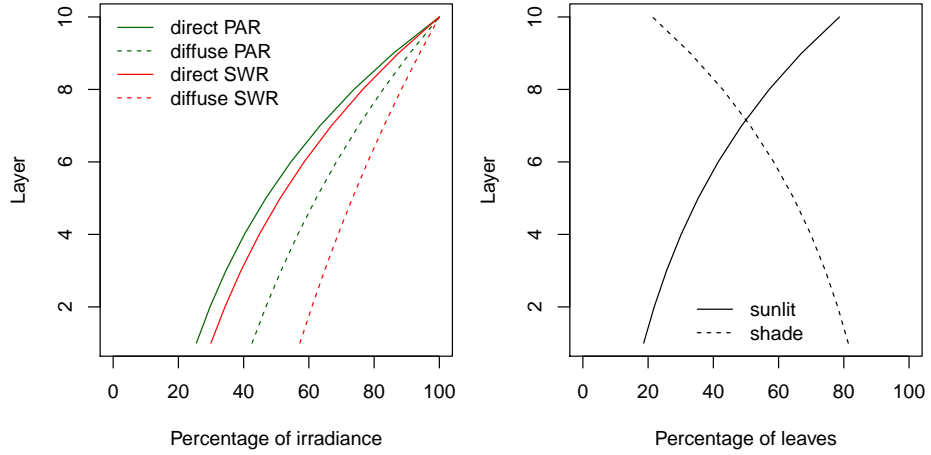
The amount of absorved diffuse radiation per leaf area unit of cohort i within a given canopy layer j is calculated as:

$$I_{dif,i,j} = I_{dif,j} \cdot k_{d,i} \cdot \alpha_i^{0.5} \exp\left[\sum_{h}^{c} -k_{d,h} \cdot \alpha_h^{0.5} \cdot 0.5 \cdot LAI_{h,j}^{all}\right] \quad (9.4)$$

The amount of absorved scattered beam radiation per leaf area unit of cohort i within a given canopy layer j is calculated as:

$$I_{sca,i,j} = I_{b,j} \cdot k_{b,i} \left(\alpha_i^{0.5} \cdot \exp\left(\sum_h^c -k_{b,h} \cdot \alpha_h \cdot 0.5 \cdot LAI_{h,i}^{all} \right) - \frac{\alpha_i}{(1-\gamma)} \cdot \exp\left(\sum_h^c -k_{b,h} \cdot 0.5 \cdot LAI_{h,i}^{all} \right) \right)$$
$$(9.5)$$

Finally, the direct radiation absorbed by a unit of sunlit leaf area of cohort i in a canopy layer j does not depend on the position of the canopy layer and is:

$$I_{dir,i,j} = I_{beam} \cdot \alpha_i \cdot 0.5/\sin\beta \tag{9.6}$$

where β is the solar elevation angle, which changes throughout the day. The amount of light absorbed by shaded/sunlit foliage of cohort i in layer j per leaf area unit ($I_{SH,i,j}$ and $I_{SL,i,j}$, respectively) is:

$$I_{SH,i,j} = I_{dif,i,j} + I_{sca,i,j} \tag{9.7}$$
$$I_{SL,i,j} = I_{dif,i,j} + I_{sca,i,j} + I_{dir,i,j} \tag{9.8}$$

The total amount of light absorbed by shaded/sunlit foliage of cohort i per ground area unit is found by taking into account the proportion of sunlit foliage:

$$\Phi_{SH,i,j} = I_{SH,i,j} \cdot (1 - f_{SL,j}) \cdot LAI_{i,j}^{\phi} \tag{9.9}$$
$$\Phi_{SL,i,j} = I_{SL,i,j} \cdot f_{SL,j} \cdot LAI_{i,j}^{\phi} \tag{9.10}$$

9.2 Shortwave radiation absorbed by the soil

The instantaneous shortwave radiation reaching the soil is calculated separately for direct beam and diffuse radiation:

$$K_{beam,soil} = K_{beam} \cdot \exp\left[\sum_{h=j+1}^n \sum_i^c -k_{b,i} \cdot \alpha_i^{0.5} \cdot LAI_{i,h}^{all} \right] \tag{9.11}$$

$$K_{dif,soil} = K_{dif} \cdot \exp\left[\sum_{h=j+1}^n \sum_i^c -k_{d,i} \cdot LAI_{i,h}^{all} \right] \tag{9.12}$$

where K_{beam} and K_{dif} are the direct and diffuse irradiance at the top of the canopy, $k_{b,i}$ is the extinction coefficient of cohort i for direct light ($k_{b,i} = 0.8$)

and $k_{d,i}$ is the extinction coefficient of cohort i for diffuse SWR. From these, the SWR absorbed by the soil is found by:

$$K_{abs,sa} = (1 - \gamma_{SWR,soil}) \cdot (K_{beam,soil} + K_{dif,soil}) \qquad (9.13)$$

where $\gamma_{SWR,soil} = 0.10$ is the SWR reflectance (10% albedo) of the soil. LWR is treated in the same way as diffuse SWR. The instantaneous LWR reaching the soil is:

$$L_{abs,sa} = (1 - \gamma_{LWR,soil}) \cdot L_a \cdot \exp\left[\sum_{h=j+1}^{n} \sum_{i}^{c} -k_{LWR} \cdot LAI_{i,h}^{all}\right] \qquad (9.14)$$

where L_a is the atmosphere longwave irradiance, $k_{LWR} = 0.8$ is the extinction coefficient for LWR and $\gamma_{LWR,soil} = 0.05$ is LWR soil reflectance (5% albedo) of the soil.

9.3   Longwave soil-canopy radiation exchange

Longwave radiation (LWR) emmited by a surface at the canopy temperature T_{can} would be:

$$L_{em} = 0.95 \cdot \sigma \cdot (T_{can} + 273.16)^{4.0} \qquad (9.15)$$

where 0.95 is emissivity and $\sigma = 5.67 \cdot 10^{-8.0} W m^{-2}$ is the Stephan-Boltzmann constant. However, the canopy may only partially cover the soil surface, so the value must be reduced by the proportion of the canopy layer actually exchanging energy. We take this as the proportion between atmospheric and absorbed LWR:

$$p_{exch} = \frac{L_{abs,ca}}{L_a} \qquad (9.16)$$

$$L_{em,c} = p_{exch} \cdot L_{em} \qquad (9.17)$$

$L_{em,c}$ is discounted twice from the canopy energy balance: as losses to the atmosphere and losses to the soil.

LWR emmited by the soil is calculated from the temperature of the first soil layer:

$$L_{em,s} = 0.95 \cdot \sigma \cdot (T_{soil} + 273.16)^{4.0} \qquad (9.18)$$

Again, the canopy only absorbs part of this radiation, the remaining going to the atmosphere:

$$L_{abs,cs} = p_{exch} \cdot L_{em,s} \qquad (9.19)$$

Chapter 10

Canopy and soil energy balances

10.1 Convective energy

Convective energy fluxes between atmosphere and the canopy (H_{ca}) and between the canopy and the soil (H_{cs}) are determined as follows:

$$H_{ca} = \frac{\rho_a \cdot c_p}{r_{ca}} \cdot (T_{can} - T_a) \tag{10.1}$$

$$H_{cs} = \frac{\rho_c \cdot c_p}{r_{cs}} \cdot (T_{can} - T_{soil}) \tag{10.2}$$

where ρ_a and ρ_c are the air density above-canopy and inside-canopy, respectively, $c_p = 1013.86\ J \mathring{u} kg^{-1} \mathring{u} C^{-1}$ is the specific heat capacity of the air. r_{ca} and r_{cs} are the atmosphere-canopy and canopy-soil aerodynamic resistances (in $s\mathring{u}m^{-1}$). These, in turn, are calculated using canopy height, total LAI and above-canopy and below-canopy wind speeds.

10.2 Latent heat

As mentioned above, the model only considers latent heat exchanged from plant transpiration, neglecting energy fluxes corresponding to evaporation from the soil and evaporation of rain intercepted by the canopy. After determining stomatal regulation and transpiration for each plant cohort, latent heat of transpiration is simply calculated as:

$$LE_c = \lambda_{T_{can}} \sum_i E_i \tag{10.3}$$

where $\lambda_{T_{can}}$ is the latent heat of vaporization at temperature T_{can} (in $J \cdot kg^{-1}$) and E_i is the instanteous transpiration flux calculated for cohort i.

10.3 Canopy capacitance and temperature changes

TO BE DONE

10.4 Soil temperature changes

Instantaneous soil temperature changes on each soil layer depend on the balance between incoming and outcoming energies (G_k and G_{k-1}):

$$\frac{\delta T_{soil,k}}{\delta t} = \frac{G_k - G_{k-1}}{C_{soil,k} \cdot \Delta z_k} \tag{10.4}$$

where Δz_k is the soil width of layer k and $C_{soil,k}$ is the thermal capacity of layer k, depending on soil moisture and texture (see function `soil_thermalcapacity`).

Energy inflow to the first layer (i.e. G_0) is the result of the soil energy balance explained above, while energy transfers between layers (i.e. G_k) depend on the soil temperature gradient:

$$G_0 = K_{abs,sa} + L_{abs,sa} - L_{em,s} + L_{abs,sc} + H_{cs} \tag{10.5}$$

$$G_k = \lambda_{soil,k} \cdot \frac{\delta T_{soil,k}}{\delta z} \tag{10.6}$$

where $\lambda_{soil,k}$ is the thermal conductivity of layer k, depending on soil moisture and texture (see function `soil_thermalconductivity`). The gradient in the bottom layer is calculated assuming a temperature of the earth (at 10 m) of 15.5 Celsius.

10.5   Bare soil evaporation

Evaporation from the soil surface is the last component of the soil water balance to be calculated. Soil evaporative demand, i.e. potential evaporation from the soil (PE_{soil}; in $mm \cdot day^{-1}$), is calculated using the Penman-Monteith combination equation:

$$PE_{soil} = \frac{1}{\lambda} \cdot \frac{\Delta \cdot R_{n,soil} + D \cdot (\rho \cdot C_p / r_a)}{\Delta + \gamma \cdot (1 + r_{soil}/r_a)} \qquad (10.7)$$

where D is the vapour pressure deficit (in kPa), Δ is the slope of the saturated vapor pressure (in $Pa \cdot K^{-1}$), γ is the psychrometer constant (in $kPa \cdot K^{-1}$), λ is the latent heat vaporization of water (in $MJ \cdot kg^{-1}$) and C_p is the specific heat of air (in $MJ \cdot kg^{-1} \cdot K^{-1}$). r_{soil} is the resistance of the soil surface, set to a constant value ($r_{soil} = 200\ s \cdot m^{-1}$). For simplicity, aerodynamic resistance (r_a) in the soil is currently set to $r_a = 208.0/u$ where u is the input wind speed.

Chapter 11

Plant hydraulics

The supply-loss theory of plant hydraulics, presented by Sperry et al. (2016a) and used in Sperry et al. (2016a), uses the physics of flow through soil and xylem to quantify how steady-state canopy water supply declines with drought and ceases by hydraulic failure. The theory builds on the hydraulic model of Sperry et al. (1998) and can be applied to different segmentations of the soil-plant continuum. In our case we considered a network of $(N{\times}2{+}S{+}1)$ resistance elements, with soil being represented in N different layers and S different stem segments. For each soil layer there is a rhizosphere element in series with a root xylem element. The N soil layers are in parallel up to the root crown. From there there are S stem xylem segments and a final leaf segment, all in series. Althougth the model implements this network representation of the soil-plant continuum, simpler one-element, two-element and three-element representations will be used in this document to facilitate understanding.

11.1   Vulnerability curves

Each continuum element has a vulnerability curve that starts at maximum hydraulic conductance (k_{max}, flow rate per pressure drop) and monotonically declines as water pressure (Ψ) becomes more negative. Vulnerability curves form the basis of hydraulic calculations.

11.1.1   Xylem vulnerability curves

Xylem tissues are assigned a two-parameter Weibull function as the vulnerability curve $k(\Psi)$:

$$k(\Psi) = k_{max} \cdot e^{-((\Psi/d)^c)} \tag{11.1}$$

where k_{max} is the maximum hydraulic conductance (defined as flow per leaf surface unit and per pressure drop), and c and d are species-specific and tissue-specific parameters. Note that parameter d is the water potential (in MPa) at which $k(\Psi)/k_{max} = e^{-1} = 0.367$. Parameter c controls the shape of the vulnerability curve ('exponential' shape with no threshold has $c \leq 1$, sigmoidal threshold has $c > 1$).

For example, we define the following parameter values for a stem xylem ($k_{s,max}$ and parameters c_s and d_s of the vulnerability curve):

```
kstemmax = 5.0 # mmol·m-2·s-1·MPa-1
stemc = 3
stemd = -3.0 # MPa
```

For root xylem ($k_{r,max}$), we may assume a higher conductance (i.e. higher efficiency) but also higher vulnerability to cavitation (defined by parameters c_r and d_r):

```
krootmax = 6.6 # mmol·m-2·s-1·MPa-1
rootc = 2
rootd = -2.5 #MPa
```

The concept of vulnerability curve can be used to specify the relationship between pressure and conductance in any portion of the flow path. Leaf vulnerability curve $k_l(\Psi)$ can be modelled using the same equation as for xylem:

$$k_l(\Psi) = k_{l,max} \cdot e^{-((\Psi/d_l)^{c_l})} \tag{11.2}$$

where $k_{l,max}$ is the leaf maximum hydraulic conductance. Values defined below specify higher conductance for leaves but also slightly higher vulnerability:

```
kleafmax = 10
leafc = 2
leafd = -2
```

With these parameter values, the vulnerability curves for root, stem and leaf are (see `hydraulics_xylemConductance()`):
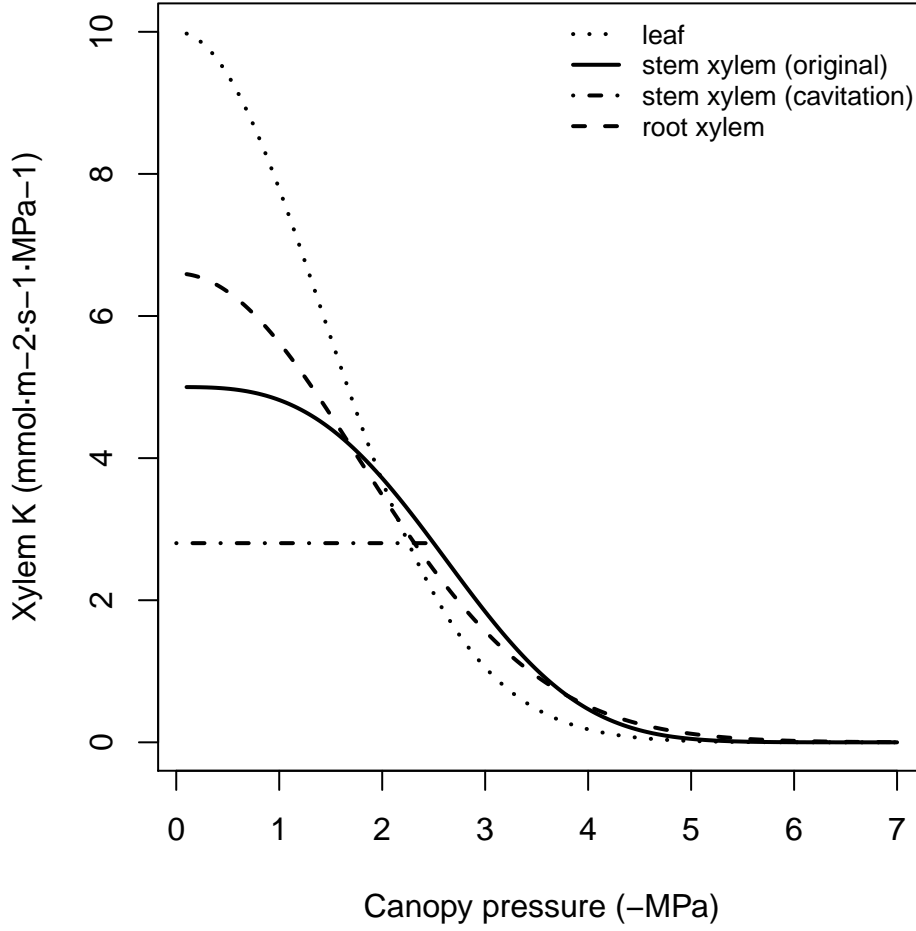
The dotted line between 0 and $\Psi_{cav} = -2.5$ MPa indicates the modification of the stem xylem vulnerability curve when cavitation has occurred (i.e., previous embolism limits a the maximum conductance value), as indicated in Sperry et al. (2016a). The corresponding proportion of conductance loss can be found using the stem vulnerability curve:

$$PLC(\Psi_{cav}) = 1.0 - \frac{k_s(\Psi_{cav})}{k_{s,max}} = 1.0 - e^{-((\Psi/d_s)^{c_s})} \tag{11.3}$$

```
1.0 - exp(-(-2.5/stemd)^stemc)
```

```
## [1] 0.4393754
```

Although root xylem are more vulnerable to the formation of emboli for a given potential, it is generally accepted that the less negative potentials of root xylem compared to the stem lead to cavitation occurring more often in the stem. The

constrain created by cavitation has an effect on the calculation of the flow rates
and derived quantities (see below).

11.1.2   Rhizosphere vulnerability curve

The rhizosphere conductance function $k_{rh}(\Psi)$ is modeled as a van Genuchten
function (Genuchten, 1980):

$$
\begin{aligned}
k_{rh}(\Psi) &= k_{rh,max} \cdot v^{(n-1)/(2 \cdot n)} \cdot \left((1-v)^{(n-1)/n} - 1 \right)^2 & (11.4) \\
v &= \left[(\alpha \Psi)^n + 1 \right]^{-1} & (11.5)
\end{aligned}
$$

where $k_{rh,max}$ is the maximum rhizosphere conductance, and n and α are
texture-specific parameters (Leij et al., 1996; Carsel and Parrish, 1988). These
are automatically set by function `soil()` when initializing soil objects (see pa-
rameters `VG_alpha` and `VG_n` in the output of `soil()`), but we can use function
`soil_vanGenuchtenParamsCarsel()` to derive them from texture types:

```
textures = c("Sandy loam","Silt loam", "Clay")
#Textural parameters
#Sandy clay loam
p1 = soil_vanGenuchtenParamsCarsel(textures[1])
p1
```

```
##     alpha         n theta_res theta_sat
##   764.983     1.890     0.065     0.410
```

```
alpha1 = p1[1]
n1 = p1[2]
#Silt loam
p2 = soil_vanGenuchtenParamsCarsel(textures[2])
p2
```

```
##     alpha         n theta_res theta_sat
##   203.9955    1.4100    0.0670    0.4500
```

```
alpha2 =  p2[1]
n2 = p2[2]
#Silty clay
p3 = soil_vanGenuchtenParamsCarsel(textures[3])
p3
```

```
##     alpha         n theta_res theta_sat
##   81.59819   1.09000   0.06800   0.38000
```

```
alpha3 =  p3[1]
n3 = p3[2]
```

We can estimate maximum rhizosphere conductance values assuming that they account for an average percentage of the resistance (e.g. 15%) across the continuum (see functions `hydraulics_averageRhizosphereResistancePercent()` and `hydraulics_findRhizosphereMaximumConductance()`):

```
percentResistance = 15
#Sandy clay loam
krmax1 =hydraulics_findRhizosphereMaximumConductance(percentResistance,
                    n1,alpha1, krootmax, rootc,rootd, kstemmax, stemc, stemd,
                    kleafmax, leafc, leafd)
krmax1
```

```
## [1] 7.375648e+14
```

```
#Silt loam
krmax2 =hydraulics_findRhizosphereMaximumConductance(percentResistance,
                    n2,alpha2, krootmax, rootc,rootd, kstemmax, stemc, stemd,
                    kleafmax, leafc, leafd)
krmax2
```

```
## [1] 3420747735
```

```
#Silty clay
krmax3 =hydraulics_findRhizosphereMaximumConductance(percentResistance,
                    n3,alpha3, krootmax, rootc,rootd, kstemmax, stemc, stemd,
                    kleafmax, leafc, leafd)
krmax3
```

```
## [1] 36831905
```

With these parameters, the resulting $k_{rh}(\Psi)$ functions can be displayed using the function `hydraulics_vanGenuchtenConductance()`:
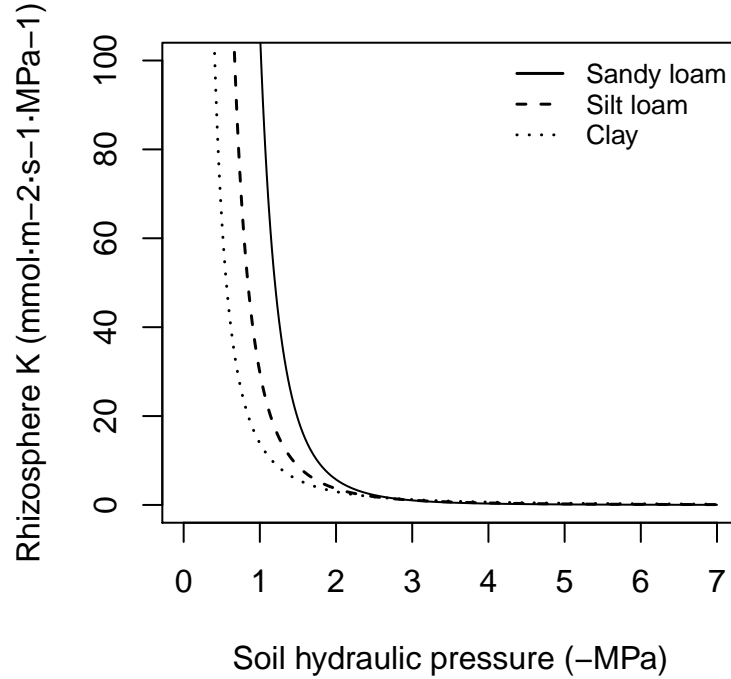
11.2 Water content of plant tissues

In **medfate** the water content of leaves and stems is tracked explicitly. Following Martin-StPaul et al. (2017), we consider two sources of water in plant segments (Tyree and Yang, 1990). The first comes from the conduits (tracheids or vessels), which will release water due to cavitation and may be refilled with water from adjacent living tissue. The second source of water is formed by more elastic living cells (i.e. parenchyma) and can potentially be a large source of water during relatively high water potentials. This source can be described using the relative water content of a symplasmic tissue. This storage compartment has its own water potential and exchanges water with the xylem conduits according to the difference in water potential.

11.2.1 Pressure-volume curves

A pressure-volume curve of a tissue relates a water potential against relative water content (RWC; $kgH_2O \cdot kg^{-1}H_2O$ at saturation) in drying tissues. Pressure-volume theory is usually applied to leaves (Bartlett et al., 2012), but it can also be applied to other tissues such as sapwood or cambium cells.

For living cells, the relationship between Ψ and RWC of the symplasmic fraction

(RWC_{sym}) is achieved by separating Ψ into osmotic (solute) potential (Ψ_S) and the turgor potential (Ψ_P):

$$\Psi = \Psi_S + \Psi_P \tag{11.6}$$

The relationship for Ψ_P is:

$$\Psi_P = -\pi_0 - \epsilon \cdot (1.0 - RWC_{sym}) \tag{11.7}$$

where π_0 (MPa) is the osmotic potential at full turgor (i.e. when $RWC_{sym} = 1$), and ϵ is the modulus of elasticity (i.e. the slope of the relationship). Assuming constant solute content, the relationship for Ψ_S is:

$$\Psi_S = \frac{-\pi_0}{RWC_{sym}} \tag{11.8}$$

When $\Psi \leq \Psi_{tlp}$, the water potential at turgor loss point, then $\Psi_P = 0$ and $\Psi = \Psi_S$. If $\Psi > \Psi_{tlp}$ then the two components are needed. The water potential at turgor loss point (Ψ_{tlp}) can be found by (Bartlett et al., 2012):

$$\Psi_{tlp} = \frac{\pi_0 \cdot \epsilon}{\pi_0 + \epsilon} \tag{11.9}$$

As an example, the following figure draws the pressure-volume curve for a tissue with $\epsilon = 12$ and $\pi_0 = -3.0$MPa:
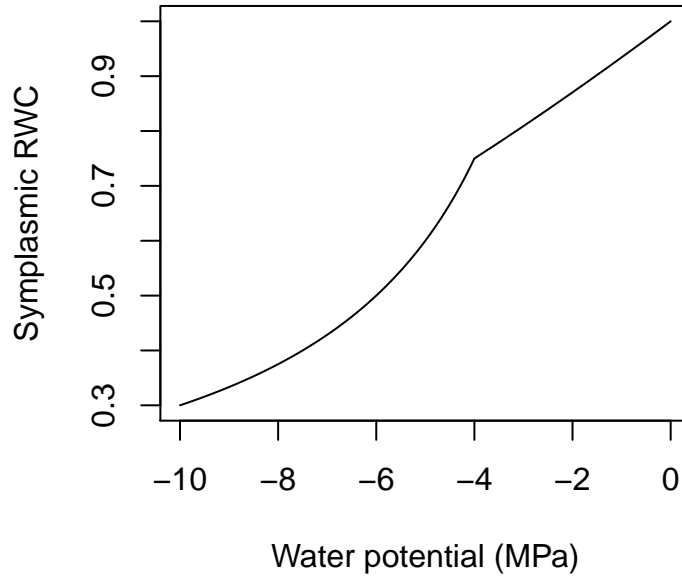
To calculate RWC_{sym} from the water potential of a tissue, the previous equations need to be combined and, after isolating RWC_{sym}, a quadratic relationship is obtained.

Apoplastic reservoirs (e.g. sapwood) consist of inelastic cells that release their water to the transpiration stream following embolism. As in Hölttä et al. (2009), we equate the relative water content of the apoplastic reservoir of a segment (leaves or stem) to the proportion of maximum conductance in the vulnerability curve:

$$RWC_{apo}(\Psi) = \frac{k(\Psi)}{k_{max}} = e^{-((\Psi/d)^c)} \tag{11.10}$$
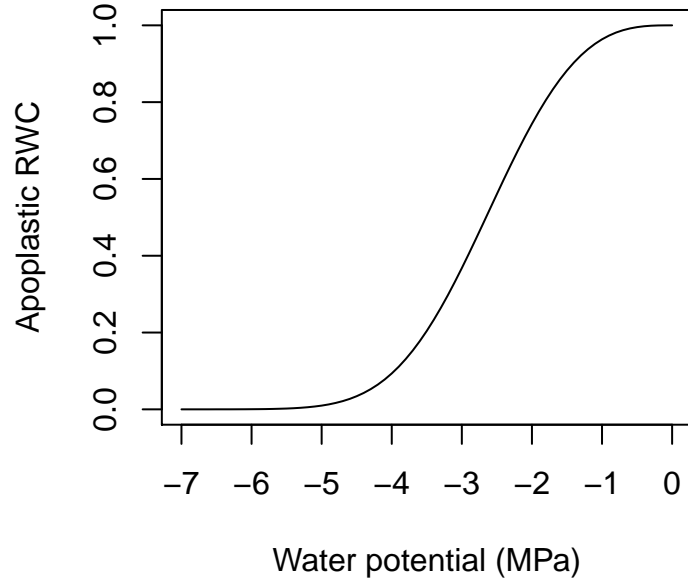
The average relative water content in a given compartment (RWC) can be obtained from Ψ_{sym} and Ψ_{apo} by calculating $RWC_{sym}(\Psi_{sym})$ and $RWC_{apo}(\Psi_{apo})$ followed by assuming a constant apoplastic fraction f_{apo}:

$$RWC = RWC_{apo}(\Psi_{apo}) \cdot f_{apo} + RWC_{sym}(\Psi_{sym}) \cdot (1 - f_{apo}) \tag{11.11}$$

11.2.2   Water content and live fuel moisture content

Pressure-volume curves are useful to determine the moisture content of live fuel elements (leaves and twigs). Given an average relative water content of a water compartment, its live fuel moisture content ($LFMC$ in $gH_2O \cdot g^{-1}$ of dry tissue) can be calculated using:

$$LFMC = RWC \cdot \Theta \cdot \frac{\rho_{H_2O}}{\rho} = RWC \cdot LFMC_{max} \tag{11.12}$$

where Θ is the tissue porosity (cm^3 of water per cm^3 of tissue), ρ is the density of the tissue and ρ_{H_2O} is the density of water.

If we know $RWC_{apo}(\Psi_{apo})$, the relative water content in conduits, and $V_{segment}$ (in m^3), the volume of conducting tissue (sapwood) in the segment, then the mass of water that is stored in conduits is:

$$S_{apo}(\Psi_{apo}) = V_{segment} \cdot f_{apo} \cdot RWC_{apo}(\Psi_{apo}) \cdot \rho_w \tag{11.13}$$

where ρ_w is the density of water ($kgH_2O \cdot m^{-3}$) and $f_{apo,s}$ is the volume fraction of apoplastic tissue within sapwood. Similarly, the amount of water stored in the symplastic tissue of the segment at any time is:

$$S_{sym}(\Psi_{sym}) = V_{segment} \cdot (1 - f_{apo}) \cdot RWC_{sym}(\Psi_{sym}) \cdot \rho_w \tag{11.14}$$

Finally, if we consider that both apoplastic and symplastic tissues are at the same water potential, the water content in the segment will be:

$$S(\Psi) = V_{segment} \cdot (f_{apo} \cdot RWC_{apo}(\Psi) + (1 - f_{apo}) \cdot RWC_{sym}(\Psi)) \cdot \rho_w \tag{11.15}$$

11.2.3   Relative water content and cavitation

In **medfate** we assume that cavitation in stems is non-reversible. Within a given sapwood segment, we further assume that the proportion of conductance loss (PLC) is related to the relative water content (RWC) in its conduit vessels (i.e. the water volume in conduit vessels with respect to the maximum water volume):

$$PLC(\Psi_{cav}) = 1 - RWC_{apo}(\Psi_{cav}) \tag{11.16}$$

where $RWC_{apo,s}$ is the function of relative water content for apoplastic stem tissue. With this assumption one can relate changes in PLC derived from cavitation with decreases in water content in xylem conduits. When PLC increases the associated change in water content is a source of water can be added to the transpirational stream (Martin-StPaul et al., 2017).

11.3   Supply functions

The supply function describes the rate of water supply (i.e. flow) for transpiration (E) as a function of pressure. The steady-state flow rate E_i through each i element of the continuum is related to the flow-induced drop in pressure across that element ($\Delta\Psi_i$) by the integral transform of the element's vulnerability curve $k_i(\Psi)$ (Sperry and Love, 2015):

$$E_i(\Delta\Psi_i) = \int_{\Psi_{up}}^{\Psi_{down}} k_i(\Psi)d\Psi \qquad (11.17)$$

where Ψ_{up} and Ψ_{down} are the upstream and downstream water potential values, respectively. The integral transform assumes infinite discretization of the flow path. The supply function can be defined for individual elements of the continuum or for the whole soil-plant continuum using different topologies. In the following subsections we illustrate the supply function for different cases.

11.3.1   Supply function for single elements

In the case of a single stem xylem element the supply function describes the flow rate as a function of canopy pressure (Ψ_{canopy}). It can be calculated by numerical integration or aproximated using an incomplete gamma function. The shape of the supply function starting at different root crown water potential values ($\Psi_{rootcrown}$) is (see function `hydraulics_EXylem()`):
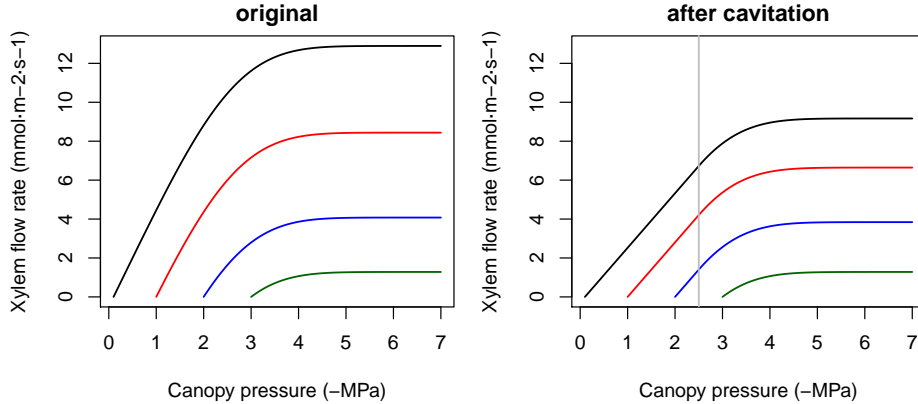
Right pane shows the supply functions that are obtained in the case of a cavitated xylem (i.e. without refilling), assuming that the minimum water potential experienced so far was -2.5 MPa. Note the linear part of the flow rate between Ψ_{soil} and this limit.

The supply function of the rhizosphere element relates the flow rate to the pressure inside the roots (Ψ_{root}). It is calculated by numerical integration of

the van Genuchten function (see function `hydraulics_EVanGenuchten()`), for which we use the analytical approximation of Van Lier et al. (2009). Here we draw the supply function for the rhizosphere starting at the four different values of bulk soil pressure (Ψ_{soil}) and for the same three texture types:
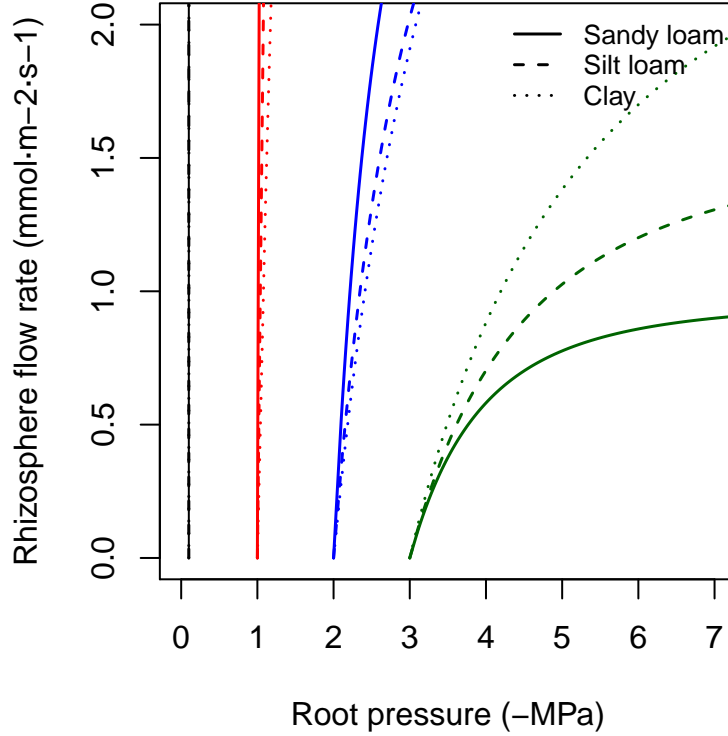
The nearly vertical lines indicate that for many values of E_i the corresponding drop in water potential through the rhizosphere will be negligible. Only for increasingly negative soil water potential values the decrease in water potential through the rhizosphere becomes relevant. Both in the case of a xylem element or a rhyzosphere element the derivative $dE_i/d\Psi$ of the supply function is equal to the corresponding vulnerability curve.

11.3.2 Supply function of two elements in series

Let us describe the soil-plant continuum is represented using *two* elements in series (rhizosphere + stem xylem). In this case, the supply function has to be calculated by sequentially using the previous supply functions. The E_i is identical for each element and equal to the canopy E. Since Ψ_{soil} is known, one first inverts the supply function of the rhizosphere to find Ψ_{root} (see function `hydraulics_E2psiVanGenuchten()`) and then inverts the supply function of the xylem to find Ψ_{canopy} (see function `hydraulics_E2psiXylem()`). The two

operations can be summarized in a single supply function describing the potential rate of water supply for transpiration (E) as function of the canopy xylem pressure (Ψ_{canopy}), starting from different bulk soil (Ψ_{soil}) values (see function hydraulics_supplyFunctionTwoElements()):
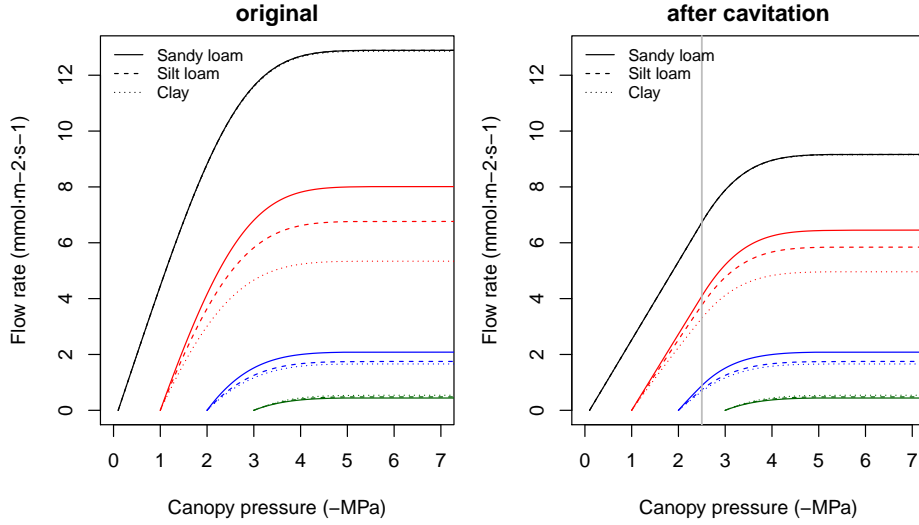
The supply function for the whole continuum contains much information. The Ψ intercept at $E = 0$ represents the predawn canopy sap pressure which integrates the rooted soil moisture profile. As E increments from zero, the disproportionately greater drop in Ψ_{canopy} results from the loss of conductance. As the soil dries the differences in flow due to soil texture become more apparent. The derivative of the whole continuum supply function, $dE/d\Psi$, is not equal to either of the vulnerability curves and it has to be obtained numerically. The derivative functions corresponding to the supply functions shown in the previous figure are:
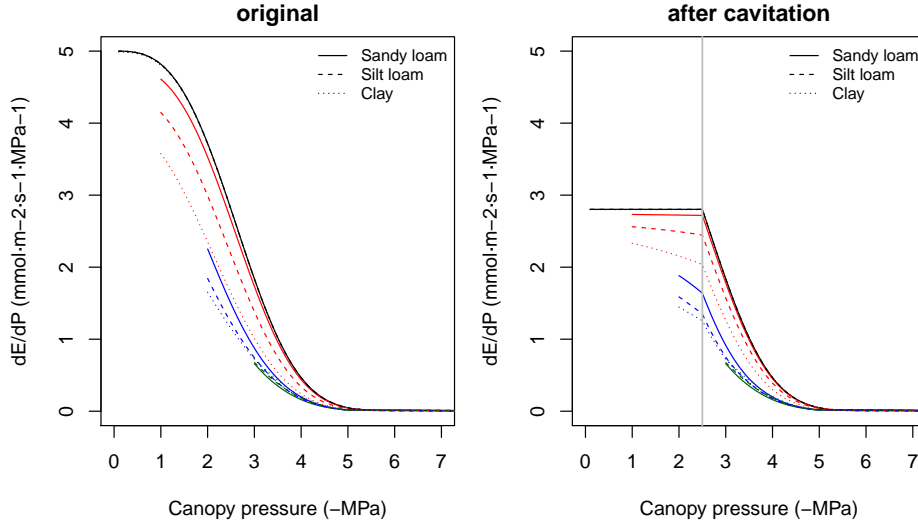
The derivative $dE/d\Psi_{canopy}$ is the conductance if the entire continuum was exposed to Ψ_{canopy} (Sperry and Love, 2015). It corresponds to the local loss of hydraulic conductance at the downstream end of the flow path. It falls towards zero for asymptotic critical values (E_{crit}). For a cavitated system $dE/d\Psi_{canopy}$ can be rather flat, in accordance with the close to linear part of the supply function.

11.3.3 Supply function of three elements in series

If the soil-plant continuum is represented using *three* elements in series (rhizosphere + stem xylem + leaf), the resulting overall conductance and resistance fractions (under wet conditions) are:

```
rstemmin = 1/kstemmax
rleafmin = 1/kleafmax

#Percentages of minimum resistance
rvec = c(rstemmin,rleafmin)
100*rvec/sum(rvec)
```

```
## [1] 66.66667 33.33333
```

```
#Maximum overall conductance
1/sum(rvec)
```

```
## [1] 3.333333
```

As before, the supply function has to be calculated by sequentially. The E_i is identical for each element. Since Ψ_{soil} is known, one first inverts the supply function of the rhizosphere to find Ψ_{root} and then inverts the supply function

of the xylem to find Ψ_{stem}. Finally, one inverts the supply function of the leaf element to find Ψ_{leaf}. As before, the three operations can be summarized in a single supply function describing the potential rate of water supply for transpiration (E) as function of the leaf pressure (Ψ_{leaf}), starting from different bulk soil (Ψ_{soil}) values (see function `hydraulics_supplyFunctionThreeElements()`):
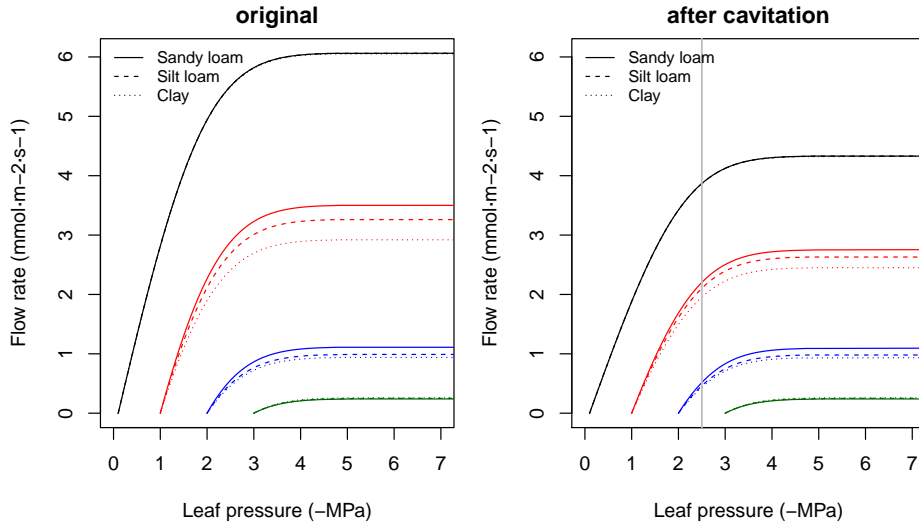
Note that overall conductance and the maximum flow of the supply function are smaller in this case than in the representation using two elements in series. While the rhizosphere component only adds a significant resistance when the soil dries, considering the leaf segment (or a root xylem segment) increases the overall resistance of the continuum. Higher vulnerability of leaves also makes the curve to saturate for less negative soil water potentials. The derivative functions corresponding to the supply functions shown in the previous figure are (note the highest value being equal to the overall maximum conductance):
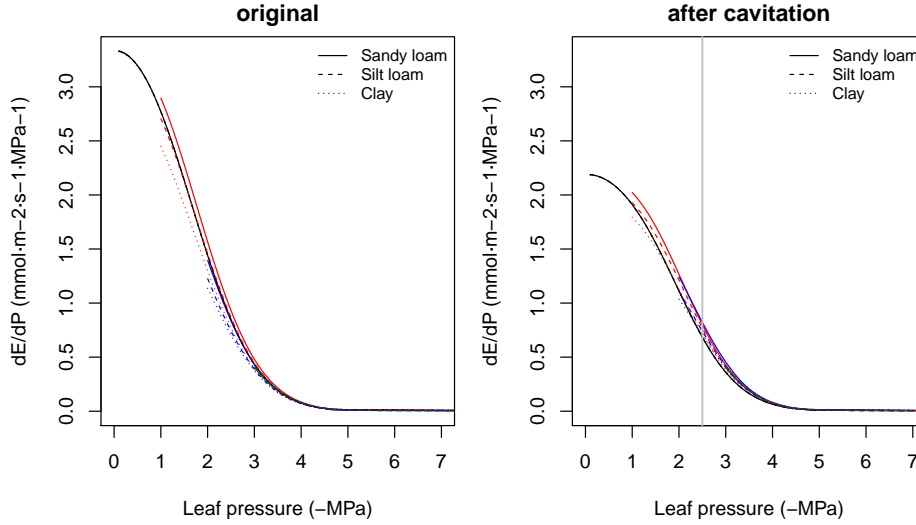
11.3.4 Supply function of a root system

So far we considered supply functions of elements in series, but resistance elements will be in parallel if soil is represented using $N > 1$ different layers. For each soil layer there is a rhizosphere element in series with a root xylem element. The N soil layers are in parallel up to the root crown.

Network of N rhizosphere components and root layers in parallel there are $N+1$ unknown pressures: the N root surface pressures $(\Psi_{rootsurf,1}, \ldots, \Psi_{rootsurf,N})$ and the root crown pressure at the downstream junction for all root components $(\Psi_{rootcrown})$. The $N + 1$ unknown pressures are solved, for each specified total flow value E, using multidimensional Newton-Raphson on a set of equations for steady-state flow (Sperry et al., 2016b):

$$E_{k,rhizosphere} - E_{k,root} = 0 \qquad (11.18)$$

$$\sum_{k}^{n} E_{k,root} - E = 0 \qquad (11.19)$$

where $E_{k,rhizosphere}$ and $E_{k,root}$ are supply flows calculated using the integrals of either van Genuchten or Weibull function as vulnerability curves, respectively. In the case of rhizosphere elements, $\Psi_{up,k} = \Psi_{soil,k}$ and in the case of root elements $\Psi_{up,k} = \Psi_{rootsurf,k}$. Solving the steady-state equations also provides values for flow across each of the parallel paths $E_{k,rhizosphere} = E_{k,root}$, which are useful to conduct water balance operations on each layer.
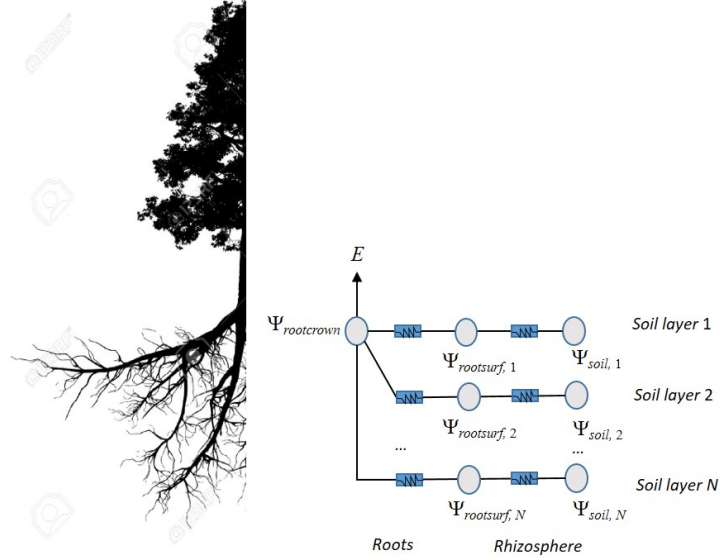
Figure 11.1: Schematic representation of hydraulics in a root network

As an example, we start by defining the water potential of three soil layers corresponding to four situations (analogously with the soil water potentials defined above):

```
psiSoilLayers1 = c(-0.3,-0.2,-0.1)
psiSoilLayers2 = c(-1.3,-1.2,-1.1)
psiSoilLayers3 = c(-2.3,-2.2,-2.1)
psiSoilLayers4 = c(-3.3,-3.2,-3.1)
```

In a network of several soil layers, one has to divide the total rhizosphere and root xylem conductances among layers. Let layer depths be:

```
d = c(300,700,3000) #Soil layer widths in mm
```

Now let v_1, v_2 and v_3 be the proportion of fine root biomass in each soil layer.

```
Z50 = 200 #Parameter of LDR root distribution
Z95 = 1200 #Parameter of LDR root distribution
v = root_ldrDistribution(Z50, Z95, d)
v
```

```
##           [,1]      [,2]       [,3]
## [1,] 0.6652935 0.2749944 0.05971209
```

In the case of the rhizosphere conductances, we can simply define them (for each

soil texture type) as:

```
krhizomaxvec1 = krmax1*v
krhizomaxvec2 = krmax2*v
krhizomaxvec3 = krmax3*v
```

To divide maximum root xylem conductance among soil layers we need weights inversely proportional to the length of transport distances (Sperry et al., 2016b). Vertical transport lengths can be calculated from soil depths and radial spread can be calculated assuming cylinders with volume proportional to the proportions of fine root biomass. The whole process can be done using function `root_rootXylemConductanceProportions()`:

```
weights = root_xylemConductanceProportions(v, d)
weights
```

```
## [1] 0.2369724 0.4214326 0.3415950
```

Transport weights are quite different than the fine root biomass proportions. This is because radial lengths are largest for the first (top) layer and vertical lengths are largest for the third (bottom) layer. The root xylem conductances are (in this case they do not depend on soil texture):

```
krootmaxvec = krootmax*weights
krootmaxvec
```

```
## [1] 1.564018 2.781455 2.254527
```

Having all these maximum conductances, we can now build the supply functions for each soil texture and starting from the different soil water potential configurations (see function `hydraulics_supplyFunctionBelowground()`):
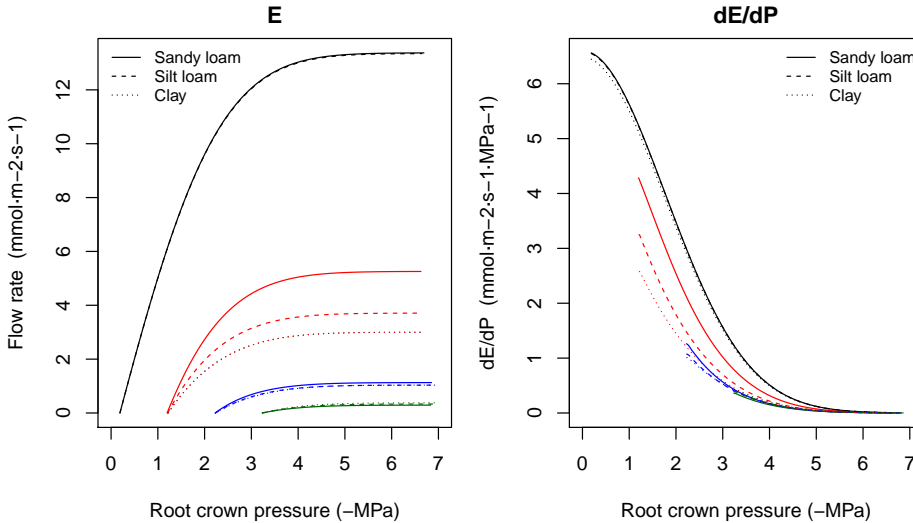
The derivative of $dE/d\Psi_{rootcrown}$ for the supply function of the root system is

again obtained numerically. Solving the previous system of equations provides the water potentials in different points of the root system. Here we plot them for the results of silt loam texture and the first and last soil potential vectors defined above:
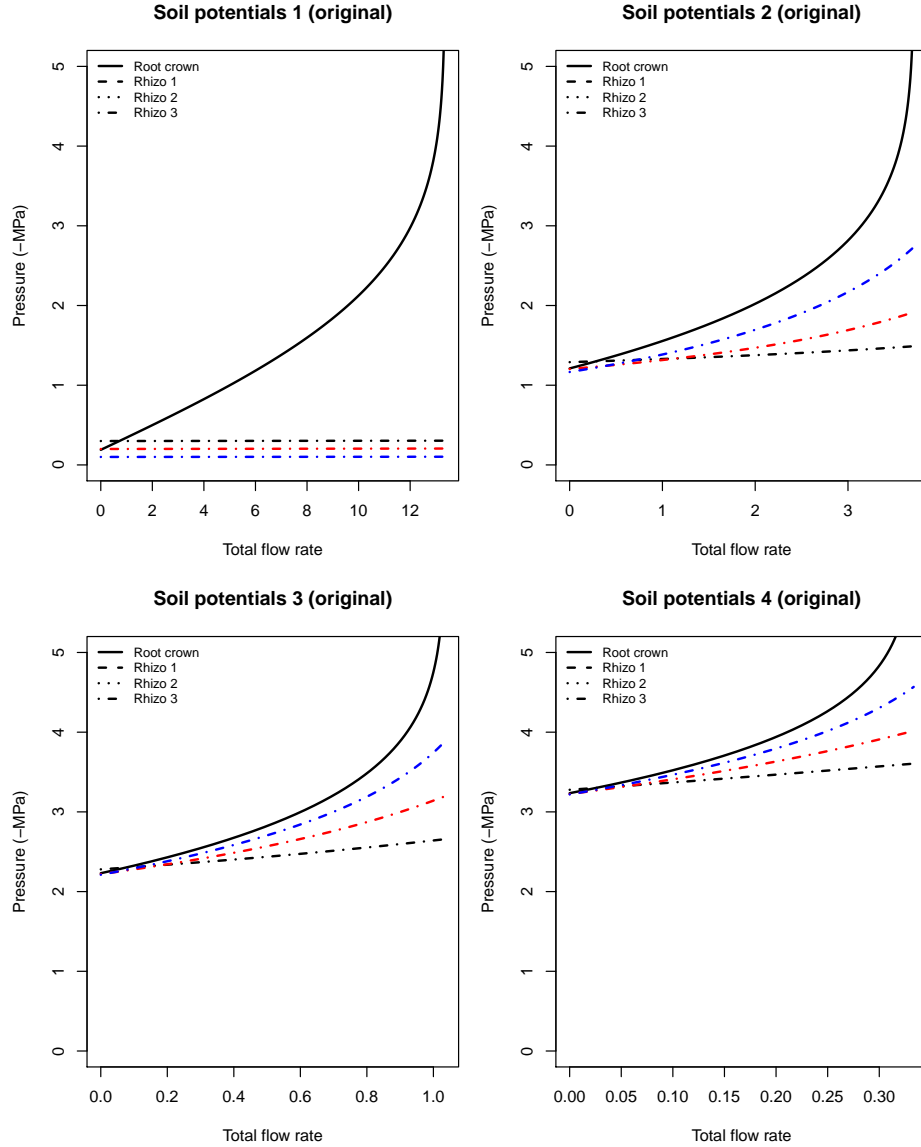
Note that when soil is not dry (first situation) pressure drop in the rhizosphere is negligible, but not the pressure drop in the root xylem. For drier soils rhizosphere becomes more relevant. We can also plot the flow rates across each of the parallel paths (again corresponding to the results of silt loam texture and

for the four soil potential vectors):

Soil potentials 1

Soil potentials 2

Soil potentials 3

Soil potentials 4
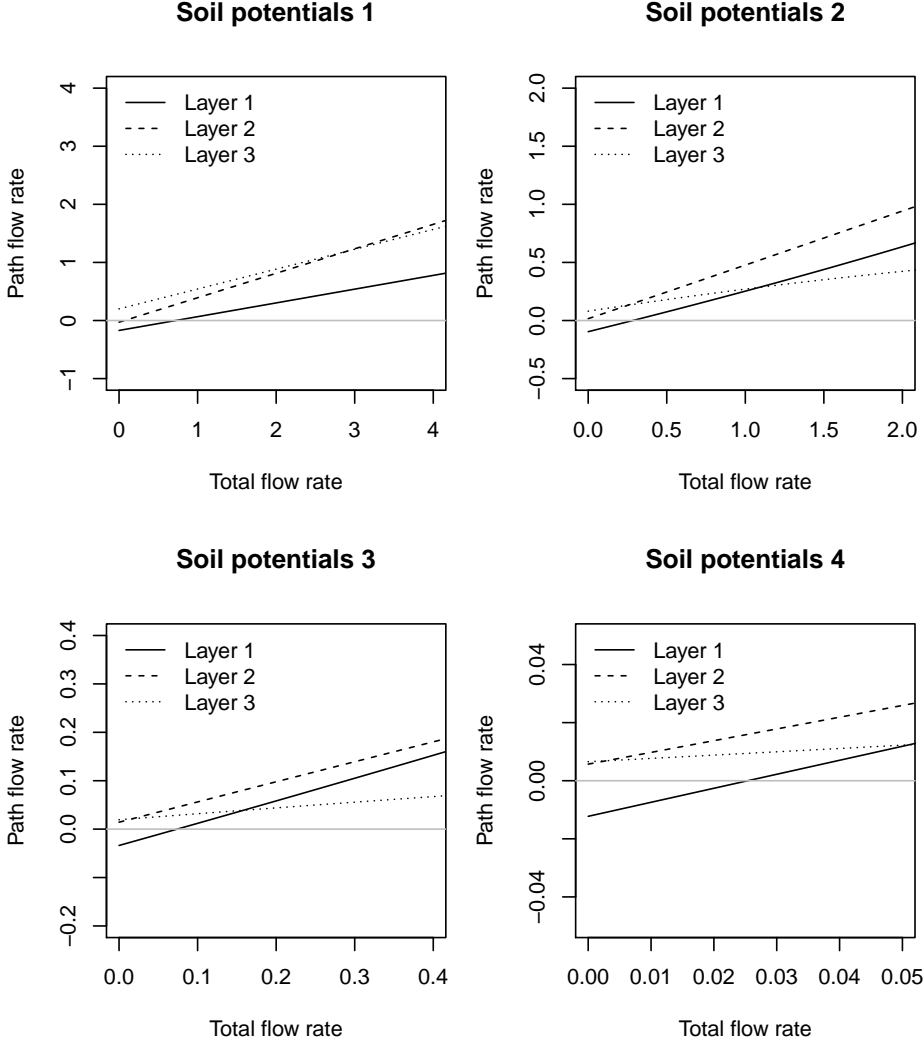
Note that the contribution of each soil layer depends on the soil conditions and the total amount of flow. For a low total flow rate some layers may have negative flows if their potential is lower than others, which in a dynamic context will cause hydraulic redistribution of water among soil layers.

11.3.5 Supply function of the soil-plant continuum

We can use a network of $(N \times 2 + S + 1)$ resistance elements to represent the soil-plant continuum, with soil being represented in N different layers. As before,
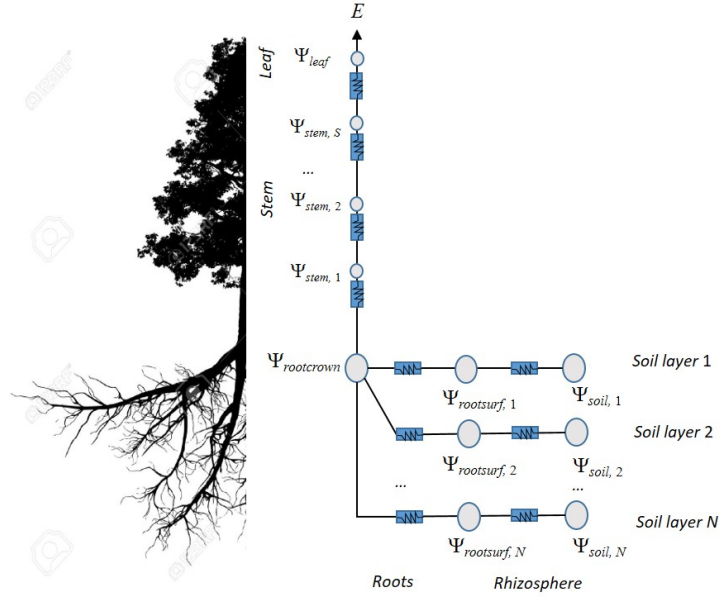
Figure 11.2: Schematic representation of hydraulics in a whole-plant network

the N soil layers are in parallel up to the root crown and each soil layer requires at least a rhizosphere and a root segment. From the root crown there are S stem xylem elements (normally $S = 1$) in series and a final leaf element. The whole hydraulic network is illustrated in the figure below.

To build the supply function for the network, we proceed by calculating water potentials in the network for each value of flow. For any given E value we start by calculating flows and potentials within the root system. After that, and assuming $S = 1$, the water potential at the upper end of the stem (Ψ_{stem}) is obtained using the inverse of the stem supply function and setting $\Psi_{up,k} = \Psi_{rootcrown}$. If $S > 1$, this is done for each of the stem segments (thus obtaining $\Psi_{stem,1}$, $\Psi_{stem,2}$, ... $\Psi_{stem,S}$), while using a maximum conductance for segments equal to $k_{max,s}$ times S. Leaf water potential (Ψ_{leaf}) is finaly obtained using the inverse of the leaf supply function and setting $\Psi_{up,k} = \Psi_{stem,S}$ and assuming a steady-state flow E. The whole supply function $E(\Psi_{leaf})$ is obtained repeating these operations from $E = 0$ to a critical value E_{crit}.

The following figure shows network supply functions (with $S = 1$) for each soil texture and starting from the different soil water potential configurations (see function `hydraulics_supplyFunctionNetwork()`):
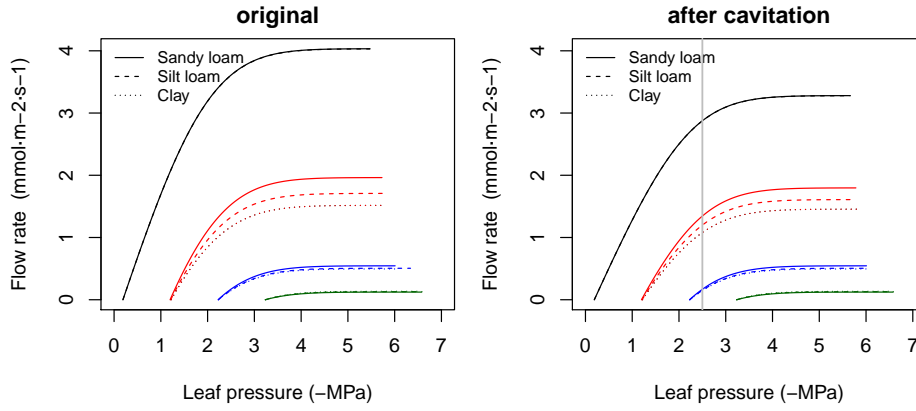
As with previous representations of the soil-plant continuum, the derivative of $dE/d\Psi_{leaf}$ for the network topology is obtained numerically:
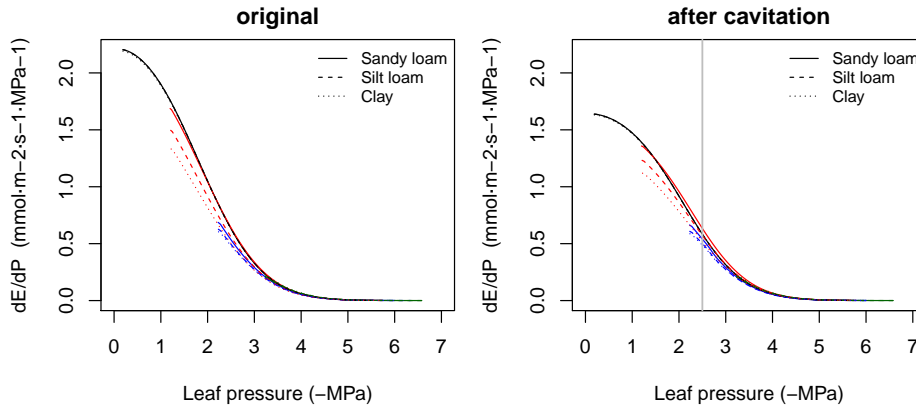
As with the root system, we can know the water potentials in different points of the continuum. Here we plot them for the results of silt loam texture and the first and last soil potential vectors defined above:

Soil potentials 1 (original)

Soil potentials 1 (cavitation)

Soil potentials 4 (original)

Soil potentials 4 (cavitation)
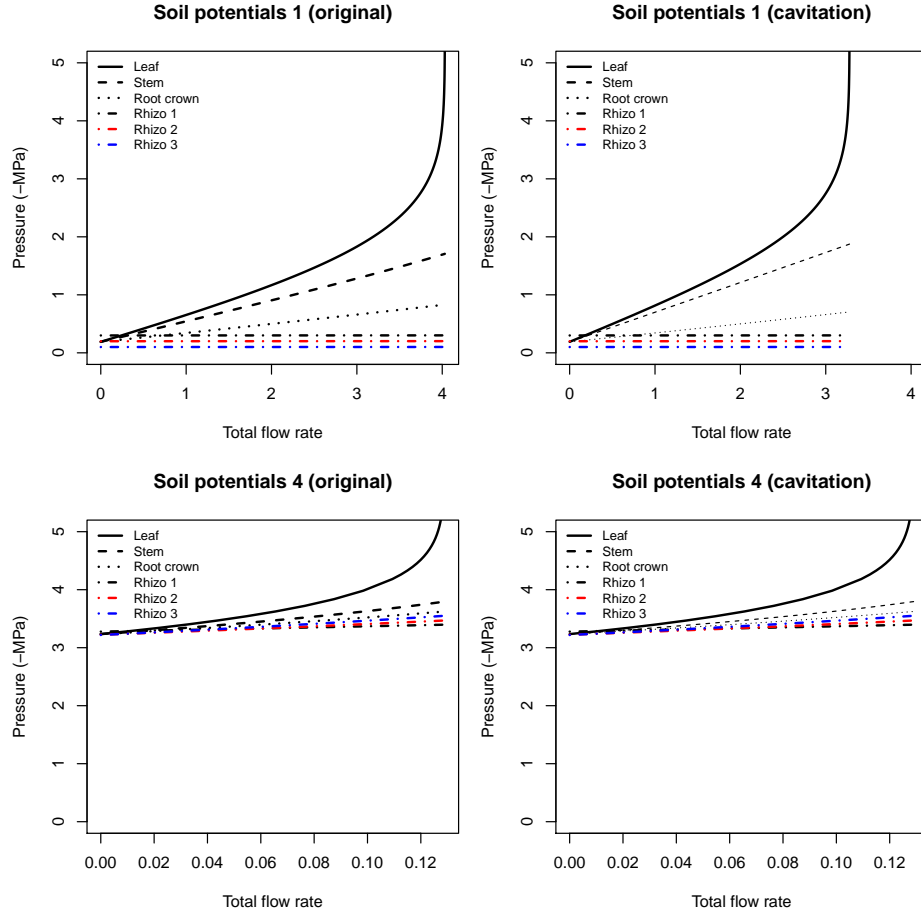
11.3.6 Supply function with water compartments

So far we assumed there are no other sources of water than the soil. In this section we consider the effect of additional water from leaf and stem tissues on the supply function. The supply function of a network representing the continuum is build for a given state of soil water potentials. This approach allows determining flows and water potential for *steady-state* conditions. In a dynamic context one has to calculate the supply function for all values of E, then to determine stomatal conductance (see sections devoted to photosynthesis and stomatal regulation) and finally to decide on a specific value of E and the corresponding steady-state configuration. Because light and temperature conditions change along the day, steady-state stomatal conductance and instantaneous E values have to be determined for subdaily steps (e.g. 1-hour steps) and then flows need to be scaled and aggregated. At the end of the day, one may substract water from soil layers and recalculate the supply function for the next day.
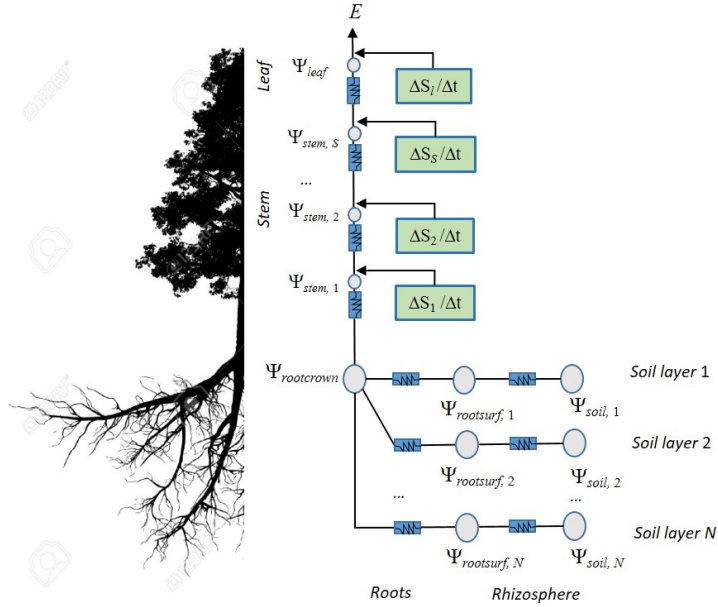
Figure 11.3: Schematic representation of hydraulics in a whole-plant network with water compartments

When considering water compartments, plant transpiration can be larger or smaller than the water extracted from the soil. Moreover, the supply function of a given time step will be dependent on the status of storage comparments in the previous time step, because this determines how much water is added or removed to the stemflow due to the effect of water compartments. For any segment (either a stem segment or the leaf segment) the flow out of it, $E_{i,out}$, is not necessarily equal to the flow entering the segment, $E_{i,in}$. Thus, instead of eq. 11.17, the equation governing the flow is (Sperry et al. 1998; Steppe et al. 2005):

$$E_{i,out} = E_{i,in} - \frac{\Delta S_i}{\Delta t} = \int_{\Psi_{up}}^{\Psi_{down}} k_i(\Psi)d\Psi - \frac{\Delta S_i}{\Delta t} \qquad (11.20)$$

When building the supply function from the root crown to the leaf, one has to consider changes in storage water of the current segment before processing the next segment. Specifically, for every segment i we take the current downstream water potential of the previous segment as upstream water potential (i.e. $\Psi_{up} = \Psi_{rootcrown,t}$ when processing the first stem segment, $\Psi_{up} = \Psi_{i-1,t}$ when processing intermediate stem segments or $\Psi_{up} = \Psi_{S,t}$ when processing the leaf segment). Then we calculate the steady-state drop in water potential (i.e., determine $\Psi_{down} = \Psi_{i,t}$) corresponding to the input flow ($E_{i,in}$) using the inverse

of the integral transform. If stem cavitation has occurred previously then $\Psi_{cav,i}$ will limit the maximum conductance. To determine $E_{i,out}$ we calculate the additional instantaneous flow due to changes in storage water volume $(\Delta S_i/\Delta t)$ using:

$$\Delta S_i = S_i(\Psi_{i,t}) - S_i(\Psi_{i,t-1}) \qquad (11.21)$$

As mentioned when describing water content functions, we consider two sources of water in plant segments (Tyree and Yang, 1990). The amount of water absorbed by or released from the storage compartment will depend on the properties of the apoplastic and symplastic tissues and the fraction of the segment that corresponds to each kind of tissue. For example, let us take the following storage capacities, fractions of apoplastic tissue and parameters of the pressure-volume curves for symplastic tissue.

```
Vmaxstem = 0.001005046
Vmaxleaf = 0.0001327463
stemfapo = 0.8
leaffapo = 0.15
stempi0 = -2
stemeps = 16
leafpi0 = -1.5
leafeps = 8
```

The following figures show the change in supply function caused by stem and leaf water compartments, assuming a 1-hr time step and either 0 MPa or -1.5 MPa as previous water potential for all segments (see function `hydraulics_supplyFunctionNetworkCapacitance()`):
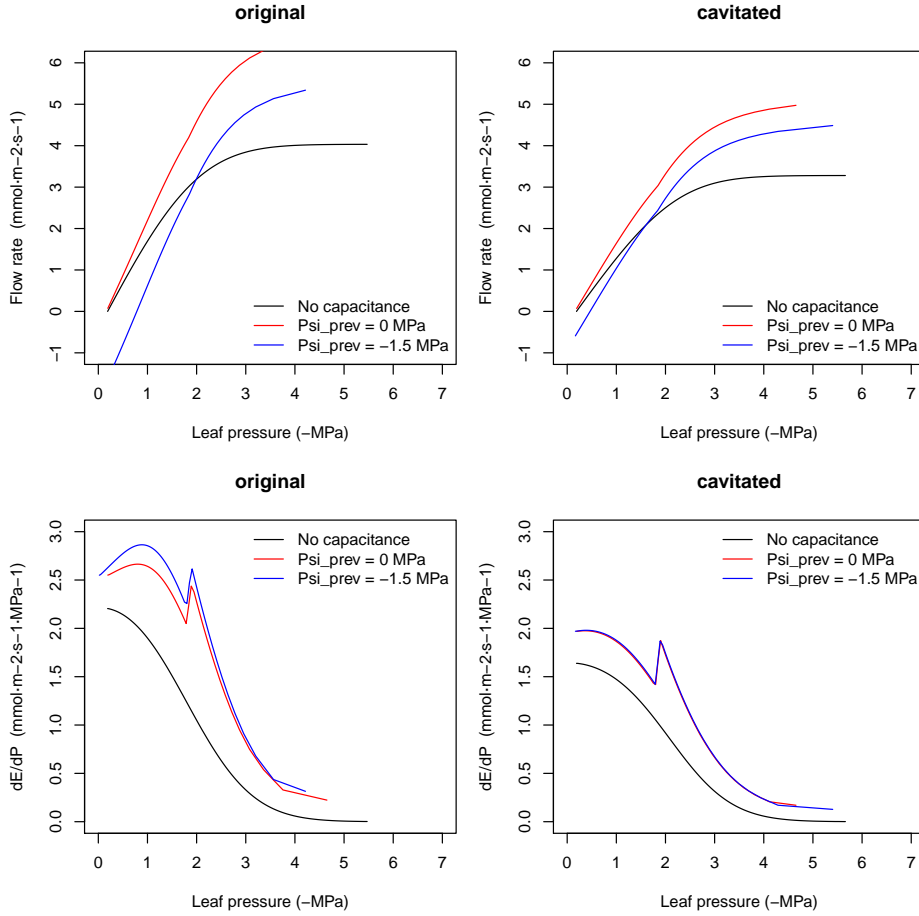
For the same water potential drop, the effect of the water compartment results in a larger transpiration flow. If the previous water potential is more negative than the root crown, negative flows may occur, because of the need to replenish the water compartment. Note, in addition, that $dE/d\Psi$ is no longer a non-increasing function of Ψ. This has important consequences for the definition of the cost function (see subsection 'Stomatal regulation'). In our opinion, the effect of water compartments on the transpiration flow are important for sub-daily variations in transpiration but are less necessary for seasonal to multi-year simulations. However, we will come back to the importance of compartments for plants being disconnected from the soil.

Chapter 12

Plant photosynthesis and stomatal regulation

12.1 Leaf energy balance, gas exchange and photosynthesis

12.1.1 Leaf VPD, conductance to water vapor and photosynthesis

The water supply function specifies the flow rate, as per leaf area, for values of leaf water potential. If we know air temperature, air vapour pressure and the light conditions in which leaves are, we can be translate the supply function into a photosynthesis function (Sperry et al., 2016a). In a nutshell, E from the supply function is used to calculate leaf temperature from an evaluation of the leaf energy balance. The diffusive conductances of the leaf to water and CO_2 are obtained from water supply and water vapor deficit. The gross assimilation rate is then obtained from the diffusive conductance and a modelled curve between assimilation and leaf internal CO_2 concentration. Gross assimilation is calculated, without subtracting autotrophic respiration, because the purpose is to represent the instantaneous gain of opening the stomata. Nevertheless autotrophic respiration is included when calculating leaf net photosynthesis.

```
Tmin = 15
Tmax = 30
RHmin = 60
RHmax = 75
Tcan = meteoland::utils_averageDaylightTemperature(Tmin, Tmax)
vpa = meteoland::utils_averageDailyVP(Tmin, Tmax, RHmin, RHmax)
Patm = meteoland::utils_atmosphericPressure(100)
```

```
Q = 2000
Catm = 386

Vmax298 = 100
Jmax298 = 1.67*Vmax298
Gmin = 0.00001;
Gmax = 0.3

Rabs = 740 #W * m-2
```

12.1.2 Leaf temperature and vapor pressure deficit

Leaf temperature (T_{leaf}; in Celsius) can be calculated for any given flow rate $E(\Psi_{leaf})$ using (Campbell and Norman, 1998):

$$T_{leaf}(\Psi_{leaf}) = T_{can} + \frac{I_{abs} - \epsilon \cdot \sigma \cdot (T_{can} + 273.15)^4 - \lambda_v \cdot E(\Psi_{leaf})}{C_p \cdot (g_r + g_{Ha})} \quad (12.1)$$

where I_{abs} (in $W \cdot m^{-2}$) is the instantaneous shortwave and longwave radiation absorbed per leaf area unit, $E(\Psi_{leaf})$ is the flow (converted to $mol \cdot s^{-1} \cdot m^{-2}$ per two-sided leaf area basis), ϵ is longwave radiation emissivity (0.97), σ is the Stephan-Boltzman constant, T_{can} is the canopy air temperature (in ºC; see Radiation and energy balance), $C_p = 29.3 \ J \cdot mol^{-1} \cdot C^{-1}$ is the specific heat capacity of dry air at constant pressure and λ_v is the latent heat of vaporization (in $J \cdot mol^{-1}$):

$$\lambda_v = (2.5023 \cdot 10^6 - (2430.54 \cdot T_{can})) \cdot 0.018 \quad (12.2)$$

Finally, g_r and g_{Ha} are the radiative and heat conductance values (in $mol \cdot m^{-2} \cdot s^{-1}$), respectively (Campbell and Norman, 1998):

$$g_r = \frac{4 \cdot \epsilon \cdot \sigma \cdot (T_{can} + 273.15)^3}{C_p} \quad (12.3)$$

$$g_{Ha} = 0.189 \cdot (u/d)^{0.5} \quad (12.4)$$

where u is wind speed (in $m \cdot s^{-1}$), taken as the wind speed at mid-crown height, and d is 0.72 times the leaf width (species parameter `LeafWidth` in cm).

The following figures illustrate the value of T_{leaf} for two leaf sizes and varying values of wind speed and flow rate, calculated for 24ºC canopy temperature and 740 $W \cdot m^{-2}$ instantaneous absorved radiation (see function `biophysics_leafTemperature`):
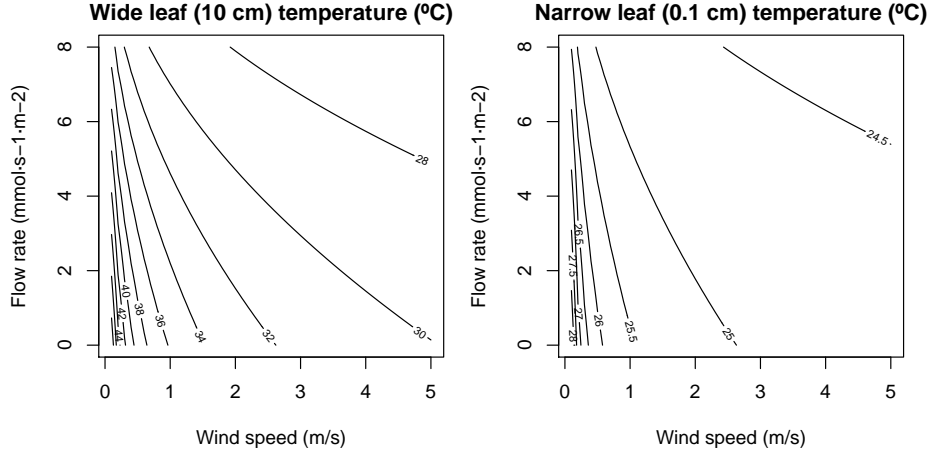
Let's now fix wind speed to 2 m/s. The application of the above equations to the $E(\Psi_{leaf})$ curves corresponding to the complete hydraulic network yields the following $T_{leaf}(\Psi_{leaf})$ curves:
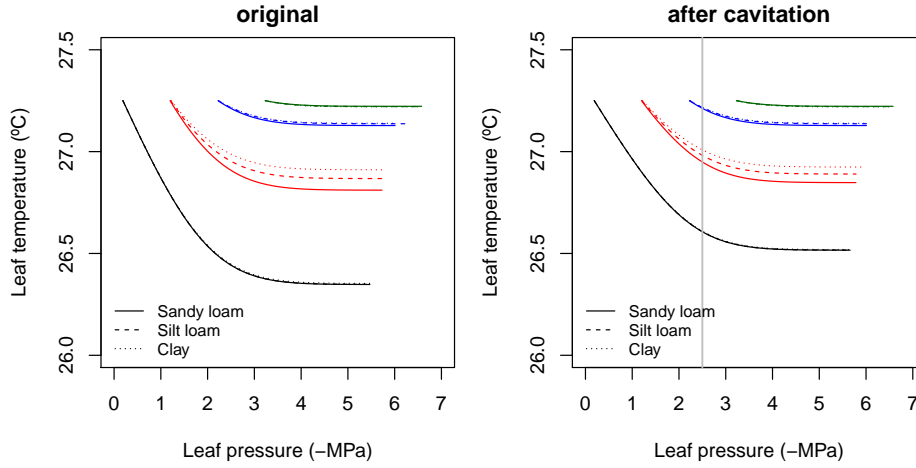
Thus, transpiration decreases leaf temperature (whereas radiation increases it and wind speed makes it more similar to air temperature). Vapor pressure deficit in the leaf (VPD_{leaf}, in kPa) is calculated as:

$$VPD_{leaf} = VP(T_{leaf}) - vp_{day} \tag{12.5}$$

Where vp_{day} is the average daily vapor pressure and $VP(T)$ is a function giving the saturated vapor pressure for temperature T. Let us assume the following values of relative humidity, yielding an average vp_{day}:

```
RHmin = 60
RHmax = 75
vpa = utils_averageDailyVP(Tmin, Tmax, RHmin, RHmax)
vpa
```

[1] 1.912181

the application of the above equation to the $T_{leaf}(\Psi_{leaf})$ curves yields the following $VPD_{leaf}(\Psi_{leaf})$ curves:
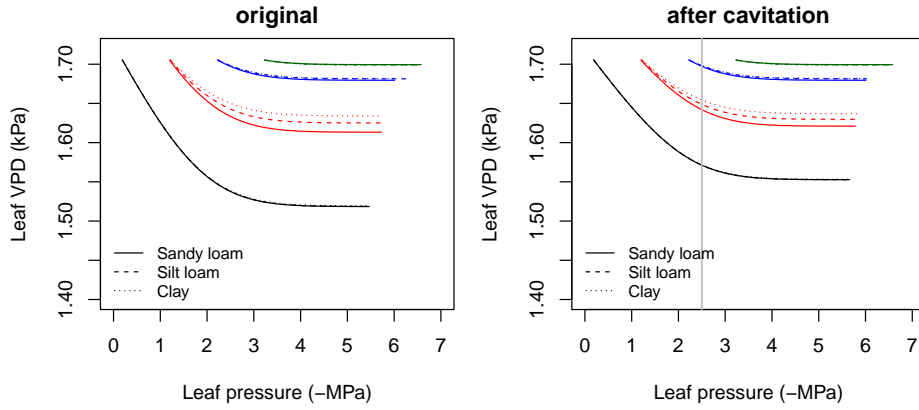
Since leaf saturated VP decreases when leaf temperature decreases, transpiration decreases leaf VPD as a result of decreasing leaf temperature.

12.1.3 Leaf conductance to water vapor

Leaf conductance to water vapor (g_{sw}; in $mol H_2O \cdot s^{-1} \cdot m^{-2}$) and to carbon dioxide (g_{sc}; in mol $CO_2 \cdot s^{-1} \cdot m^{-2}$) are obtained for each value of E (in $mol \cdot s^{-1} \cdot m^{-2}$) and VPD_{leaf} using:

$$g_{sw} = E \cdot \frac{P_{atm}}{VPD_{leaf}} \tag{12.6}$$

$$g_{sc} = g_{sw}/1.6 \tag{12.7}$$

the application of the equation for g_{sw} to the $VPD_{leaf}(\Psi_{leaf})$ curves yields the following $g_{sw}(\Psi_{leaf})$ curves:
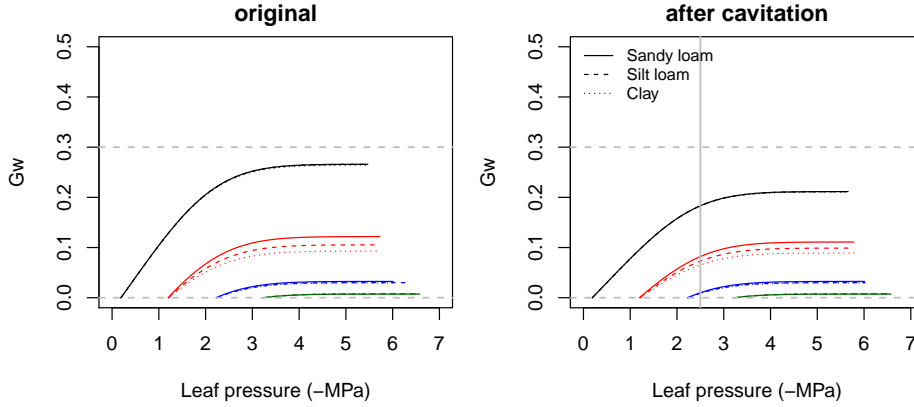
Hence, larger values of transpiration require larger values of leaf water vapour conductance. In the previous figure we have indicated the thresholds of g_{swmin} and g_{swmax}, the species-specific minimum and maximum water vapour conductances (i.e. conductances when stomata are fully closed and fully open, respectively; see parameters `Gwmin` and `Gwmax` in `SpParamsMED`).

```
Gmin = 0.0045;
Gmax = 0.3
```

g_{sw} cannot exceed g_{swmax} so that some flow rates may not be possible (see stomatal regulation below). However, g_{swmax} should quickly become non-limiting as soil dries (i.e. reducing E) or VPD_{leaf} increases (Sperry et al., 2016a). Minimum stomatal conductance is also used in **medfate** when building the supply function, as it specifies the minimum flow rates that will occur for completely-closed stomata, i.e. the minimum flow from which supply function is build.

12.1.4 Leaf photosynthesis

Rubisco-limited photosynthesis rate A_c (in $\mu mol CO_2 \cdot s^{-1} \cdot m^{-2}$) is modelled using (Collatz et al., 1991; Medlyn et al., 2002):

$$A_c = \frac{V_{max} \cdot (C_i - \Gamma*)}{C_i + K_c \cdot (1 + O_a/K_o)} \qquad (12.8)$$

where V_{max} is Rubisco's maximum carboxylation rate (in $\mu mol CO_2 \cdot s^{-1} \cdot m^{-2}$), C_i is the internal carbon dioxide concentration (in $\mu mol \cdot mol^{-1}$), $\Gamma*$ is the compensation point (in $\mu mol \cdot mol^{-1}$), K_c (in $\mu mol \cdot mol^{-1}$) and K_o (in $mmol \cdot mol^{-1}$) are Michaelis-Menten constants for carboxylation and oxygenation, respectively, and O_a is the atmospheric oxygen concentration (i.e. 209 $mmol \cdot mol^{-1}$). $\Gamma*$, K_c and K_o depend on leaf temperature (T_{leaf}, in Celsius) (Bernacchi et al., 2001):

$$\Gamma* \quad = \quad 42.75 \cdot e^{\frac{37830 \cdot (T_{leaf} - 25)}{298 \cdot R \cdot (T_{leaf} - 273)}} \tag{12.9}$$

$$K_c \quad = \quad 404.9 \cdot e^{\frac{79430 \cdot (T_{leaf} - 25)}{298 \cdot R \cdot (T_{leaf} - 273)}} \tag{12.10}$$

$$K_o \quad = \quad 278.4 \cdot e^{\frac{36380 \cdot (T_{leaf} - 25)}{298 \cdot R \cdot (T_{leaf} - 273)}} \tag{12.11}$$

Electron transport-limited photosynthesis A_e (in $\mu mol CO_2 \cdot s^{-1} \cdot m^{-2}$) was obtained from Medlyn et al. (2002):

$$A_e \quad = \quad \frac{J}{4} \cdot \frac{C_i - \Gamma*}{C_i + 2 \cdot \Gamma*} \tag{12.12}$$

$$J \quad = \quad \frac{(\alpha \cdot Q + J_{max}) - \sqrt{(\alpha \cdot Q + J_{max})^2 - 4.0 \cdot c \cdot \alpha \cdot Q \cdot J_{max}}}{2 \cdot c} \tag{12.13}$$

where α is the quantum yield of electron transport (0.3 *molelectrons $\cdot$ molphotons^{-1}*), Q is the PAR photon flux density ($\mu mol photons \cdot m^{-2} \cdot s^{-1}$), which is calculated from leaf irradiance (I_{par}; in $W \cdot m^{-2}$):

$$Q = I_{par} \cdot 546 \cdot 0.836 \cdot 10^{-2} \tag{12.14}$$

J_{max} and J are the maximum and actual rate of electron transport (both in $\mu mol electrons \cdot m^{-2} \cdot s^{-1}$) and $c = 0.9$ defines the curvature of the light-response curve. The gross assimilation rate A at a given C_i is the minimum of A_e and A_c. To obtain a smooth A-vs-C_i curve we used (Collatz et al., 1991):

$$A = \frac{(A_c + A_e) - \sqrt{(A_c + A_e)^2 - 4.0 \cdot c' \cdot A_e \cdot A_c}}{2 \cdot c'} \tag{12.15}$$

where $c' = 0.98$ is a curvature factor. The temperature dependence of J_{max} and V_{max} relative to 25ºC was modelled using Leuning (2002) (his eq. 1 with parameters from his Table 2). The internal CO_2 concentration, C_i, needs to be known to calculate A using the previous equations. Sperry et al. (2016b) use a second equation for A which uses g_{cs}:

$$A = g_{sc} \cdot (C_{atm} - C_i) \tag{12.16}$$

where C_{atm} is the atmospheric CO_2 concentration (in $\mu mol \cdot mol^{-1}$; see parameter `Catm` in function `defaultControl()`). Combining the two equations for A and finding the root of the resulting equation using Newton-Raphson method allows determining C_i and therefore A. Thus, after defining PAR photon flux density, atmosphere CO_2 concentration and maximum rate parameters:

```
Q = 2000
Catm = 386
Vmax298 = 100
Jmax298 = 1.67*Vmax298
```

one can obtain the following $A(\Psi_{leaf})$ curves from $T_{leaf}(\Psi_{leaf})$ and $g_{sc}(\Psi_{leaf})$:
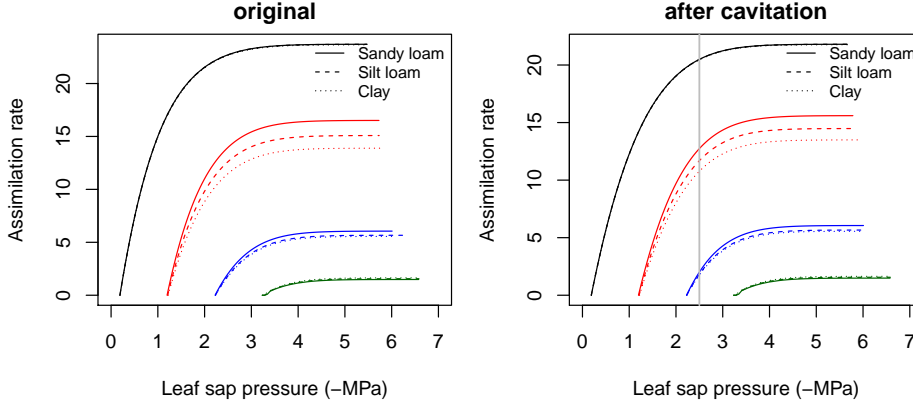
Finally, leaf net photosynthesis (i.e. accounting for autotrophic respiration) is calculated as:

$$A_n = A - 0.015 \cdot V_{max} \tag{12.17}$$

12.2 Crown photosynthesis

In the previous subsection we calculated photosynthesis at the leaf level. However, the function $A(\Psi_{leaf})$ can be calculated for a whole crown. Essentially we need to repeat the calculations of leaf temperature, leaf VPD, leaf gas conductance and photosynthesis for every leaf to be considered in the crown. Gross and net photosynthesis values can be then aggregated across the crown for each value of Ψ_{leaf}, so that the function $A(\Psi_{leaf})$ is obtained. Here we will consider a crown of one species divided into 10 layers, with constant leaf density:

```
LAI = 2
nlayer = 10
LAIlayerlive = matrix(rep(LAI/nlayer,nlayer),nlayer,1)
LAIlayermax = matrix(rep(LAI/nlayer,nlayer),nlayer,1)
LAIlayerdead = matrix(0,nlayer,1)
kb = 0.8
kd_PAR = 0.5
kd_SWR = kd_PAR/1.35
alpha_PAR = 0.9
```

```
gamma_PAR = 0.04
gamma_SWR = 0.05
alpha_SWR = 0.7
```

Many aspects may vary across the crown, including environmental conditions (such as direct/diffuse light or wind speed) and photosynthesis parameters (e.g. `Vmax298`). The previous crown definition and light parameters lead to a percentage of the above-canopy irradiance reaching each layer (Anten and Bastiaans, 2016). Furthermore, it is generally accepted that sunlit and shade leaves need to be treated separately (De Pury and Farquhar, 1997).Extinction of direct radiation also defines the proportion of leaves of each layer that are affected by direct light beams (i.e. the proportion of sunlit leaves).
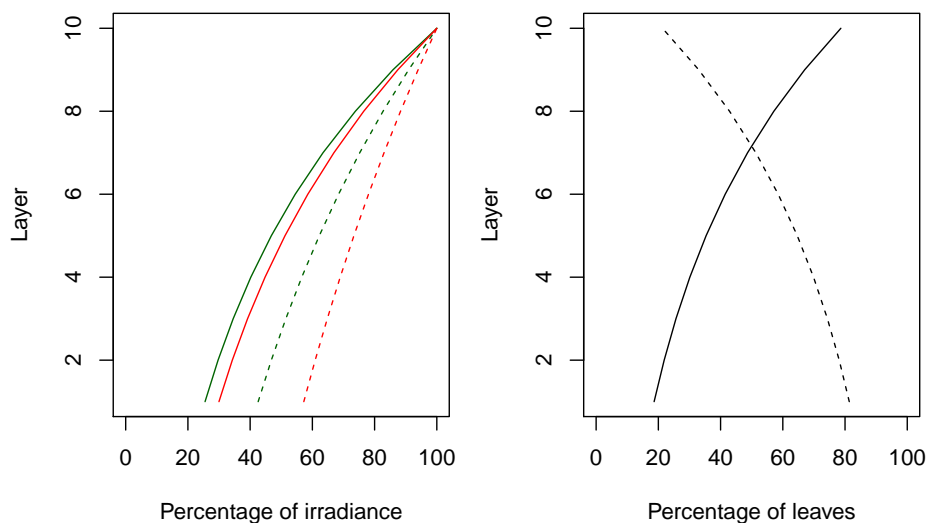
For simplicity, here we will assume constant windspeed in all layers:

```
ulayer = rep(2, 10)
```

Regarding incoming light, we assume the following direct and diffuse irradiance at the top of the canopy:

```
solarElevation = 0.67
SWR_direct = 1100
SWR_diffuse = 300
PAR_direct = 550
PAR_diffuse = 150
```

Solar elevation is the angle between the sun and the horizon (i.e. the complement of the zenith angle). Under these conditions, the amount of shortwave and PAR radiation absorbed per unit of leaf area at each canopy layer is (Anten and Bastiaans, 2016):
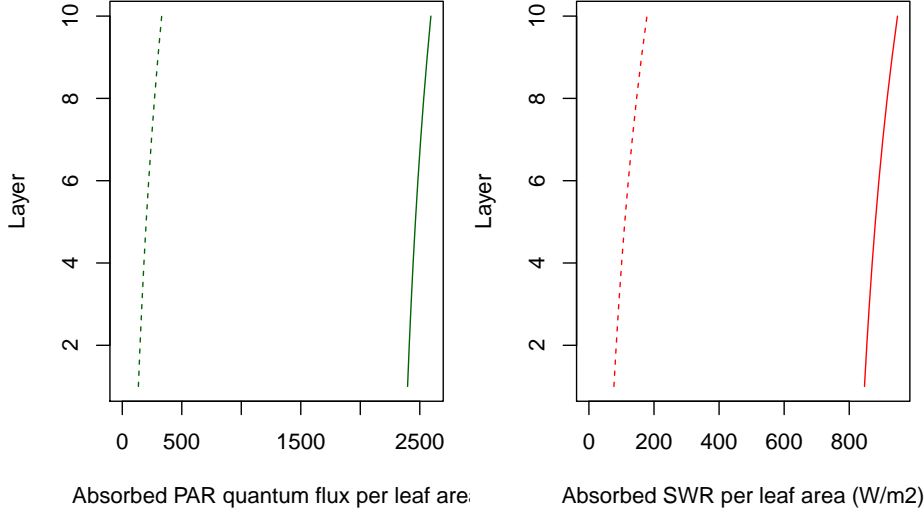
Following De Pury and Farquhar (1997), we further assume that maximum assimilation rates are highest for leaves at the top of the canopy and there is a exponential decrease from there towards the bottom, where maximum rates are 50% of those at the top:

$$V_{max,298}(L_i) = V_{max,298} \cdot exp(-0.713 \cdot L_i/LAIc) \qquad (12.18)$$

where L_i is the cumulative LAI value at a given canopy layer i and $LAIc$ is the canopy LAI.

Multilayer canopy models allow evaluating leaf conditions, stomatal conductance and photosynthesis for different points of the canopy. However, this comes at high computational cost. While big-leaf canopy models are known to be unaccurate under some situations, sun-shade canopy models (De Pury and Farquhar, 1997) provide estimates that are close to multiple layer models (Hikosaka et al., 2016). Sun-shade models involve: (a) aggregating the leaf area of sunlit/shade leaves across layers; (b) aggregating the light absorbed by leaves of each kind across layers; and (c) aggregating maximum assimilation rates across layers, again separating sunlit and shade leaves. One then calls the photosynthesis model twice (i.e. once for shade leaves and once for sunlit leaves), using the aggregated maximum assimilation rates. Separating the two kinds of leaves acknowledges that they operate at different parts of the light-saturation curve. The following figure provides the canopy photosynthesis functions obtained, under different situations, using a full 10-layer canopy description (top), a sunshade canopy model (center) or a big-leaf model (bottom). These were generated using functions `photo_multilayerPhotosynthesisFunction()`, `photo_sunshadePhotosynthesisFunction()` and `photo_leafPhotosynthesisFunction()`, respectively. Note the coincidence between the multi-layer and the sun-shade

models.
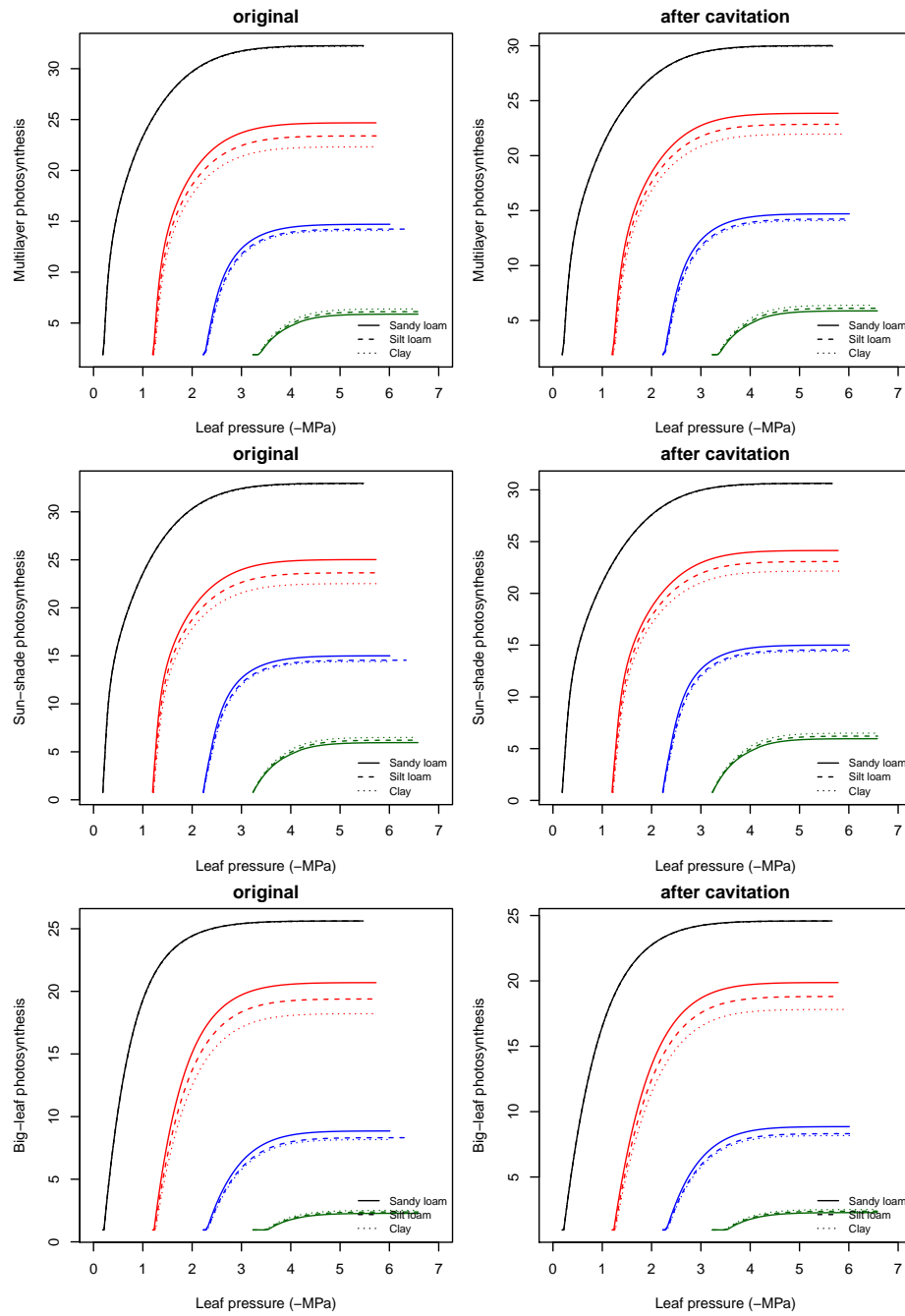
12.3 Stomatal regulation

Sperry et al. (2016a) presented a profit maximization approach where hydraulic costs of opening the stomata are compared against photosynthetic gain. Details of their approach, and two suggested variants, a given in the next two subsections. The final subsection explains how to scale stomatal regulation (and hence, transpiration and photosynthesis) from leaf to plant.

12.3.1 Cost and gain functions

The hydraulic supply function is used to derive a transpirational *cost function* $\theta_1(\Psi_{leaf})$ that reflects the increasing damage from cavitation and the greater difficulty of moving water along the continuum (Sperry et al., 2016b):

$$\theta_1(\Psi_{leaf}) = \frac{k_{c,max} - k_c(\Psi_{leaf})}{k_{c,max} - k_{crit}} \tag{12.19}$$

where $k_c(\Psi_{leaf}) = dE/d\Psi(\Psi_{leaf})$ is the slope of the supply function, $k_{c,max} = dE/d\Psi(\Psi_{soil})$ and $k_{crit} = dE/d\Psi(\Psi_{crit})$ is the slope of the supply function at $E = E_{crit}$ the critical flow beyond which hydraulic failure occurs.

Alternatively, we considered a second cost function ($\theta_2(\Psi_{leaf})$) using the vulnerability curve of the leaf:

$$\theta_2(\Psi_{leaf}) = \frac{k_{l,max} - k_l(\Psi_{leaf})}{k_{l,max} - k_{l,min}} \tag{12.20}$$

$$\tag{12.21}$$

where k_l is the leaf conductance function; and $k_{l,min}$ and $k_{l,max}$ are the minimum and maximum leaf conductance values found in the supply function. Using the leaf vulnerability curve for the cost function is grounded on the fact that stomatal regulation occurs at leaves, so that instantaneous regulation should respond to the loss of hydraulic conductance at this point, independently of what happens to the rest of the continuum. Hormonal signals from root to leaf are assumed to regulate stomatal aperture at longer time scales. Obviously, θ_2 is the same before irreversible cavitation. The difference between them may be interpreted as the following. θ_2 strictly follows the potential at the leaf level (and hence could be related to a loss of turgor).

The type of cost function can be specified by the user by setting parameter `hydraulicCostFunction` (see function `defaultControl()`). The following figures illustrate the θ_1 and θ_2 curves corresponding to the supply functions:
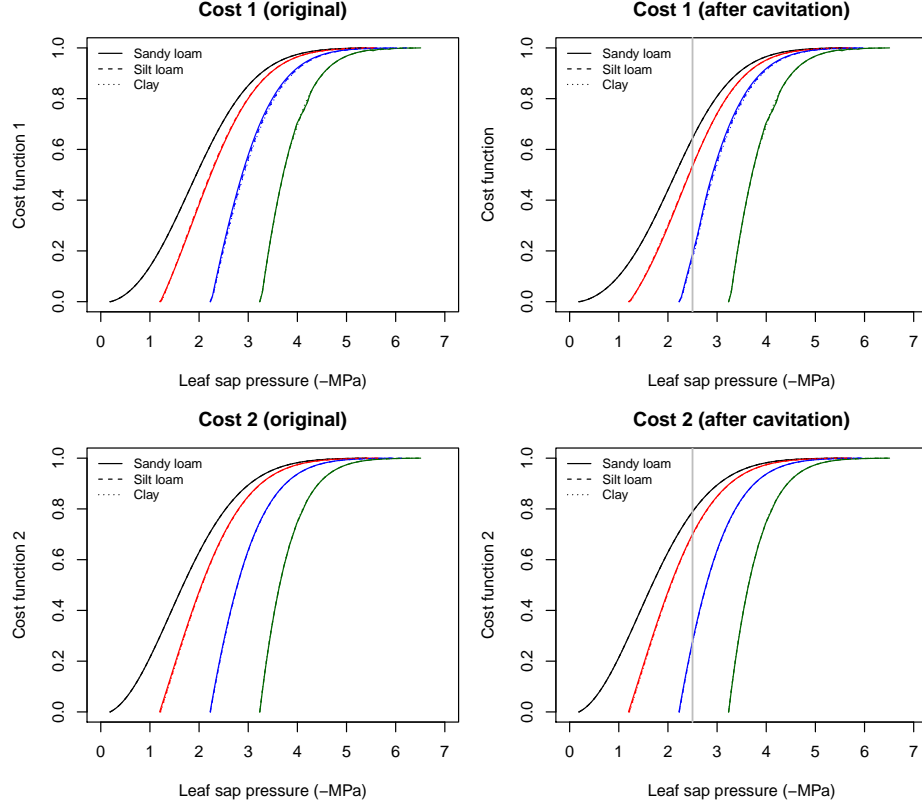
The normalized photosynthetic *gain function* $\beta(\Psi_{leaf})$ reflects the actual assimilation rate with respect to the maximum:

$$\beta(\Psi_{leaf}) = \frac{A(\Psi_{leaf})}{A_{max}} \tag{12.22}$$

where A_{max} is the instantaneous maximum assimilation rate estimated over the full Ψ_{leaf} range. The following figures illustrate the $\theta(\Psi_{leaf})$ and $\beta(\Psi_{leaf})$ curves corresponding to the supply and assimilation functions:

Gain (original)   **Gain (after cavitation)**
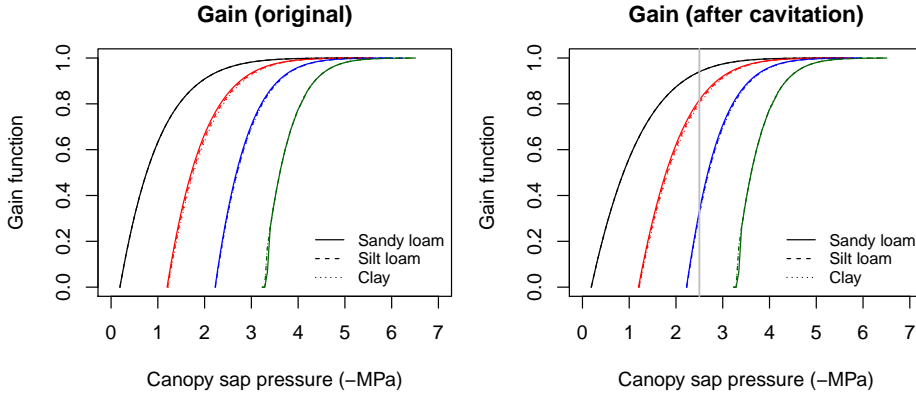
12.3.2 Profit maximization at the leaf level

According to Sperry et al. (2016a), stomatal regulation can be effectively estimated by determining the maximum of the *profit function* ($Profit(\Psi_{leaf})$), for which we consider three alternatives corresponding to the two cost functions:

$$Profit_1(\Psi_{leaf}) = \beta(\Psi_{leaf}) - \theta_1(\Psi_{leaf}) \tag{12.23}$$
$$Profit_2(\Psi_{leaf}) = \beta(\Psi_{leaf}) - \theta_2(\Psi_{leaf}) \tag{12.24}$$
$$\tag{12.25}$$

Once Ψ_{leaf} that maximizes profit is determined, the values of the remaining variables are also determined. At this point, it may happen that $g_{sw}(\Psi_{leaf})$ is lower than the minimum (i.e. cuticular) water vapor conductance (g_{swmin}) or larger than the maximum water vapor conductance (g_{swmax}). These thresholds need to be taken into account when determining the maximum of the profit function. The following figures illustrate the $Profit_1(\Psi_{leaf})$ and $Profit_2(\Psi_{leaf})$ curves of corresponding to the previous cost and gain curves: \begin{center}
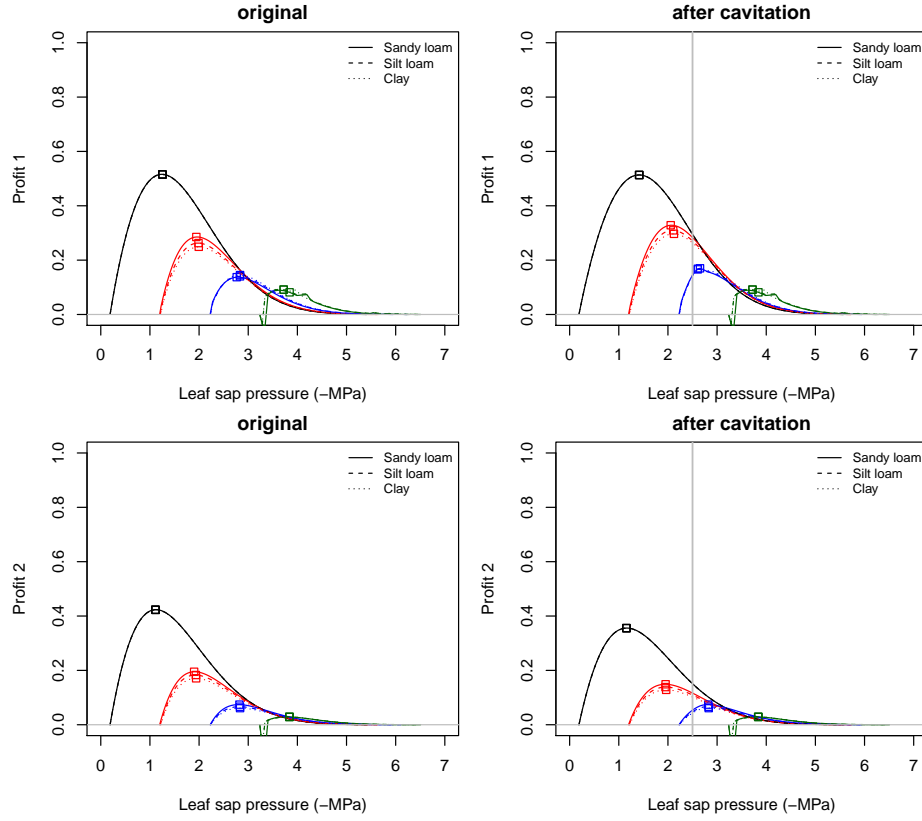
Squares in the previous figures indicate the maximum profit points in each situation. In the case of non-cavitated system (left panels), the drier the soil, the closer is the maximum profit Ψ_{leaf} to soil water potential as one would expect intuitively. This occurs for all three profit functions. Unlike θ_1 which is different for each soil texture (and soil potential), θ_2 is the same for all soil textures. As a result, the regulation points do not differ much among textures in $Profit_2$ and $Profit_3$ because the only difference is in the gain function. For a system with xylem cavitation (right panel), the maximum $Profit_1$ curves behave strangely. In particular may get a more negative value for Ψ_{canopy} for wet soils than for dry soils. This effect does not occur when using $Profit_2$. $Profit_2$ brings plant water potentials to more negative values after cavitation. Although cavitation did not change the θ_2 function, the supply function is flatter and this affects the gain function, making it increase less steeply with lower potentials.

Differences between profit functions can be more easily seen when plotting the change from original (uncavitated) regulation to the cavitated one, in terms of both canopy sap pressure and flow rate:
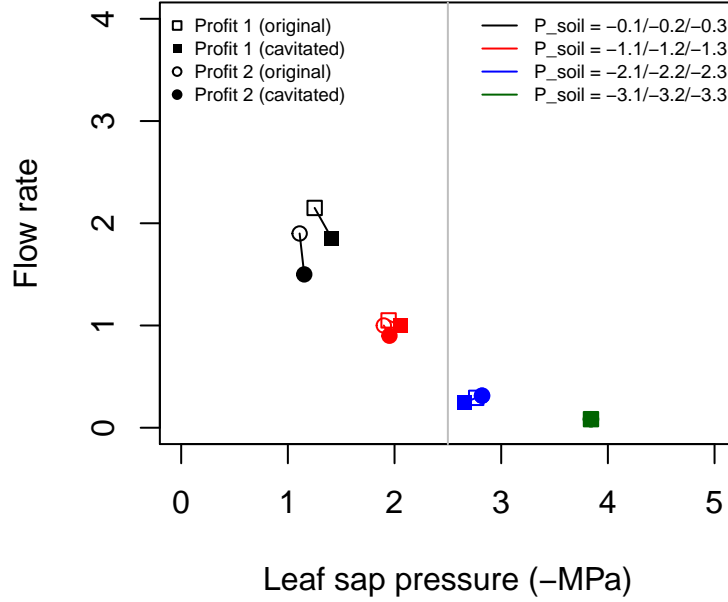
In $Profit_1$ irreversible cavitation often brings, after soil rewetting, less conservative stomatal regulation that enables higher flow rates. This does not seem to happen in $Profit_2$, where despite irreversible cavitation leads to more negative water potentials, predicted flow rates after rewetting are not above those predicted before cavitation.

12.3.3 Scaling to the plant level

So far, we have considered stomatal regulation by at the leaf level only. At the plant level, the gain function could be build from the crown photosynthesis function $A(\Psi_{leaf})$ that we defined in subsection 'Crown photosynthesis'. However, using the crown photosynthesis function would imply the assumption that the same stomatal aperture occurs in all leaves of the crown, independently of whether they are in shade or sunlit. A more realistic approach is to determine stomatal regulation by profit maximization for sunlit and shade leaves separately; and then determining the average photosynthesis and flow rate from the leaf area of each leaf type. The gain function and profit maximization calculations conducted for each leaf type yield instantaneous water potentials Ψ_{sunlit} and Ψ_{shade}. They also yield flow values E_{shade} and E_{sunlit}, in $mmol H_2O \cdot s^{-1} \cdot m^{-2}$ of leaf area unit. The average flow rate in $mmol H_2O \cdot s^{-1} \cdot m^{-2}$ per leaf area unit at the plant level is the weighed average:

$$E_{plant} = \frac{E_{sunlit} \cdot LAI_{sunlit} + E_{shade} \cdot LAI_{shade}}{LAI_{sunlit} + LAI_{shade}} \qquad (12.26)$$

where LAI_{sunlit} and LAI_{shade} are the cohorts LAI values for sunlit and shade leaves, respectively. Net photosynthesis per leaf area of sunlit and shade leaves (i.e. $A_{n,sunlit}$ and $A_{n,shade}$) is aggregated similarly:

$$A_{n,plant} = \frac{A_{n,sunlit} \cdot LAI_{sunlit} + A_{n,shade} \cdot LAI_{shade}}{LAI_{sunlit} + LAI_{shade}} \qquad (12.27)$$

Profit maximization calculations for shade and sunlit leaves imply different amount of water extracted from the soil layers and different plant water potentials. To overcome this issue, we must use the hydraulic supply function to find the extraction flows from soil layers, the water potential at the root crown and the 'average' water potential of the crown all corresponding to the average flow E_{plant}.

Chapter 13

Transpiration and photosynthesis under Sperry's model

The model determines transpiration and photosynthesis for each plant cohort separately as follows. First, it updates the hydraulic supply function depending on plant hydraulic characteristics and soil moisture status. Then, transpiration of the plant cohort is estimated for each of them following the framework of Sperry et al. (2016a), who suggest estimating stomatal conductance from the instantaneous maximization of profit, defined as the difference between photosynthesis gain and hydraulic cost (both normalized for comparability). Since the continuum representation implies several soil layers in parallel but joining at the root crown, the hydraulic submodel yields instantaneous water flow and carbon assimilation rates from (or to) each soil layer. Finally, the instantaneous transpiration and assimilation rates of each time step are scaled to the duration of the time step and to the leaf area of the plant cohort. The following provides details for these processes (see further details in Appendices).

13.1 Water supply function

The supply-loss theory of plant hydraulics of Sperry and Love (2015) uses the physics of flow through soil and xylem to quantify how canopy water supply declines with drought and ceases with hydraulic failure. The theory can be applied to different networks representing the soil-plant continuum, but in our case the continuum is represented using a network of $(N \times 2 + 2)$ resistance elements, with soil being represented in N different layers. For each soil layer there is a rhizosphere element in series with a root xylem element. The N

different layers are in parallel up to the root crown. From there there is a stem xylem element and a final leaf element.

The *supply function* describes the rate of water supply (i.e. flow) for transpiration (E) as a function of the pressure drop between the soil and the leaf, and incorporates both soil, xylem and leaf hydraulic constrains (Sperry et al., 1998; Sperry and Love, 2015; Sperry et al., 2016b). Assuming that maximum conductance values are in mmol $H_2O \cdot s^{-1} \cdot m^{-2}$ per leaf area unit, transpiration rate ($E(\Psi_{leaf})$; in mmol $H_2O \cdot s^{-1} \cdot m^{-2}$ per leaf area unit) is a function of leaf water potential (Ψ_{leaf}; in MPa). The supply function for the whole continuum contains much information. The Ψ intercept at $E = 0$ represents the predawn canopy sap pressure which integrates the rooted soil moisture profile. As E increments from zero, the disproportionately greater drop in Ψ_{leaf} results from the loss of conductance. As the soil dries the differences in flow due to soil texture become more apparent. More details of the calculation of the supply function are given in Appendices.

13.2   Leaf energy balance

Leaf temperature (T_{leaf}; in Celsius) can be calculated for any given flow rate $E(\Psi_{leaf})$ using (Campbell and Norman, 1998):

$$T_{leaf}(\Psi_{leaf}) = T_{can} + \frac{I_{abs} - \epsilon \cdot \sigma \cdot (T_{can} + 273.15)^4 - \lambda_v \cdot E(\Psi_{leaf})}{C_p \cdot (g_r + g_{Ha})} \quad (13.1)$$

where I_{abs} (in $W \cdot m^{-2}$) is the instantaneous shortwave and longwave radiation absorbed per leaf area unit, $E(\Psi_{leaf})$ is the flow (converted to $mol \cdot s^{-1} \cdot m^{-2}$ per two-sided leaf area basis), ϵ is longwave radiation emissivity (0.97), σ is the Stephan-Boltzman constant, T_{can} is the canopy air temperature (in ºC; see 'Complex model: Radiation and energy balance'), $C_p = 29.3\ J \cdot mol^{-1} \cdot C^{-1}$ is the specific heat capacity of dry air at constant pressure and λ_v is the latent heat of vaporization (in $J \cdot mol^{-1}$):

$$\lambda_v = (2.5023 \cdot 10^6 - (2430.54 \cdot T_{can})) \cdot 0.018 \quad (13.2)$$

Finally, g_r and g_{Ha} are the radiative and heat conductance values (in $mol \cdot m^{-2} \cdot s^{-1}$), respectively (Campbell and Norman 1998):

$$g_r = \frac{4 \cdot \epsilon \cdot \sigma \cdot (T_{can} + 273.15)^3}{C_p} \quad (13.3)$$

$$g_{Ha} = 0.189 \cdot (u/d)^{0.5} \quad (13.4)$$

where u is wind speed (in $m\mathring{u}s^{-1}$), taken as the wind speed at mid-crown height, and d is 0.72 times the leaf width (species parameter `LeafWidth` in cm).

13.3 Leaf photosynthesis functions

Each water supply value implies an energy balance at the leaf level and a degree of stomatal openness, which ultimately leads to a particular value of leaf photosynthesis. At this point, the model has not decided the amount of water transpired. Therefore, it determines curves depending on leaf water potential for several parameters, as done for $E(\Psi_{leaf})$. More specifically, for each Ψ_{leaf} value, the model calculates the corresponding leaf temperature (T_{leaf}; in ºC), leaf-to-air vapor pressure deficit (VPD_{leaf}; in kPa), leaf water vapor conductance (g_{sw}; in $molH_2O\mathring{u}s^{-1}\mathring{u}m^{-2}$) and, finally the leaf gross and net (i.e. after accounting for autotrophic respiration) photosynthesis assimilation rates (A_g and A_n; both in $\mu molCO_2\mathring{u}s^{-1}\mathring{u}m^{-2}$). More details of the calculation of these functions are given in Appendices.

Since the model deals with canopies and not single leaves, different parts of the crowns of plant cohorts may be in different canopy positions, which leads to differences in radiation and leaf energy balance. Moreover radiation, energy balance and photosynthesis of leaves vary through the day. Therefore, calculating photosynthesis at the canopy level requires dividing the canopy into c layers, while differentiating between **sunlit** and **shade** leaves. Photosynthesis is calculated by separately for sunlit/shade leaves (De Pury and Farquhar 1997). For each time step, the leaf temperature, leaf VPD and leaf water vapor conductance functions are determined separately for the different leaves.

13.4 Stomatal regulation

Plants must open their stomata to acquire CO_2 and perform photosynthesis, but doing so promotes water loss. This trade-off has resulted in a tight coordination between capacity to supply and transpire water (hydraulic conductance and diffusive conductance to water vapor) and the maximum capacity for photosynthesis (carboxylation rate and electron-transport rate). For modelling purposes, this carbon-for-water trade-off means that hydraulics, stomatal conductance, transpiration and photosynthesis need to be estimated simultaneously. Here we adopt the framework of Sperry et al. (2016a), who suggest estimating stomatal conductance from the instantaneous maximization of profit, defined as the difference between photosynthesis gain and hydraulic cost (both normalized for comparability).

Stomatal regulation and plant transpiration are determined for each time step separately. The model transforms the slope of the hydraulic supply function

into a **cost function** and the cohort's gross photosynthesis function into a **gain function**. Then, it finds the Ψ_{leaf} that maximizes the difference between gain and cost. This simultaneously determines E and A_n at the plant cohort level (and also T_{leaf}, VPD_{leaf}, g_{sw} and A_n for each sunlit/shade leaf in the canopy). The details of all these calculations can be found in Appendices.

While the cost function is the same for the whole day, the gain function and profit maximization calculations are conducted for each of the time steps, yielding instantaneous flow values $E_{t,s}$ for each soil layer s, in mmol $H_2O \cdot s^{-1} \cdot m^{-2}$ of leaf area unit and instantaneous net assimilation values $A_{n,t}$ in μmol $C \cdot s^{-1} \cdot m^{-2}$ of ground area (i.e. at the cohort level). To obtain daily values of transpiration at the cohort level the instantaneous flow rates $E_{t,s}$ need to be scaled to $E_{step,s}$ using:

$$E_{step,s} = E_{t,s} \cdot 10^{-3} \cdot 0.01802 \cdot LAI_i^\phi \cdot \Delta t \tag{13.5}$$

where 0.01802 is the molar weight (in kg = L = mm) of water, LAI_i^ϕ is the leaf area index of plant cohort i and $\Delta t = \tau_{day}/n_t$, being n_t the number of time steps. The flow rates $E_{step,s}$ of all steps are added to yield E_s (in mm $H_2O \cdot day^{-1}$):

$$E_s = \sum_{n=1}^{n_t} E_{step,s} \tag{13.6}$$

and substracted from the water content of the corresponding soil layer. Daily values of net carbon assimilation for plant cohorts are obtained similarly. The instantaneous rates $A_{n,t}$ are scaled to $A_{n,step}$ using:

$$A_{n,step} = A_{n,t} \cdot 10^{-6} \cdot 12.01017 \cdot \Delta t \tag{13.7}$$

where 12.01017 is the molar weight of carbon (in g). $A_{n,step}$ values of all steps are added to obtain A_n, the daily net assimilation at the cohort level (in g $C \cdot m^{-2} \cdot day^{-1}$):

$$A_{n,step} = \sum_{n=1}^{n_t} A_{n,step} \tag{13.8}$$

13.5   Plant drought stress and water potentials

Because the model determines optimum transpiration for each time step, this leads to a daily sequence of leaf water potential ($\Psi_{leaf,t}$) and root crown water potential ($\Psi_{rootcrown,t}$) values. The model chooses as the leaf water potential

of the day for cohort i ($\Psi_{leaf,i}$) the minimum of $\Psi_{leaf,t}$ values. Analogously, the model chooses as the root crown water potential of the day for cohort i ($\Psi_{rootcrown,i}$) the minimum of $\Psi_{rootcrown,t}$ values. They represent water potential values that would occur at mid-day. Unlike under the simple transpiration mode, here there is no need to average water potentials under the Sperry transpiration mode, because the differences in potential of soil layers are already integrated in the hydraulic supply function.

In order to have an estimate of daily drought stress for the plant cohort, the model uses the stem vulnerability curve of the plant to find the conductance relative to maximum stem conductance and turns it into its complement:

$$DDS_i = \phi_i \cdot \left(1.0 - \frac{k_{stem,i}(\Psi_{rootcrown,i})}{k_{\max stem,i}}\right) = \phi_i \cdot \left(1.0 - e^{-(\Psi_{rootcrown,i}/d_{stem})^{c_{stem}}}\right)$$
(13.9)

where ϕ_i is the leaf phenological status. Note the use of $\Psi_{rootcrown,i}$ (and not $\Psi_{leaf,i}$) to determine drought stress index. Thus the model tracks the degree of conductance decrease at the beginning of the stem as a measure of drought stress. This choice makes daily drought stress values of the Simple and Complex transpiration modes more comparable (because leaf mid-day water potentials are usually much more negative than soil water potentials) and is a sensible choice if one wants to run the model in irreversible cavitation mode (see below).

13.6 Irreversible cavitation and hydraulic disconnection

Like with the 'Granier' transpiration mode, the water balance model with 'Sperry' transpiration mode is normally run assuming that although soil drought may reduce transpiration, embolized xylem conduits are automatically refilled when soil moisture recovers. When setting `cavitationRefill = FALSE` the model tracks the maximum value of drought stress as before:

$$P_{embolized,i} = \max\{P_{embolized,i}, DDS_i\} \qquad (13.10)$$

However, the way that previous cavitation levels are taken into account differs from the 'Simple' transpiration mode. In this mode, the stem xylem vulnerability curve is modified by specifying that the maximum conductance value is reduced and set to $k_{stem,i} \cdot (1.0 - P_{embolized,i})$. This effectively causes the supply function to reach lower flow values for the same water potential drop (see details in Appendices).

When running the model using the 'Complex' transpiration mode plants may be allowed to disconnect from the soil when its potential becomes too negative.

Parameter $P_{rootdisc,i}$ can be used to specify the minimum relative conductance value that the plant will tolerate without disconnecting hydraulically from the soil (in normal simulations $P_{rootdisc,i} = 0$). Again, this affects the model in a way slightly different than when running the model in 'Simple' transpiration mode. Before building the supply function, the model checks if there are layers where the relative conductance of roots (i.e. $k_{root,i,s}(\Psi_s)/k_{\max root,i,s}$) is lower than $P_{rootdisc,i}$. Those layers where this happens are not considered in the calculation of the supply function and do not contribute to transpiration or to the determination of plant water potentials.

13.7   Transpiration and photosynthesis after soil disconnection

Considering water compartments allows tracking leaf and stem (i.e. plant) *dessication*, either when the plant is connected to the soil or when transpiration flow comes from the plant itself. In **medfate**, disconnection from a given soil layer occurs when its water potential is too low with respect to the root xylem vulnerability curve. The user can control this behaviour by specifying a p_{root} threshold for relative conductance, and the plant will be disconnected from a soil layer if $k_r(\Psi_{soil})/k_{r,max} < p_{root}$. An interesting situation arises when a plant is disconnected from all soil layers. In this case, the steady-state calculations cannot be used to determine flows, so one is forced to use a full discrete time approximation, with compartments and flows indicated in the figure below.

As before, each time step Δt is divided into m substeps and instantaneous lateral flows between symplastic and apoplastic compartments are calculated as before. In this case, however, one needs to calculate instantaneous flows between stem apoplastic compartments using:

$$F_{i,i+1} = k_s(\min(\Psi_{apo,i}, \Psi_{cav,i})) \cdot (\Psi_{apo,i} - \Psi_{apo,i+1}) \tag{13.11}$$

and between the last stem compartment and the leaf using:

$$F_{S,l} = k_l(\Psi_{apo,l}) \cdot (\Psi_{apo,S} - \Psi_{apo,l}) \tag{13.12}$$

The flow from the leaf to the atmosphere is dictated by the minimum stomatal conductance and the vapour pressure deficit. For each time substep all flows are calculated and water content of compartments is updated. Then the equations of relative water content are inversed to find the water potentials for the next time substep.

The instantaneous flow rate between symplastic and apoplastic compartments can be approximated using a lateral conductance k_{lat} and the difference in water potentials. For the leaf we have:
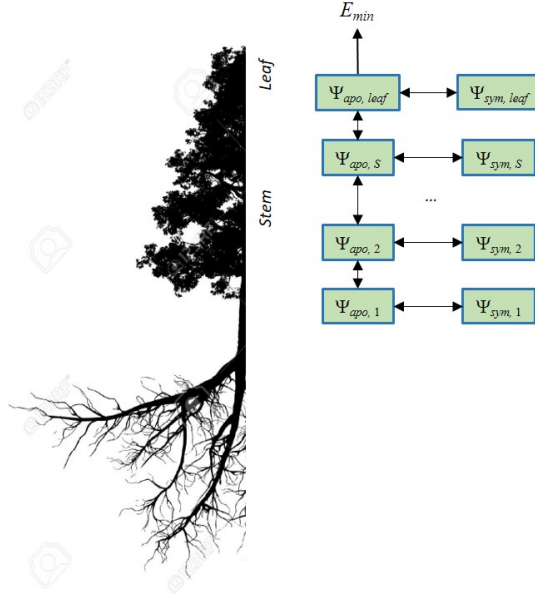
Figure 13.1: Schematic representation of hydraulics in a whole-plant network after disconnection from soil

$$F_{lat,l} = k_{lat} \cdot (\Psi_{sym,l} - \Psi_{apo,l}) \tag{13.13}$$

where $\Psi_{sym,l}$ is the water potential of the symplastic leaf compartment and $\Psi_{apo,l}$ is the water potential in the apoplastic leaf compartment. If $\Psi_{sym,l} > \Psi_l$ then the flow will be positive towards the leaf apoplasm and if $\Psi_{sym,l} < \Psi_l$ the flow will instead refill the leaf symplastic tissue. An analogous equation can be used to calculate the instantaneous lateral flow between symplastic and apoplastic compartments in any stem segment:

$$F_{lat,i} = k_{lat} \cdot (\Psi_{sym,i} - \Psi_{apo,i}) \tag{13.14}$$

Part IV

Forest growth modelling

Chapter 14

Forest growth model

14.1 Design principles

The physical structure of the stand is represented in one (vertical) dimension. Height (or depth) is the only dimension that matters (i.e. the coordinates of plants are not explicit). The model is cohort-based, meaning that similar plant individuals are represented using a single entity with average properties (e.g. tree height or diameter) and a density variable is used to scale from individual level to the cohort level. Processes are implemented either at the cohort-level (water balance and photosynthesis) or at the individual level (carbon balance and growth). The model has been designed to be executed on forest inventory plots, but it can be run on other kind of vegetation (e.g. shrublands or crops) provided vegetation is described using the appropriate variables (i.e. diameter and height for trees, percent cover and height for shrubs). The model tries to reproduce the physiological processes that modulate leaf area changes and plant growth rates. Nevertheless, since the model does not implement all processes that may affect growth (such as nutrient availability), maximum growth rates and maximum plant sizes are constrained from user inputs, to ensure that model can be more easily calibrated and validated with observations. Consequently, we believe the model is suited to study variations of plant growth derived from environmental conditions and competition for light and water.

Leaf area of each plant cohort is divided between live (wether in resistance buds or unfolded leaves) and dead (standing dead trees). Expanded leaf area corresponds to the portion of live leaf area that is unfolded at any given moment through the leaf phenological cycle. Leaf area density of individuals is considered constant across the crown. Sapwood area of individuals is another important state variable. The Pipe model (Shinozaki et al., 1964) is adopted to link increments of leaf area, sapwood area and fine root biomass. Ratios of leaf area to sapwood area (Huber value) can vary within species, due to environmen-

tal conditions (Mencuccini and Grace, 1995). The model assumes a constant, species-specific Huber value, but allows deviations from the pipe model caused by drought-related leaf area reductions.

Water fluxes, soil water balance and plant photosynthesis processes follow the design of the soil water balance model and this part of the model design will not be repeated here. Plant respiration is calculated at the individual level, by estimating the respiration of leaves, stem and fine root compartments. While fine root respiration is proportional to leaf respiration, and hence to expanded leaf area, stem respiration depends on plant size.

Growth is determined taking into account environmental limitations on both source (i.e. carbon assimilation) and sink (i.e. carbon investment on plant tissue expansion) (Fatichi et al., 2014; Guillemot et al., 2015; Körner, 2015). With respect to carbon availability for growth, the model offers three alternatives. In the first one, carbon available for growth is simply the daily difference between net photosynthesis and maintenance respiration (i.e. no carbon storage). The second alternatives involves a single (fast) carbon storage pool that allows decoupling assimilation from growth. Finally, the third alternative involves two carbon storage pools ('fast' and 'slow') with a transfer rate between them (Richardson et al., 2013; Dietze et al., 2014), which we assume to be regulated by the need to maintain, as much as possible, a minimum amount of carbon in the fast pool (i.e. for metabolic and osmotic purposes). In the second and third modes, maximum overall C storage capacity is proportional to plant size.

The LPG model (Sitch et al., 2003) applies different turnover rates for different tissues, but then tries to satisfy the pipe model (Shinozaki et al., 1964) by allocating C where it is more limiting. Instead, we assume that baseline leaf and fine root turnover rates are linearly related to conversion from sapwood to heartwood. Similarly to 3-PG (Landsberg and Waring, 1997) we assume that the turnover rate is smallest for young plants, and it increases up to a maximum value. The model assumes that plants cannot suffer from cavitation if the leaf water potential is large enough for growth to occur (i.e. if cell turgidity is large enough for cell elongation). Similarly, it also assumes that growth stops before cavitation starts during drought events. When sapwood area reduction occurs, this not only reduces leaf area, but also decreases the amount of fast C reserves available for future growth. Thus it is assumed that parts of the plant are effectively disconnected.

Tree structural variables are updated as in forest gap models (Lindner et al., 1997).

14.2   State variables

14.3   Process scheduling

Every day the growth model first updates the expanded leaf area of living plants according to the phenology of species and the day of the year. Then the model performs soil water balance, transpiration and photosynthesis calculations by calling the soil water balance submodel. After dealing with water fluxes and photosynthesis, the model determines the amount of respiratory biomass, the maximum storage value per individual and maintenance respiration at the individual level. The comparison between photosynthesis and respiration leads to an amount of carbon available for growth (if no carbon pools are considered) or a change in the amount of fast carbon storage pool (if one or two carbon pools are considered). After that, the model determines variations in sapwood area, dead leaf area and live leaf area, which can originate due to conversion from sapwood to heartwood, growth or drought-induced cavitation. If two carbon storage pools are considered, at the end of the day the model determines the direction and amount of carbon transfer between them. Once a year (or by the end of the simulated period) the model translates sapwood area growth into structural variables (i.e., plant height, tree DBH, tree crown ratio and shrub cover).

14.3.1   Water balance, plant transpiration and photosynthesis

The growth model calls the soil water balance model as a submodel to perform soil water balance and photosynthesis calculations. We only summarize the steps here. The submodel first increases soil moisture due to precipitation, accounting for canopy interception loss, surface runoff and deep drainage. To calculate water losses due to transpiration, the submodel acts differently depending on whether transpiration mode is set to 'Granier' or 'Sperry'. Generally speaking, though, the submodel determines stomatal conductance of each plant cohort according to the environmental conditions (i.e. light, leaf temperature, water vapor deficit and soil moisture) and this leads to an estimation of transpiration and net photosynthesis. The submodel then decreases water content due to bare soil evaporation, and plant transpiration, which completes the daily water balance.

Among other outputs, the soil water balance submodel provides values of leaf water potential Ψ_{leaf} (in MPa) and net photosynthesis calculated at the plant cohort level, A_n^{coh} (in $gC\,\mathring{u}m^{-2}\mathring{u}day^{-1}$). Ψ_{leaf} is used in the growth model to modulate drought effects on growth and leaf area losses (see below), whereas A_n is obviously needed to determine carbon balance and growth. Since carbon

balance is calculated at the individual level, A_n^{coh} needs to be scaled to net photosynthesis per individual (in $gC \cdot ind^{-1} \cdot day^{-1}$) using:

$$A_n^{ind} = 10000 \cdot A_n^{coh}/N \tag{14.1}$$

where N is the density of individuals per hectare.

14.4   Model input

14.4.1   Vegetation state variables and parameters

Vegetation in the stand is described using a set of plant cohorts, described in an object of class `growthInput`. This function assembles all parameters needed for the simulation of a given stand in a single list. Model parameters are grouped by category. Regarding physical aboveground description of the stand, each plant cohort is defined by its species identity (SP; with R name [`SP`]). In addition, each cohort needs to be defined regarding the following state variables:

- N [`N`]: The density of individuals (in $ind \cdot ha^{-1}$).
- DBH [`DBH`]: Tree diameter at breast height (in cm).
- $Cover$ [`Cover`]: Shrub percent cover (in %).
- H [`H`]: Total tree or shrub height (in cm).}
- CR [`CR`]: Crown ratio (i.e. the ratio between crown length and total height).}
- LAI^{live} [`LAI_live`]: Live leaf area index (one-side live leaf area of plants in the cohort per surface area of the stand) (in $m^2 \cdot m^{-2}$).}
- LAI^{ϕ} [`LAI_expanded`]: Expanded leaf area index (one-side expanded leaf area of plants in the cohort per surface area of the stand) (in $m^2 \cdot m^{-2}$).}
- LAI^{dead} [`LAI_dead`]: Dead leaf area index (one-side dead leaf area of plants in the cohort per surface area of the stand) (in $m^2 \cdot m^{-2}$).}
- $LAI^{predrought}$ [`LAI_predrought`]: Live leaf area index before the current drought started (one-side dead leaf area of plants in the cohort per surface area of the stand) (in $m^2 \cdot m^{-2}$).}
- SA [`SA`]: Area of functional sapwood per individual (in $cm^2 \cdot ind^{-1}$).}
- C_{fast} [`fastCstorage`]: Amount of C in the fast carbon storage pool (in g $C \cdot ind^{-1}$).}
- C_{slow} [`slowCstorage`]: Amount of C in the slow carbon storage pool (in g $C \cdot ind^{-1}$).}

Excepting SP (species identity) and N (density), the remaining aboveground state variables are modified during growth simulations. Belowground parameters are the following:

- Z [`Z`]: The rooting depth (in cm).}
- V [`V`]: A matrix with the proportion of fine roots in each soil layer.}

Additional belowground variables are included if 'transpirationMode = "Complex"}. These, and the parameters needed for water balance calculations are described in vignette '**Soil description and root system architecture**'.

The following physiological parameters are needed for growth calculations:

- *SLA* [`SLA`]: Specific leaf area (m$^2 \cdot$ kg^{-1}).
- *Hv* [`Al2As`]: Huber value. Leaf area to sapwood area ratio (in m$^2 \cdot$ m^{-2}).}
- W_{dens} [`WoodDens`]: Wood density (at 0% humidity) (in g $\cdot$ cm^{-3}).}
- W_C [`WoodC`]: Wood carbon content in relation to dry weight (in g $\cdot$ g^{-1}).}
- $C_{p,\max}$ [`Cstoragepmax`]: Maximum storage capacity, expressed as C per total respiratory C (in gC $\cdot$ gC^{-1}).
- $RGR_{\max}$ [`RGRmax`]: Maximum daily relative growth rate (in sapwood area basis) (in cm$^2 \cdot$ cm^{-2}).

Another set of parameters is needed to transform changes in sapwood area and leaf area to changes in the structural variables such as tree height, tree crown ratio or shrub cover:

- $H_{\max}$ [`Hmax`]: Maximum plant height (in cm).
- $f_{HD,\min}$, $f_{HD,\max}$ [`fHDmin}`,fHDmax']: Minimum and maximum values of the height-diameter ratio (in cm $\cdot$ cm^{-1}).
- $Z_{\max}$ [`Zmax`]: Maximum rooting depth (in mm).
- a_{ash} [`Aash`]: Regression coefficient for the quadratic relationship between shrub height and shrub area.
- a_{bsh}, b_{bsh} [`Absh, Bbsh`]: Allometric coefficients relating crown phytovolume with dry weight of shrub individuals.
- *CR* [`cr`]: Ratio between crown length and total height (constant value for shrubs).
- $r_{6.35}$ [`r635`]: Ratio between the dry weight of leaves plus branches and the dry weight of leaves alone for branches of 6.35 mm of diameter.
- a_{cr}, b_{1cr}, b_{2cr}, b_{3cr}, c_{1cr}, c_{2cr} [`B1cr, B2cr, B3cr, C1cr, C2cr`]: Regression coefficients used to update the crown ratio of trees.
- a_{cw}, b_{cw} [`Acw, Bcw`]: Regression coefficients used to calculate the crown width of trees (as intermediary step to obtain the crown ratio).

14.4.2 Metereological input

Weather input data must include variables calculated at the **daily** scale. The variables required by function `growth()` depend on the transpiration mode, similarly to function `spwb()`. We recommend meteorological input to be generated using package **meteoland** (De Cáceres et al., 2018).

14.5 Model output

Chapter 15

Plant compartments, respiration and carbon balance

15.1 Biomass compartments

Biomass of leaves, sapwood and fine roots is needed in the model to estimate respiratory costs (and, if needed, the size of the C storage pools). Respiratory leaf biomass per individual (B_{leaf}; $gC\mathring{u}ind^{-1}$) is the result of dividing live expanded leaf area by SLA ($kgdry\mathring{u}m^{-2}$), the specific leaf area coefficient of the species, and multypling by a carbon conversion factor (0.3 $gC\mathring{u}gdry^{-1}$):

$$B_{leaf} = 0.3 \cdot 1000 \cdot LA^{\phi}/SLA \tag{15.1}$$

where $LA^{\phi} = 10000 \cdot LAI^{\phi}/N$ is the expanded leaf area per individual (in m^2) and factor 1000 is used to convert from kg to g. Hence, only expanded leaf area has respiratory cost (i.e. winter resistance buds do not) and counts for C storage purposes.

Respiratory sapwood biomass per individual (B_{stem}; $gC\mathring{u}ind^{-1}$) represents the sapwood biomass of stems (including trunks and branches) and coarse roots. It is defined as the product of sapwood area (SA; in cm^2) per individual times the sum of height (H; in cm) and rooting depth (Z; cm), transformed to carbon biomass using species-specific parameters of wood C density (W_{dens}; $gdry\mathring{u}cm^{-3}$) and carbon content (W_C; $gC\mathring{u}gdry^{-1}$):

$$B_{stem} = SA \cdot (H + Z) \cdot W_{dens} \cdot W_C \tag{15.2}$$

Finally, the biomass of fine roots per individual (B_{root}; g C $\cdot$ ind^{-1}) is simply assumed proportional to expanded leaf biomass per individual:

$$B_{root} = B_{leaf}/2.5 \tag{15.3}$$

where 2.5 is a ratio between leaf biomass and fine root biomass. Hence, fine-root maintenance respiration costs are also influenced by leaf-phenological status (Sitch et al., 2003).

15.2   Maximum capacity of C pools

If carbon pools are considered, their maximum capacity is updated at this point. If there is a single (fast) carbon pool, its maximum storage capacity per individual ($C_{fast,\max}$; $gC\mathring{u}ind^{-1}$) is defined proportional to the total living biomass (i.e., easily accessed C sources like sugars are assumed to be stored in all living parts of the plant):

$$C_{fast,\max} = C_{p,\max} \cdot (B_{leaf} + B_{stem} + B_{root}) \tag{15.4}$$

where $C_{p,\max}$ is the amount of C storage per plant respiratory C weight. If two carbon pools are considered, their maximum capacity is updated assuming that the fast pool corresponds to 5% of plant respiratory weight, and the slow pool corresponds to the remaining:

$$
\begin{aligned}
C_{fast,\max} &= 0.05 \cdot (B_{leaf} + B_{stem} + B_{root}) \tag{15.5}\\
C_{slow,\max} &= \max\left(C_{slow,\max}, (C_{p,\max} - 0.05) \cdot (B_{leaf} + B_{stem} + B_{root})\right) \tag{15.6}
\end{aligned}
$$

Note the maximum function for the slow C pool, which ensures that the size of the slow pool will not decrease if there is a decrease in leaf area. Thus, while the slow C pool is still calculated in relation to the total living biomass, it is assumed to be primarily found in long-lasting organs (stem, roots, lignotubers, ...).

15.3   Maintenance respiration and C balance

Individual daily maintenance respiration (R^{ind}; in $gC\mathring{u}ind^{-1}$) is calculated for each of the three compartments (leaves, alive vascular tissues (stem and coarse roots), and fine roots) (Mouillot et al. 2001). The model uses a Q_{10} relationship with temperature, which means that for every 10ºC change in temperature there is a Q_{10} factor change in respiration. Baseline respiration rates (r_{leaf}, r_{stem} and

r_{root} for leaves, vascular tissues and fine roots, respectively; in $gC·gC^{-1}$) are not species-specific and all refer to 20ºC:

$$R_{leaf} = B_{leaf} \cdot r_{leaf} \cdot Q_{10}^{(T_{mean}-20)/10} \tag{15.7}$$

$$R_{stem} = B_{stem} \cdot r_{stem} \cdot Q_{10}^{(T_{mean}-20)/10} \tag{15.8}$$

$$R_{root} = B_{root} \cdot r_{root} \cdot Q_{10}^{(T_{mean}-20)/10} \tag{15.9}$$

$$R^{ind} = R_{leaf} + R_{stem} + R_{root} \tag{15.10}$$

where T_{mean} is the average daily temperature (in ºC). Note that the output of `growth()` regarding respiration is actually the result of scaling R^{ind} to the cohort level (R^{coh} in $gC·m^{-2}·day^{-1}$), for comparability with photosynthesis and transpiration:

$$R^{coh} = R^{ind} \cdot N/10000 \tag{15.11}$$

If no carbon pools are considered, the carbon available for growth is simply the difference between individual's net photosynthesis and maintenance respiration:

$$C_{available} = \max(0, A_n^{ind} - R^{ind}) \tag{15.12}$$

whereas if carbon pools are considered, the fast C pool is updated with the result of adding photosynthesis and subtracting respiration; and the resulting pool size sets the amount of C available for growth:

$$C_{fast} = \max(0, C_{fast} + A_n^{ind} - R^{ind}) \tag{15.13}$$

$$C_{available} = C_{fast} \tag{15.14}$$

Chapter 16

Sapwood conversion to heartwood, embolism and growth

16.1 Sapwood conversion to heartwood, embolism and growth

Prentice et al. (1993) assumed a constant annual rate of 4% for the conversion from sapwood to heartwood. Similarly, Sitch et al. (2003) assumed a sapwood annual turnover rate of 5% for all biomes. A reasonable value for maximum daily turnover rate would be (assuming an annual rate 4.5%):

$$1 - 0.955^{(1/365)} = 0.0001261398 \tag{16.1}$$

The actual proportion of sapwood area that is transformed into heartwood is:

$$p_{heartwood} = \frac{0.0001261398}{1 + 15 \cdot e^{-0.01 \cdot H}} \tag{16.2}$$

where 0.01 is a constant causing short plants to have slower turnover rates.

Sapwood turnover is applied at the same rate in evergreen and deciduous species. The amount of sapwood that is converted to heartwood every day, $\Delta SA_{turnover}$, is thus:

$$\Delta SA_{turnover} = SA \cdot p_{heartwood} \tag{16.3}$$

Before applying either growth or cavitation the model determines the extent to which cell turgor allows growth using a negative exponential function:

$$f_{turgor}(\Psi_{leaf}) = 1 - \left[e^{(\Psi_{leaf}/\Psi_{tlp})-1} \right]^5 \tag{16.4}$$

where $f_{turgor}(\Psi_{leaf}) = 0$ if $\Psi_{leaf} > \Psi_{tlp}$. The following figure illustrates the function for $\Psi_{tlp} = -1.5$ MPa:
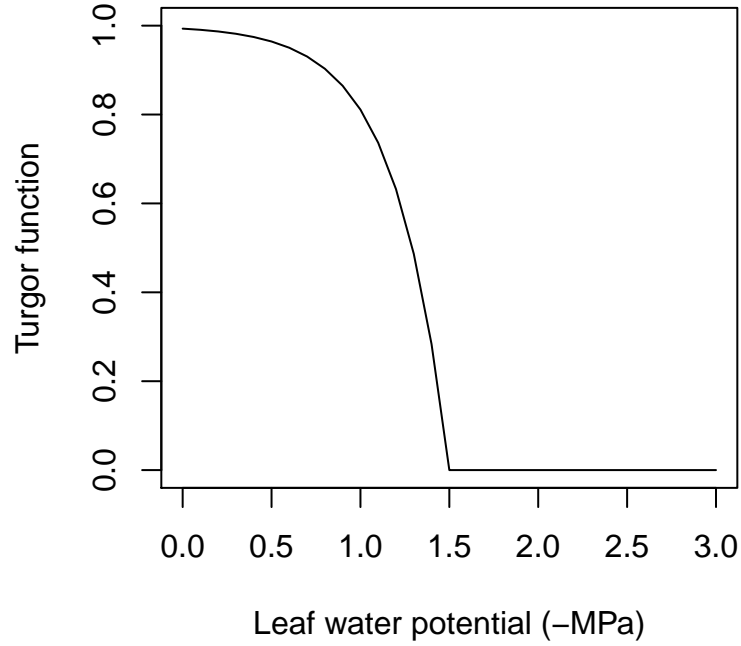
If $f_{turgor}(\Psi_{leaf}) > 0$ growth is applied, but there can be leaf area losses from sapwood turnover, whereas if $f_{turgor}(\Psi_{leaf}) = 0$ growth does not occur and cavitation is possible. The following two subsection detail the behavior of the growth model in each case.

16.2 Growth and turnover during non-drought periods

If (i.e. $f_{turgor}(\Psi_{leaf}) > 0$) the model determines growth, expressed as formation of new sapwood and leaf area increase. Daily sapwood growth rate is assumed to depend on the availability of carbon (i.e., $C_{available} > 0$), but also requires temperature to be within acceptable ranges (because it affects biochemical rates) and minimum turgor for cell elongation.

The adoption of the pipe model (Shinozaki et al. 1964) implies that the addition of new foliage requires building a proportional amount of xylem conduits and fine roots. This is represented in the model by a species-specific Huber value Hv (in $m^2 \mathring{u} m^{-2}$). Since all living biomass equations are linearly related to sapwood area, the total cost in g C per 1 cm^2 of newly formed sapwood area:

$$
\begin{aligned}
C_{cost,leaf} &= 0.3 \cdot \frac{0.1 \cdot Hv}{SLA} & (16.5) \\
C_{cost,stem} &= (H + Z) \cdot W_{dens} \cdot W_C & (16.6) \\
C_{cost,root} &= C_{cost,leaf}/2.5 & (16.7) \\
C_{cost,overall} &= 1.3 \cdot (C_{cost,leaf} + C_{cost,stem} + C_{cost,root}) & (16.8)
\end{aligned}
$$

where 0.1 is needed to express $C_{cost,leaf}$ in units of $g\mathring{u}cm^{-2}$ and factor 1.3 is used in the calculation of $C_{cost,overall}$ because growth respiration is assumed to be a constant proportion of all new tissue growth (30% of new tissue is respired, Ryan 1990). Note that carbon allocation to the three compartments does not follow constant proportions for different plants because the larger the size of a plant, the more C will need to be allocated in the vascular system per unit of sapwood area increment, and hence the proportion of C allocated to leaves and fine roots will decrease. The maximum increase in sapwood area according to the availability of C is:

$$
\Delta SA_{available} = \frac{C_{available}}{C_{cost,overall}} \tag{16.9}
$$

Several sink limitations may occur. One is the turgor limitation, which is represented in the model by f_{turgor}. If carbon pools are considered, then the C concentration in the fast pool (i.e. $C_{fast}/C_{fast,\max}$) may also limit the rate of growth. We model this sink limitation by assuming that the maximum rate of growth will decrease with decreasing concentration, following a sigmoidal function:

$$
f_{conc} = \frac{1}{1 + \exp\left(-5 \cdot \frac{(C_{fast}/C_{fast,\max})-0.5}{0.5}\right)} \tag{16.10}
$$
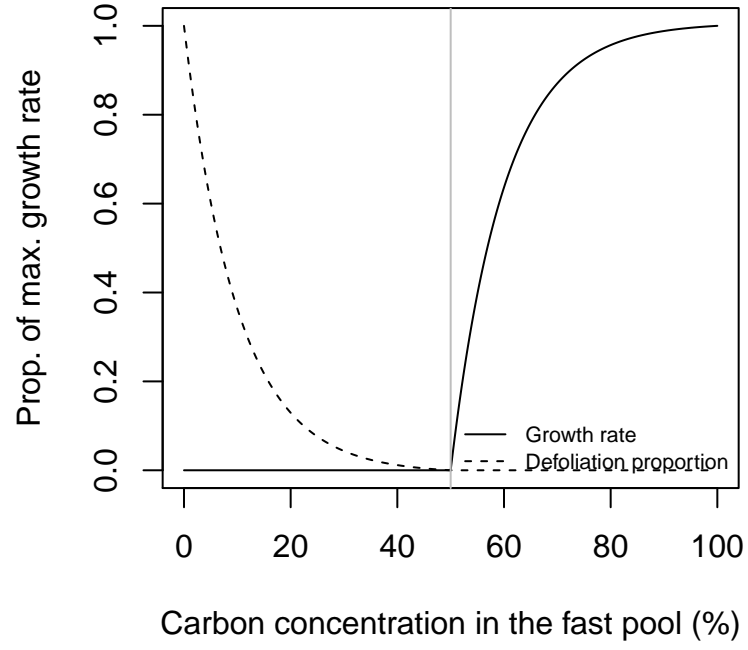
Obviously, if carbon pools are not considered $f_{conc} = 1$.

Growth modulation due to temperature is incorporated through $f_{temp}(T_{mean})$, using a truncated parabolic function as in Poyatos et al. (2007):

$$f_{temp}(T) = \frac{(T - T_{low}) \cdot (T_{high} - T)}{(T_{opt} - T_{low}) \cdot (T_{high} - T_{opt})} \tag{16.11}$$

where $0 \leq f_{temp}(T) \leq 1$, T_{low} and T_{high} minimum and maximum temperature values for growth and T_{opt} is the optimum growth temperature.
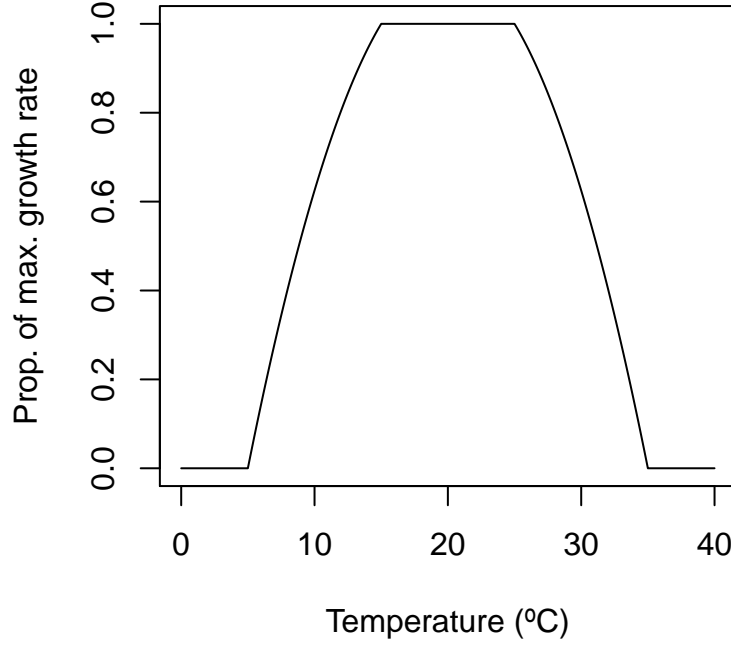
The rate of daily increase in sapwood area taking into account sink limitations is (ΔSA_{sink}; cm^2):

$$\Delta SA_{sink} = RGR_{max} \cdot SA \cdot f_{turgor}(\Psi_{leaf}) \cdot f_{conc} \cdot f_{temp}(T_{mean}) \qquad (16.12)$$

where RGR_{max} is the user-defined, species-specific maximum relative growth rate in sapwood area (in $cm^2 \mathring{u} cm^{-2}$), which can incorporate nutrient deficiency effects.

The final growth rate of sapwood area per individual, ΔSA_{growth} (in cm^2), is found by combining the potential increase in sapwood area according to availability and cost with the sink limitations:

$$\Delta SA_{growth} = \min(\Delta SA_{available}, \Delta SA_{sink}) \qquad (16.13)$$

If carbon pools are considered the actual carbon growth consumption (i.e. $C_{cost,overall} \cdot \Delta SA_{growth}$) has to be subtracted from C_{fast}:

$$C_{fast} = C_{fast} - C_{cost,overall} \cdot \Delta SA_{growth} \qquad (16.14)$$

Sapwood area is updated considering both new sapwood formation and sapwood conversion to heartwood ($\Delta SA_{turnover}$):

$$SA = SA + \Delta SA_{growth} - \Delta SA_{turnover} \qquad (16.15)$$

After updating sapwood area, the model updates living, expanded and dead leaf area accordingly:

$$LAI^{live} = LAI^{live} + N \cdot (\Delta SA_{growth} - \Delta SA_{turnover}) \cdot Hv \quad (16.16)$$
$$LAI^{\phi} = LAI^{live} \cdot \phi \quad (16.17)$$
$$LAI^{dead} = LAI^{dead} + N \cdot \Delta SA_{turnover} \cdot Hv \quad (16.18)$$

During non-drought periods the state variables regulating drought effects are kept at initial values (i.e. $\Psi_{\min} = 0$ and $LAI^{predrought} = LAI^{live}$).

16.3 Leaf area losses during drought-periods

During drought-periods (i.e. if $f_{turgor}(\Psi_{leaf}) = 0$) cavitation may occur. However, cavitation is applied at the leaf area level and not at the sapwood area level. During drought periods reductions of live leaf area can come from either sapwood conversion into heartwood or cavitation. First, the model compares the current Ψ_{leaf} value with $\Psi_{\min}$ the minimum potential experienced since drought started:

$$\Psi_{\min} = \min(\Psi_{leaf}, \Psi_{\min}) \quad (16.19)$$

Then the model determines the proportion of embolized conducts as the complement of hydraulic conductance corresponding to $\Psi_{\min}$, relative to the maximum hydraulic conductance. If the transpiration mode is "Simple", this is done using a whole-plant conductance function:

$$P_{embolism} = 1 - K(\Psi_{\min}) = \exp\left\{ \ln(0.5) \cdot \left[\frac{\Psi_{\min}}{\Psi_{extract}} \right]^r \right\} \quad (16.20)$$

where $\Psi_{extract}$ is the potential at which conductance is 50% of maximum and $r = 3$. If the transpiration mode is "Complex", $P_{embolism}$ is calculated using the stem-leaves vulnerability curve:

$$P_{emb} = 1 - \frac{k_{stem}(\Psi_{\min})}{k_{stem}(0)} = 1 - \exp\left\{ -\left[\frac{\Psi_{\min}}{d_{stem}} \right]^{c_{stem}} \right\} \quad (16.21)$$

Since leaf area reduction may also come from sapwood conversion into heartwood, the model determines which process leads to a larger reduction in leaf area:

$$LAI^{live} = \min(LAI^{live} - N \cdot \Delta SA_{turnover} \cdot Hv, \, LAI^{predrought} \cdot (1 - P_{emb}))$$
$$(16.22)$$

and expanded leaf area (LAI^{ϕ}) and dead leaf area (LAI^{dead}) are modified accordingly.

16.4 Transfer between carbon pools

If two carbon pools are considered then carbon can be transferred from one to the other. The model assumes that the direction of transfer depends on the C concentration in the fast pool. When the pool is at full capacity its C should be converted to long-term storage, whereas if the pool is empty C stored in the slow pool should be mobilised. The relative rate of transfer ($r_{transfer}$; in $gC\mathring{u}gC^{-1}$) is modelled using a sigmoidal function:

$$r_{transf} = 0.1 \cdot \frac{2}{1 + \exp\left(-5 \cdot \frac{(C_{fast}/C_{fast,\max}) - 0.5}{0.5}\right)} - 1 \qquad (16.23)$$
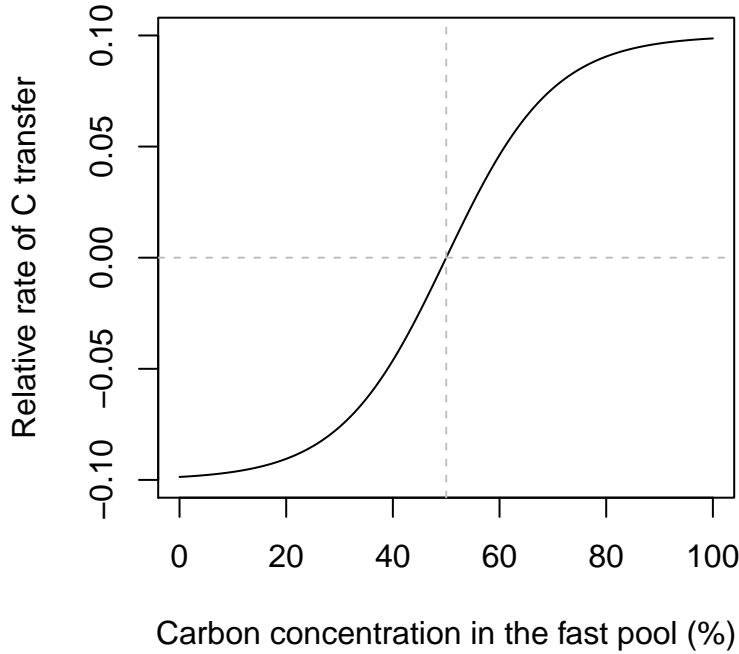
where 0.1 indicates that the maximum daily transfer rate is 10% of the source C pool size. If $r_{transf} < 0$ then $-r_{transf} \cdot C_{slow,\max}$ g of carbon are taken from the slow C pool and 90% of this amount is added into the fast C pool (the

remaining 10% is assumed to be the transfer cost). Similarly, if $r_{transf} > 0$ then $r_{transf} \cdot C_{fast,\max}$ g of carbon are taken from the fast C pool and 90% of this amount is added into the slow C pool (again, the remaining 10% is assumed to be the transfer cost). The amounts of C transferred are also limited by the amount that would be needed to fill the sink pool (i.e., if the sink pool is already full, no carbon is transferred).

16.5 Update of maximum stem conductance

The inclusion of Hv in the initialization of SA and in growth equations causes sapwood area and leaf area to maintain a constant ratio equal to Hv. However, this rule may be broken by leaf phenology or when losing leaves because of drought stress. Leaf area reductions cause transpirational demand to be reduced accordingly. Moreover, in the case of Complex's transpiration mode leaf loss causes variations in leaf area to sapwood area ratio, which may become lower than Hv and, hence, maximum stem hydraulic conductance may increase. Tree size controls much of the variation in stem hydraulic conductance, since hydraulic path length increases with tree height. We modelled stem conductance per leaf area unit ($k_{stem,\max}$; in $mmol\,\mathring{u}m^{-2}\mathring{u}s^{-1}\mathring{u}MPa^{-1}$) as a function of species-specific xylem conductivity ($k_{xylem,\max}$; in $kg\mathring{u}m^{-1}\mathring{u}s^{-1}\mathring{u}MPa^{-1}$), leaf area to sapwood area ratio and tree height (Christoffersen et al., 2016):

$$k_{stem,\max} = \frac{1000}{0.018} \cdot \frac{k_{xylem,\max} \cdot (SA/10000)}{(H/100) \cdot LA^{\phi}} \cdot \chi_{taper} \qquad (16.24)$$

where χ_{taper} is a factor to account for taper of xylem conduit with height (Savage et al., 2010; Christoffersen et al., 2016), 0.018 is the molar weight of water (in $kg \cdot mol^{-1}$). This way, if the leaf-to-sapwood area ratio decreases with tree height, as has been documented in several species (McDowell et al. 2002), the decreasing conductance effects with height may be partially overcome (Christoffersen et al., 2016). A drought-induced decrease in LA^{ϕ} alleviate drought effects (i.e. a lower decrease in water potential across the stem for the same flow) because of an increase in conductance.

Chapter 17

Update of structural variables

Unlike functional variables, structural variables are updated for simplicity once a year only (or before the end of the simulated period).

17.1 Tree diameter, height and crown ratio

In the case of tree cohorts, the cumulated new sapwood area $(\sum SA_{growth})$ is translated to an increment in DBH (ΔDBH, in cm) following:

$$\Delta DBH = 2 \cdot \sqrt{(DBH/2)^2 + (\sum SA_{growth}/\pi)} - DBH \qquad (17.1)$$

Furthermore, the model assumes that increments in height are linearly related to increments in diameter through a function f_{HD} (Lindner et al. 1997):

$$\Delta H = f_{HD} \cdot \Delta DBH \qquad (17.2)$$

Hence, f_{HD} represents the height increment (in cm) per each cm of diameter increment. It was customary in forest gap models to prevent height from being larger than a species-specific value $H_{\max}$, so that beyond some point trees only grew in size by increasing their diameter. Moreover, light conditions influence growth in height with trees living under the shade of others generally showing larger increases in height than trees living in open conditions. Hence, our formulation for f_{HD} is (Lindner et al., 1997; Rasche et al., 2012):

$$f_{HD} = [f_{HD,\min} \cdot L + f_{HD,\max} \cdot (1 - L)] \cdot \left(1 - \frac{H - 137}{H_{\max} - 137}\right) \qquad (17.3)$$

where $f_{HD,\min}$ would be the height-diameter ratio for a tree of 137 cm height growing in full light and $f_{HD,\max}$ would be the same ratio for a tree of the same height growing in the shadow. This formulation seems slightly easier to calibrate than that presented in Rasche et al. (2012). $H_{\max}$ could be dependent on environmental conditions, but we skip this here, because environmental conditions already affect growth rate and carbon balance.

After updating tree diameter (DBH) and tree height (H), the model updates tree crown ratio (CR) by applying allometric relationships that take into account tree size and competition (see details in vignette XX).

17.2   Shrub height and cover

Since shrub structural variables are height and cover, shrub growth is done in a way somewhat different from trees. Shrubs are often multi-stemmed (some trees also are), so that increases in sapwood area are not easily related to diameter growth. Since leaf biomass is related to sapwood area, one may model shrub growth assuming an allometric relationship between phytovolume of individual shrub crowns and photosynthetic biomass. This strategy entails that shrubs may grow or shrink in size depending on their C balance, in the same way that tree crowns would become denser or sparser depending on their C balance. Hence, shrubs can be understood as crowns in the floor.

Starting from live leaf area ($m^2 \mathring{u} m^{-2}$) we can calculate the foliar weight per shrub individual (in $kg \mathring{u} ind^{-1}$):

$$W_{leaves} = \frac{LAI^{live}}{(N/10000) \cdot SLA} \qquad (17.4)$$

An allometric relationship relating the biomass of leaves plus small branches and crown phytovolume (PV; in $m^3 \mathring{u} ind^{-1}$) can be drawn from fuel calculations:

$$W_{leaves+branches} = W_{leaves} \cdot r_{6.35} = a_{bsh} \cdot PV^{b_{bsh}} \qquad (17.5)$$

where a_{bsh} and b_{bsh} are allometric relationships and $r_{6.35}$ is a species-specific ratio relating the dry weight of leaves plus small branches to the dry weight of leaves. Inverting this relationship we obtain an expression of shrub crown phytovolume:

$$PV = \left[\frac{W_{leaves} \cdot r_{6.35}}{a_{bsh}}\right]^{1/b_{bsh}} \qquad (17.6)$$

Phytovolume is defined as the volume occupied by the shrub crown, i.e.:

$$PV = (A_{sh}/10000) \cdot (H/100) \cdot CR \tag{17.7}$$

where A_{sh} is the area of a single shrub individual (in cm^2). If we use the following quadratic relationship between A_{sh} and H:

$$A_{sh} = a_{ash} \cdot H^2 \tag{17.8}$$

we can calculate shrub height from phytovolume using:

$$H = \left[\frac{10^6 \cdot PV}{a_{ash} \cdot CR} \right]^{1/3} \tag{17.9}$$

Finally, the new value for shrub cover (in percent) can be obtained from H and N (in $\text{ind} \cdot \text{ha}^{-1}$):

$$Cover = 100 \cdot (N/10000) \cdot (A_{sh}/10000) = \frac{N \cdot a_{ash} \cdot H^2}{10^6} \tag{17.10}$$

Note that crown ratio for shrubs is assumed constant in the model. Like for trees, shrub height is limited to a maximum height $H_{\max}$. However, unlike trees, shrubs are not allowed to continue growing once this maximum size is attained. When the estimated height is over the maximum value, the exceeding amount of live leaf area is allocated to dead live area.

Part V

Static modules

Chapter 18

Leaf biomass, leaf area and vertical profiles

18.1 Input data

18.1.1 Forest inventory data

The input data for tree cohorts are:

- SP_i: Species identity}
- DBH_i: Diameter at breast height (in cm) of the representative tree.
- H_i: Height (in cm) of the representative tree.
- N_i: Cohort density (in $ind. \cdot ha^{-1}$).

The input data for shrub cohorts are:

- SP_i: Species identity
- C_i: Plant cover (in percent).
- H_i: Mean plant height (in cm).

18.1.2 Allometric species-specific parameters

- $a_{fbt}, b_{fbt}, c_{fbt}, d_{fbt}$ [`a_fbt`, `b_fbt`, `c_fbt`, `d_fbt`]: Regression coefficients used to calculate foliar biomass of an individual tree from its DBH and the cummulative basal area of larger trees.
- a_{ash} [`a_ash`]: Regression coefficient relating the square of shrub height with shrub area.
- a_{bsh} and b_{bsh} [`a_bsh`, `b_bsh`]: Allometric coefficients relating phytovolume with dry weight of shrub individuals.

- $cr(SP_i)$: [cr]: Ratio between crown length and total height for shrubs.

18.2 Allometric relationships

18.2.1 Leaf biomass for tree cohorts

Foliar biomass for a single tree of cohort i ($FB_{tree,i}$; in kg) is calculated using:

$$FB_{tree,i} = a_{fbt} \cdot DBH_i^{b_{fbt}} \cdot e^{c_{fbt} \cdot BAL_i} \cdot DBH_i^{d_{fbt} \cdot BA_{sup}} \tag{18.1}$$

where DBH_i is the diameter of the tree (in cm), BAL_i is the cummulative basal area ($m^2 \cdot ha^{-1}$) of trees having a larger diameter, and a_{fbt}, b_{fbt}, c_{fbt} and c_{fbt} are species-specific regression coefficients. The foliar biomass of the whole tree cohort (FB_i; in $kg \cdot m^{-2}$) is obtained multiplying tree foliar biomass by tree density (N_i; in $ind. \cdot ha^{-1}$):

$$FB_i = FB_{tree,i} \cdot (N_i/10000) \tag{18.2}$$

18.2.2 Leaf biomass for shrub cohorts

To calculate the leaf biomass of a shrub cohort, we first determine $A_{sh,i}$, the area (in cm^2) occupied by one average individual of height H_i (in cm), using the quadratic relationship:

$$A_{sh,i} = a_{ash} \cdot H_i^2 \tag{18.3}$$

where a_{ash} is a species-specific parameter. The model then estimates the dry weight of leaves and branches up to 6.35mm in diameter ($B_{sh,i}$, in kg) of this average individual (i.e. fine fuel biomass), using an allometric relationship with shrub crown phytovolume assuming a cylinder (in cm^3):

$$B_{sh,i} = a_{bsh} \cdot (A_{sh,i} \cdot H_i \cdot cr(SP_i))^{b_{bsh}} \tag{18.4}$$

where a_{bsh} and b_{bsh} are species-specific parameters and $cr(SP_i)$ is a species-specific crown ratio (a proportion between 0 and 1, the ratio between crown length and total height). Shrub density (N_i; in $ind. \cdot m^{-2}$) can be grossly estimated from percent cover (C_i, in percent) and $A_{sh,i}$ (in cm^{-2}):

$$N_i = \frac{C_i/100}{A_{sh,i}/10000} \tag{18.5}$$

The fine fuel biomass of a shrub cohort (W_i, in $kg \cdot m^{-2}$) is simply the product of $B_{sh,i}$ (kg of dry weight) and N_i:

$$W_i = B_{sh,i} \cdot N_i \tag{18.6}$$

Foliar biomass (in $kg \cdot m^{-2}$) can be obtained using the species-specific ratio $r_{6.35}(SP_i)$:

$$FB_i = W_i / r_{6.35}(SP_i) \tag{18.7}$$

If not known, $r_{6.35}(SP_i)$ can be set to a default value of 2 (equivalent to %50 of weight corresponding to leaves).

18.2.3   Leaf area and LAI

Leaf area index (LAI in $m^2 \cdot m^{-2}$) of a given cohort i can be calculated from its foliar biomass (in $kg \cdot m^{-2}$) by using a *specific leaf area* coefficient (SLA, in $m^2 \cdot kg^{-1}$) that in **medfate** is species-specific:

$$LAI_i = FB_i \cdot SLA \tag{18.8}$$

The leaf area (LA in m^2) of an individual of the cohort is found by dividing it by plant density (N_i, in $ind. \cdot ha^{-1}$) and multiplying by 10000 $m^2 \cdot ha^{-1}$:

$$LA_i = 10000 \cdot LAI_i / N_i \tag{18.9}$$

18.2.4   Crown base height

In the case of shrubs the crown ratio is simply equal by a species-specific parameter: $CR_i = cr(SP_i)$. In the case of trees, the crown ratio is modelled as a function of tree size and stand competition, following a modification of the logistic equation of Hasenauer and Monserud (1996):

$$CR_i = \frac{1}{1 + e^{-(a_{cr} + b_{1cr} \cdot HD + b_{2cr} \cdot (H_i/100) + b_{3cr} \cdot DBH_i^2 + c_{1cr} \cdot BAL_i + c_{2cr} \cdot ln(CCF))}} \tag{18.10}$$

where $HD = H_i / (100 \cdot DBH_i)$ is the height to diameter ratio (in $m \cdot cm^{-1}$), H_i is the tree height, DBH_i is the diameter, CCF is the crown competition factor and a_{cr}, b_{1cr}, b_{2cr}, b_{3cr}, c_{1cr} and c_{2cr} are species-specific parameters. The crown competition factor is in turn calculated using (Krajicek et al., 1961):

$$CCF = \sum_i N_i \cdot MCA_i = \sum_i N_i \cdot \pi \cdot (CW_i/2)^2/100 \qquad (18.11)$$

where N_i is the tree density, MCA_i is the maximum crown area (in percent of unit area) and CW_i is the crown width (in m) assuming an open-grown tree, estimated from an allometric relationship with tree diameter:

$$CW_i = a_{cw} \cdot BDH_i^{b_{cw}} \qquad (18.12)$$

where again a_{cw} and b_{cw} are species-specific parameters.

Chapter 19

Fuel characteristics and fire behaviour

19.1 Purpose

Functions `fuel_FCCS()` and `fire_FCCS()` allow calculating potential fire behaviour for forest inventory plots. Formulation of fuel characteristics and fire behaviour is an adaptation of the Fuel Characteristics Classification System (FCCS; Prichard et al., 2013). In FCCS, fuelbed is divided into six strata, including canopy, shrub, herbaceous vegetation, dead woody materials, leaf litter and ground fuels. All except ground fuels are considered here. The intensity of burning depends on several factors, including topography, wind conditions, fuel structure and its moisture content, which is determined from antecedent and current meteorological conditions. A modification of the Rothermel's (1972) model is used to calculate the intensity of surface fire reaction (in kW/m^2) and the rate of fire spread (in m/min) of surface fires assuming a steady-state fire. Both quantities are dependent on fuel characteristics, windspeed and direction, and topographic slope and aspect. The model returns the following results: (1) Fuel characteristics by stratum; (2) Surface fire behavior (i.e. reaction intensity, rate of spread, fireline intensity and flame length); (3) Crown fire behavior; (4) Fire potential ratings of surface fire behavior and crown fire behavior.

19.2 Input data

19.2.1 Forest inventory plot data

The input data for tree cohorts are:

- SP_i: Species identity}
- DBH_i: Diameter at breast height (in cm) of the representative tree.
- H_i: Height (in cm) of the representative tree.
- N_i: Cohort density (in $ind. \cdot ha^{-1}$).

The input data for shrub cohorts are:

- SP_i: Species identity
- C_i: Plant cover (in percent).
- H_i: Mean plant height (in cm).

Cohorts are not distinguished for the herbaceous stratum, and the variables needed are:

- C_{he}: Herbaceous cover (in percent).
- H_{he}: Mean herb height (in cm).

Finally, the model also requires the percent cover of trees in the canopy (C_{ca}). This is easily available from forest inventory data, but could also be derived from the description of tree cohorts.

19.2.2   Species-specific parameters

- $r_{6.35}(SP_i)$ [`r635`]: Ratio between the weight of leaves plus branches and the weight of leaves alone for branches of 6.35 mm.
- $\rho_p(SP_i)$ [`PD`]: Particle density.
- $\sigma(SP_i)$ [`SAV`]: Surface-area-to-volume ratio of the small fuel (1h) fraction (leaves and branches < 6.35mm).
- $h(SP_i)$ [`HeatContent`]: High fuel heat content.
- $\eta_F(SP_i)$ [`Flammability`]: Flammability value (either 1 or 2 for normal or high, respectively).
- $LD(SP_i)$ [`LeafDuration`]: Leaf duration (in years).
- $LI(SP_i)$ [`PercentLignin`]: Percentage of lignin in leaves.

19.2.3   Other inputs

Other inputs may be given by expert opinion or they may be calculated from another model. Specifically, for each plant cohort (and for any day of application) the fire behaviour model requires:

- $P_{dead,i}$: Proportion of the plant that is dead.
- M_i: Foliar moisture value (in percent of dry weight).

Analogously, the same variables are needed for the herbaceous stratum.

- $P_{dead,he}$: Proportion of herb fuels that respond to humidity changes as 1-h dead fuels.
- $M_{live,he}$: Foliar moisture value of live herb fuels (in percent of dry weight).

The model also needs the following input parameters:

- M_{dead}: the moisture of 1-h dead fuels (in percent of dry weight).
- U: Midflame windspeed (in $m \cdot s^{-1}$).
- S: Slope (in percent).

19.3 Fuel characteristics

19.3.1 Fuel strata

The Fuel Characteristics Classification System (FCCS) on which this document is based, defines six fuel strata (Prichard et al., 2013):

- *Canopy*: Trees, snags and ladder fuels.
- *Shrubs*: Primary and secondary layers.
- *Non-woody vegetation (herbs)*: grasses, sedges, rushes and forbs.
- *Woody fuels*: All downed and dead wood, sound wood, rotten wood and stumps.
- *Litter-lichen-moss*: Lichen, litter and moss layers.
- *Ground fuels*: Duff, basal accumulation and squirrel middens.

Shrubs, herbs and woody fuels are constitute the **upper surface fuels**, whereas herbs and woody fuels alone consitute the **lower surface fuels**. FCCS summarizes and calculates characteristics for each fuelbed stratum and layer. Our model estimates fuel loading and characteristics for canopy, shrub, non-woody vegetation, as well as fine (1h) woody fuels and litter fuels. Larger woody fuels (10h or 100h) could be considered if information about forest management actions is available. Ground fuels are not included here.

19.3.2 Cohort fuel loading

Here we consider as burnable fuels foliage and branches up to 6.35 mm = 0.25 in in diameter. The same consideration applies to both trees and shrubs.

Fine fuel loading for a tree cohort (W_i; in $kg \cdot m^{-2}$), including its leaves and branches with diameter up to 6.35 mm = 0.25 in, is calculated from foliar biomass (FB_i, see eq. (18.2)) using:

$$W_i = r_{6.35}(SP_i) \cdot FB_i \tag{19.1}$$

where $r_{6.35}(SP_i)$ is the ratio between the weight of leaves plus branches and the weight of leaves alone for branches of 6.35 mm in diameter for the species of cohort i. The biomass corresponding to branches of less than < 6.35 mm (SBB_i, also in $kg \cdot m^{-2}$) is obtained by subtraction:

$$SBB_i = (r_{6.35}(SP_i) - 1) \cdot FB_i \qquad (19.2)$$

Whereas W_i is the cohort loading variable influencing fire behavior, FB_i and SBB_i are cohort variables used to estimate fine dead woody and leaf litter loadings.

Our procedure to estimate shrub fuel loading differs from Prichard et al. (2013) because they calculate first total biomass of the shrub species and then consider the percentage of total weight that corresponds to leaves and small branches. In our case, we estimate fine fuel loading (W_i, in $kg \cdot m^{-2}$) and foliar biomass (FB_i, in $kg \cdot m^{-2}$) of shrubs from eqs. (18.6) and (18.7). Biomass of small branches (in $kg \cdot m^{-2}$) can be obtained from :

$$SBB_i = W_i - FB_i \qquad (19.3)$$

19.3.3 Vertical distribution of cohort fuels

For all tree or shrub cohorts fuels are assumed to be homogeneously distributed between the crown base height ($H_{b,i}$; in cm) and the total height (H_i). Crown base height of trees is calculated as explained in 18.2.4. The loading of a cohort that occurs within a given height interval of limits H_1 and H_2 is calculated as:

$$W_i(H_1, H_2) = W_i \cdot p_i(H_1, H_2) \qquad (19.4)$$

where $p_i(H_1, H_2)$ is the proportion of the crown of cohort i that corresponds to the height interval (H_1, H_2):

$$p_i(H_1, H_2) = \frac{\max(0, \min(H_i, H_2) - \max(H_{b,i}, H_1))}{H_i - H_{b,i}} \qquad (19.5)$$

19.3.4 Fuel bulk density profile

Knowing at which height fuels are placed, the **fuel bulk density profile** (Reinhardt et al., 2006) is defined for any given interval (H_1, H_2) as the bulk density (kg/m^3) of fine fuels corresponding to that interval:

$$BDP(H_1, H_2) = \frac{\sum_i W_i(H_1, H_2)}{H_2 - H_1} \qquad (19.6)$$

Canopy bulk density normally ranges between 0 and 0.4 kg/m^3 (Scott and Reinhardt, 2002). Sando and Wick (1972) arbitrarily defined canopy base height as the lower vertical 0.3-m section with a weight greater than $0.01124 kg/m^3$. A

user-defined threshold t_{BDP} (in kg/m^3) in 0.1-m sections is used to differentiate the surface fuelbed from canopy fuels. Using this threshold the model calculates the following three heights (Reinhardt et al., 2006):

- *Shrub stratum base height*, H_{sb} (in cm): the minimum height between 0 and 2 m where fuel bulk density is larger than t_{BDP}.
- *Shrub stratum top height*, H_{st} (in cm): the maximum height between 0 and 2 m where fuel bulk density larger than t_{BDP}. With this definition h_s cannot be higher than 2 m (corresponding to fuel model 4 in Anderson 1982).
- *Canopy base height*, H_{cb} (in cm): In terms of its consequences to crown fire initiation, canopy base height can be defined as the lowest height above the ground at which there is sufficient canopy fuel to propagate fire vertically through the canopy. It is calculated as the minimum height over $H_s t$ when the bulk density starts again to be larger than t_{BDP}.
- *Canopy top height*, H_{ct} (in cm): the maximum height where bulk density is larger than t_{BDP}.
- *Canopy gap*, H_{gap} (in cm): the difference between H_{cb} and H_{st}. The canopy gap is used to calculate crown initiation potential.

The following figure illustrates the definition and analysis of the fuel bulk density profile for a given forest stand. Following Mitsopoulos and Dimitrakopoulos (2007), a threshold $t_{BDP} = 0.04$ has been used to determine shrub and canopy heights.
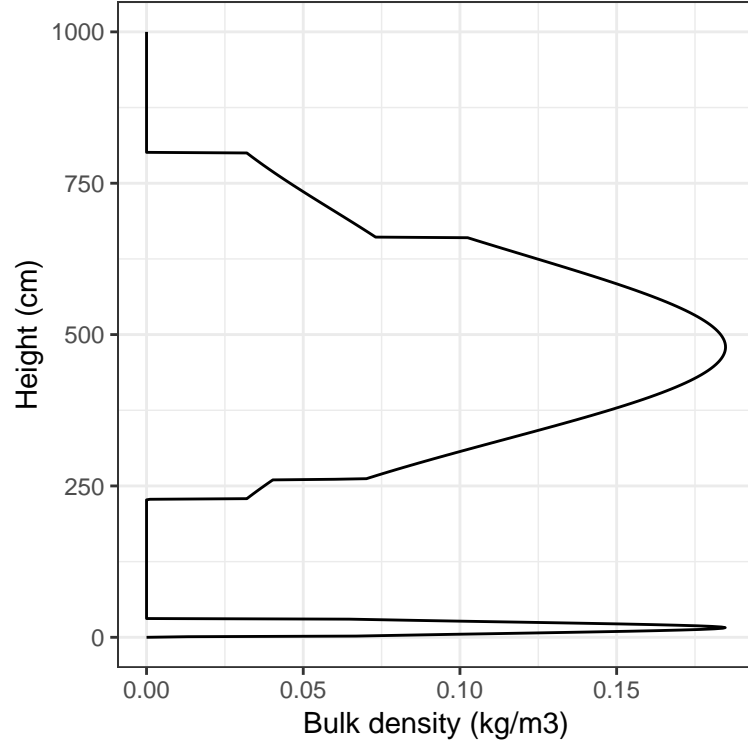
19.3.5   Fuel loading (w) and fuel depth (δ)

19.3.5.1   Canopy stratum

Canopy loading (in $kg \cdot m^{-2}$) is the sum of (tree and shrub) cohort loadings above 2 m (i.e. 200 cm):

$$w_{ca} = \sum_i w_{i,ca} = \sum_i W_i(200, \infty) \tag{19.7}$$

where $w_{i,ca}$ is the canopy stratum loading of cohort i. Canopy depth (in m) is defined as the average of tree (or shrub) crown lengths above 2 m, weighted by the loadings of cohorts in the canopy:

$$\delta_{ca} = \frac{1}{100} \cdot \frac{\sum_i w_{i,ca} \cdot (H_i - H_{b,i}) \cdot p_{i,ca}}{\sum_i w_{i,ca}} \tag{19.8}$$

where the proportion of a tree (or shrub) cohort in the canopy stratum is $p_{i,ca} = p_i(200, \infty)$.

19.3.5.2 Shrub stratum

Shrub loading (in $kg \cdot m^{-2}$) is the sum of (tree and shrub) cohort loadings between the ground and 2 m (i.e. 200 cm):

$$w_{sh} = \sum_i w_{i,sh} = \sum_i W_i(0, 200) \tag{19.9}$$

where $w_{i,sh}$ is the shrub stratum loading of cohort i. The depth of the shrub stratum (in m) is defined as the average of tree (or shrub) crown lengths below 2 m, weighted by the loadings of cohorts in the shrub stratum:

$$\delta_{sh} = \frac{1}{100} \cdot \frac{\sum_i w_{i,sh} \cdot (H_i - H_{b,i}) \cdot p_{i,sh}}{\sum_i w_{i,sh}} \tag{19.10}$$

where the proportion of a shrub (or tree) cohort in the shrub stratum is $p_{i,sh} = p_i(0, 200)$.

19.3.5.3 Non-woody stratum

Herb percent cover and average herb height are transformed into herbaceous loading ($kg \cdot m^{-2}$) using (ref piropinos):

$$w_{he} = 0.014 \cdot C_{he} \cdot (H_{he}/100) \tag{19.11}$$

The depth of the herbaceous stratum (in m) is simply the mean height of herbs:

$$\delta_{he} = H_{he}/100 \tag{19.12}$$

19.3.5.4 Woody and litter strata

In FCCS (Prichard et al., 2013), woody surface loading includes several fuel sizes. However, when calculating surface fire behavior w_{wo} includes 100% of 1h fuels, 25% of 10h fuels and 12.5% of 100h fuels, which represents the material available for flaming combustion. Obtaining loading estimates for 10h- and 100h-fuels is very difficult without field fuel sampling. However, we might estimate 1h woody fuels and leaf litter from standing biomass of small branches (< 6.35mm) and leaves for trees and shrubs. Hence, our treatment of surface woody fuels includes only fine (1h) fuels.

Assuming a continuous input of litter, the variation in accumulated litter is described by a simple differential equation (Birk and Simpson, 1980):

$$\frac{\mathrm{d}X}{\mathrm{d}t} = L - k \cdot X \tag{19.13}$$

where k is the decay constant, L is the rate of litterfall and X is the litter mass accumulated in the forest floor. Assuming that litter mass has reached a steady state, X can be estimated as the ratio between L and k. If litterfall is estimated as the total foliar biomass divided by leaf duration, the amount of steady state leaf litter corresponding to each tree and srhub cohort can be estimated using:

$$w_{li,i} = \frac{FB_i}{LD(SP_i) \cdot k_i} \tag{19.14}$$

where FB_i is the foliar biomass of cohort i, $LD(SP_i)$ is the species-specific average leaf duration (in years) and k_i is the rate of decay of leaves of cohort i, which is given by the regreession model of Meentemeyer (1978):

$$k_i = (-0.5365 + 0.00241 \cdot AET) - (-0.01586 + 0.000056 \cdot AET) \cdot LI(SP_i) \tag{19.15}$$

where $LI(SP_i)$ is the species-specific percentage of lignin content in leaves and AET is actual evapotranspiration (default $AET = 1000mm$). Litter loadings are summed for four litter types (short pine needles, long pine needles, other conifers, broadleaves). In the case of fine dead woody materials (small fallen branches), loading of small branches is taken as woody litter and it is assumed that small branch litterfall occurs at the same time as leaf litterfall (i.e. according to leaf duration):

$$w_{wo} = \sum_i w_{wo,i} = \sum_i \frac{SBB_i}{LD(SP_i) \cdot k_{wo}} \tag{19.16}$$

where $k_{wo} = 0.95y^{-1}$ is a constant rate of decomposition for small branches.

In FCCS, the depth of woody and LLM strata are inputs. In our case the depth of the woody and litter strata are estimated from the corresponding fuel loadings:

$$\delta_{wo} = w_{wo}/\rho_{b,wo} \tag{19.17}$$
$$\delta_{li} = w_{li}/\rho_{b,li} \tag{19.18}$$

where $\rho_{b,wo}$, $\rho_{b,li}$ are the woody and litter bulk density (in $kg \cdot m^{-3}$), respectively. Litter bulk density $\rho_{b,li}$ is calculated as a weighted average of litter types:

$$\rho_{b,li} = \frac{\sum_k \rho_{b,k} \cdot w_{li,k}}{\sum_k \cdot w_{li,k}} \tag{19.19}$$

where k indicates litter type. The bulk density for litter types are [Prichard et al. (2013); Table 1]:

$$\rho_{b,shortneedlepine} = \rho_{b,longneedlepine} = \rho_{b,otherconifer} = 1.65 lb \cdot ft^{-3} = 26.43 kg \cdot m^{-3} \tag{19.20}$$

$$\rho_{b,hardwood} = 0.83 lb \cdot ft^{-3} = 13.30 kg \cdot m^{-3} \tag{19.21}$$

19.3.6 Other fuel characteristics

All the following characteristics are calculated in metric units (although British units are indicated to qualify specific values for compatibility).

19.3.6.1 Particle density (ρ_p)

Particle density is the ratio of dry weight over volume for fuel particles (in $kg \cdot m^{-3}$). When species have different values, particle density averages for shrub and canopy strata can be obtained as:

$$\rho_{p,sh} = \frac{\sum_i w_{i,sh} \cdot \rho_p(SP_i)}{\sum_i w_{i,sh}} \tag{19.22}$$

$$\rho_{p,ca} = \frac{\sum_i w_{i,ca} \cdot \rho_p(SP_i)}{\sum_i w_{i,ca}} \tag{19.23}$$

where $\rho_p(SP_i)$ is the species-specific particle density. $\rho_{p,he}$, $\rho_{p,wo}$ and $\rho_{p,li}$ are all set to a default value $\rho_p = 400 kg \cdot m^{-3} = 25 lb \cdot ft^{-3}$ (Prichard et al., 2013).

19.3.6.2 Particle volume (PV)

Particle volume is defined as the volume of particles per surface area (in $m^3 \cdot m^{-2}$). Is calculated as dry weight loading divided by particle density. If species have different particle density values, the particle volume for canopy (PV_{ca}) and shrub(PV_{sh}) strata can be calculated using:

$$PV_{ca} = \sum_i PV_{i,ca} = \sum_i w_{i,ca}/\rho_p(SP_i) \tag{19.24}$$

$$PV_{sh} = \sum_i PV_{i,sh} = \sum_i w_{i,sh}/\rho_p(SP_i) \tag{19.25}$$

where $PV_{i,ca}$ and $PV_{i,sh}$ are the particle volume of cohort i in the canopy and shrub strata, respectively. The particle volume for woody and herb strata are simply:

$$PV_{wo} = w_{wo}/\rho_{p,wo} \tag{19.26}$$
$$PV_{he} = w_{he}/\rho_{p,he} \tag{19.27}$$

The particle volume for the litter stratum is the sum of particle volume of litter components:

$$PV_{li} = \sum_i PV_{li,k} = \sum_i w_{li,k}/\rho_{p,li} \tag{19.28}$$

19.3.6.3   Packing ratio (β)

The proportion of fuelbed stratum volume occupied by fuel particles is an important factor to predict fire behavior. At low packing ratios (low particle density) fire intensity is limited by excessive heat loss. At high packing ratios (high particle density), lack of oxygen limits combustion. The packing ratios for the canopy and shrub stratum (β_{ca} and β_{sh}; dimensionless) are given by:

$$\tag{19.29}$$
$$eqrefeq : packingratioshrub\beta_{ca} = \frac{PV_{ca}}{\delta_{ca}} \tag{19.30}$$
$$\beta_{sh} = \frac{PV_{sh}}{\delta_{sh}} \tag{19.31}$$

where $w_{i,ca}$ and $w_{i,sh}$ are the contribution of cohort i to canopy and shrub strata loading (in $kg \cdot m^{-2}$), respectively, and $\rho_p(SP_i)$ is the particle density (in $kg \cdot m^{-3}$) of fuels in cohort i. The packing ratio for the herbaceous, woody and litter strata are:

$$\beta_{he} = \frac{PV_{he}}{\delta_{he}} \tag{19.32}$$
$$\beta_{wo} = \frac{PV_{wo}}{\delta_{wo}} = \frac{\rho_{b,wo}}{\rho_{p,wo}} \tag{19.33}$$
$$\beta_{li} = \frac{PV_{li}}{\delta_{li}} = \frac{\rho_{b,li}}{\rho_{p,li}} \tag{19.34}$$

Note that the packing ratio expressions for woody and litter strata as a ratio of bulk and particle density arises as a consequence of how fuel depth and particle volume are estimated.

19.3.6.4   Surface-area-to-volume ratio (σ)

The surface-area-to-volume ratio (in $m^2 \cdot m^{-3}$) for the canopy or shrub strata are calculated using weighted averages:

$$\sigma_{ca} = \frac{\sum_i w_{i,ca} \cdot \sigma(SP_i)}{\sum_i w_{i,ca}} \tag{19.35}$$

$$\sigma_{sh} = \frac{\sum_i w_{i,sh} \cdot \sigma(SP_i)}{\sum_i w_{i,sh}} \tag{19.36}$$

where $w_{i,ca}$ and $w_{i,sh}$ are the contribution of cohort i to canopy and shrub strata loading (in $kg \cdot m^{-2}$), respectively, and $\sigma(SP_i)$ is the species-specific surface-area-to-volume ratio. The surface-area-to-volume ratio of herbs is assumed constant $\sigma_{he} = 11483 m^2 \cdot m^{-3} = 3500 ft^2 \cdot ft^{-3}$ and that of small (1-h) woody fuels is $\sigma_{wo} = 1601.05 m^2 \cdot m^{-3} = 488 ft^2 \cdot ft^{-3}$. The surface-area-to-volume ratio for the litter stratum is:

$$\sigma_{li} = \frac{\sum_k w_{li,k} \cdot \sigma_k}{\sum_k w_{li,k}} \tag{19.37}$$

and the surface-area-to-volume ratio for litter types are:

$$\sigma_{shortneedlepine} = 6562 m^2 \cdot m^{-3} = 2000 ft^2 \cdot ft^{-3} \tag{19.38}$$

$$\sigma_{longneedlepine} = 4921 m^2 \cdot m^{-3} = 1500 ft^2 \cdot ft^{-3} \tag{19.39}$$

$$\sigma_{otherconifer} = 8202 m^2 \cdot m^{-3} = 2500 ft^2 \cdot ft^{-3} \tag{19.40}$$

$$\sigma_{hardwood} = 8202 m^2 \cdot m^{-3} = 2500 ft^2 \cdot ft^{-3} \tag{19.41}$$

19.3.6.5   Fuel area index (FAI)

The fuel area index (FAI) is the total fuel surface area per unit of ground area (unitless). It is analogous to leave area index (LAI), and it is used to calculate FCCS fire potentials (Schaaf et al., 2007). For shrub and canopy strata, FAI is calculated as:

$$FAI_{ca} = \sum_i FAI_{i,ca} = \sum_i PV_{i,ca} \cdot \sigma(SP_i) \tag{19.42}$$

$$FAI_{sh} = \sum_i FAI_{i,sh} = \sum_i PV_{i,sh} \cdot \sigma(SP_i) \tag{19.43}$$

where $FAI_{i,ca}$ and $FAI_{i,sh}$ are the FAI of cohort i in the canopy and shrub strata, respectively. The FAI of herbs and woody strata are given by:

$$FAI_{he} \quad = PV_{he} \cdot \sigma_{he} \tag{19.44}$$

$$FAI_{wo} \quad = PV_{wo} \cdot \sigma_{wo} \tag{19.45}$$

For the litter layer, FAI is calculated as a sum of FAI for litter components:

$$FAI_{li} = \sum_k FAI_{li,k} = \sum_k PV_{li,k} \cdot \sigma_k \tag{19.46}$$

19.3.6.6   Moisture (M)

Live foliar moisture (in percent of dry weight) is also averaged across cohorts composing the shrub or canopy strata:

$$M_{live,sh} \quad = \frac{\sum_i w_{i,sh} \cdot M_i}{\sum_i w_{i,sh}} \tag{19.47}$$

$$M_{live,ca} \quad = \frac{\sum_i w_{i,ca} \cdot M_i}{\sum_i w_{i,ca}} \tag{19.48}$$

Live foliar moisture of herb stratum ($M_{live,he}$) is an input. The moisture of dead plant in the canopy and shrub layers ($M_{dead,ca}$ and $M_{dead,sh}$), the moisture of dead herbs ($M_{dead,he}$), as well as that of litter (M_{li}) and woody (M_{wo}) strata are all assumed equal to the moisture of 1-h dead fuels, which is an input of the model.

19.3.6.7   Proportion of dead fuel (P_{dead})

Woody and litter strata are dead fuels, but for canopy, shrub and herb strata the proportion of fuels that are dead are variable. The proportion of dead fuels in the herbaceous stratum ($P_{dead,he}$) is an input of the model, but for the shrub and canopy strata these are calculated from the proportion of dead fuels in each cohort:

$$P_{dead,sh} \quad = \frac{\sum_i w_{i,sh} \cdot P_{dead,i}}{\sum_i w_{i,sh}} \tag{19.49}$$

$$P_{dead,ca} \quad = \frac{\sum_i w_{i,ca} \cdot P_{dead,i}}{\sum_i w_{i,ca}} \tag{19.50}$$

19.3.6.8 Low heat content (h)

The low fuel heat content of each surface fuel stratum (in $kJ \cdot kg^{-1}$) is used for the calculation of reaction intensity. Heat content values are adjusted for live foliar moisture content in canopy, shrub and herb strata; and are left to the default value for woody and litter strata:

$$
\begin{aligned}
h_{ca} &= h_{ca,def} - (M_{live,ca}/100) \cdot V & (19.51)\\
h_{sh} &= h_{sh,def} - (M_{live,sh}/100) \cdot V & (19.52)\\
h_{he} &= h_{def} - (M_{live,he}/100) \cdot V & (19.53)\\
h_{wo} &= h_{li} = h_{def} & (19.54)
\end{aligned}
$$

where $h_{def} = 18608 kJ \cdot kg^{-1} = 8000 Btu \cdot lb^{-1}$ is the default low heat content value for herbs, woody and litter strata, and $V = 2596 kJ \cdot kg^{-1} = 1116 Btu \cdot lb$ is the latent heat of vaporisation of water. The default low heat of contents for the canopy and shrub strata ($h_{ca,def}$ and $h_{sh,def}$) are calculated as a weighted average across cohorts:

$$
\begin{aligned}
h_{ca,def} &= \frac{\sum_i w_{i,ca} \cdot h(SP_i)}{\sum_i w_{i,ca}} & (19.55)\\
h_{sh,def} &= \frac{\sum_i w_{i,sh} \cdot h(SP_i)}{\sum_i w_{i,sh}} & (19.56)
\end{aligned}
$$

where $h(SP_i)$ is a species-specific low heat content value.

19.3.6.9 Flammability index (η_F)

Flammability index ($\eta_F \in [1, 2]$) is a multiplier of reaction efficiency based on expert opinion applied to species that burn with more intensity than others, resulting from differences in fuel chemistry. Flammability index of canopy and shrub strata are the result of averaging the flammability of cohorts using loading as weights:

$$
\begin{aligned}
\eta_{F,ca} &= \frac{\sum_i w_{i,ca} \cdot \eta_F(SP_i)}{\sum_i w_{i,ca}} & (19.57)\\
\eta_{F,sh} &= \frac{\sum_i w_{i,sh} \cdot \eta_F(SP_i)}{\sum_i w_{i,sh}} & (19.58)
\end{aligned}
$$

where $\eta_F(SP_i)$ is a species-specific flammability value. Flamability index for other strata are set to default values:

$$\eta_{F,he} \quad = \eta_{F,li} = 1.5 \tag{19.59}$$
$$\eta_{F,wo} \qquad = 1.0 \tag{19.60}$$

19.3.6.10   Reactive volume (RV)

The volume per surface unit ($m^3 \cdot m^{-2}$) that would be involved in flaming combustion.

$$
\begin{aligned}
RV_{sh} &= w_{shrub}/\rho_{p,sh} & (19.61)\\
RV_{he} &= w_{he}/\rho_{p,he} & (19.62)\\
RV_{wo} &= w_{wo}/\rho_{p,wo} & (19.63)\\
RV_{li} &= \min(w_{li}, w_{\max,li})/\rho_{p,li} & (19.64)
\end{aligned}
$$

In the case of litter, the flame loading is limited by $w_{\max,li}$, the maximum loading that would be consumed in the flaming stage of combustion, calculated as a weighted average of litter types:

$$w_{\max,li} = \frac{\sum_k w_{\max,k} \cdot w_{li,k}}{\sum_k \cdot w_{li,k}} \tag{19.65}$$

where k indicates litter type. The maximum combustion loadings for litter types are [Prichard et al. (2013); Table 2]:

$$
\begin{aligned}
w_{\max,shortneedlepine} &= w_{\max,otherconifer} = 0.3248 kg \cdot m^{-2} = 2900 lb \cdot ac^{-1} & (19.66)\\
w_{\max,longneedlepine} &= 0.6496 kg \cdot m^{-2} = 5800 lb \cdot ac^{-1} & (19.67)\\
w_{\max,hardwood} &= 0.3472 kg \cdot m^{-2} = 3100 lb \cdot ac^{-1} & (19.68)
\end{aligned}
$$

19.3.7   Unit conversion of fuel characteristics

FCCS calculations employ empirical equations that were derived in British units system. Hence, all the fuel characteristics and model inputs that are in metric units have to be translated into British units prior to fire behaviour calculations:

- Loading: $1 kg \cdot m^{-2} = 0.204918 lb \cdot ft^{-2}$
- Depths: $1m = 3.2808399 ft$
- Particle density and bulk density: $1 kg \cdot m^{-3} = 0.06242796 lb \cdot ft^{-3}$
- Particle volume and reactive volume: $1 m^3 \cdot m^{-2} = 3.2808399 ft^3 \cdot ft^{-2}$
- Surface-to-area-volume ratio: $1 m^2 \cdot m^{-3} = 0.3048 ft^2 \cdot ft^{-3}$
- Heat content: $1 kJ \cdot kg^{-1} = 0.429922614 Btu \cdot lb^{-1}$
- Wind speed: $1 m \cdot s^{-1} = 2.23693629 mph$

19.4 Surface fire behavior

19.4.1 Surface rate of spread (R)

In the Rothermel (1972) model, surface rate of spread is defined as the ratio of heat source (i.e. the surface fire energy propagated to unburned fuels) to surface fuel heat sink (i.e. the energy required to preheat fuels). Owing to the difference in packing ratio between the litter stratum and the other surface fuels, litter-dominated fuelbeds may have substantially different spread rates than other fuelbeds. For this reason, in FCCS the rate of spread (in $ft \cdot min^{-1}$) is calculated separately for litter stratum and the final rate of spread is the maximum of the rate of spread of all surface fuels and that of the litter stratum. Rate of spread is also limited to a maximum based in windspeed and slope.

$$R = \min(WindSlopeCap, \max(R_{surf}, R_{litter})) \tag{19.69}$$

The surface fuel and litter fuel rates of spread are given by the application of Rothermel's (1972) equation to each case:

$$R_{surf} \quad = \frac{I_{R,surf} \cdot \xi_{surf} \cdot (1 + \phi_W + \phi_S)}{q_{surf}} \tag{19.70}$$

$$R_{litter} \quad = \frac{I_{R,litter} \cdot \xi_{litter} \cdot (1 + \phi_W + \phi_S)}{q_{litter}} \tag{19.71}$$

where $I_{R,surf}$ and $I_{R,litter}$ are the reaction intensities (in $Btu \cdot ft^{-2} \cdot min^{-1}$), ξ_{surf} and ξ_{litter} are the propagating flux ratios, q_{surf} and q_{litter} are the heat sinks. Finally, ϕ_W and ϕ_S are the slope and wind modifiers. All of them are explained in the following sections. The maximum rate of spread calculated from windspeed and slope is:

$$WindSlopeCap = 88 \cdot U \cdot (1 + \phi_S) \tag{19.72}$$

where U is windspeed (in mph) and 88 is a conversion factor (from mph to ft/min).

19.4.1.1 Reaction intensity (I_R)

Reaction intensity of surface fuels (in $Btu \cdot ft^{-2} \cdot min^{-1}$) is calculated as the sum of component reaction intensities of the four different surface fuel strata, whereas the reaction intensity in the litter uses this strata alone:

$$I_{R,surf} \quad = I_{R,sh} + I_{R,he} + I_{R,wo} + I_{R,li} \tag{19.73}$$

$$I_{R,litter} \qquad \qquad = I_{R,li} \tag{19.74}$$

Each component reaction intensity is calculated using:

$$I_{R,sh} = (\eta_{\beta'_{allsurf}})^{A_{sh}} \cdot \Gamma'_{\max,sh} \cdot w_{sh} \cdot h_{sh} \cdot \eta_{M,sh} \cdot \eta_{K,sh} \cdot \eta_{F,sh} \quad (19.75)$$

$$I_{R,he} = (\eta_{\beta'_{lowsurf}})^{A_{he}} \cdot \Gamma'_{\max,he} \cdot w_{he} \cdot h_{he} \cdot \eta_{M,he} \cdot \eta_{K,he} \cdot \eta_{F,he} \quad (19.76)$$

$$I_{R,wo} = (\eta_{\beta'_{lowsurf}})^{A_{wo}} \cdot \Gamma'_{\max,wo} \cdot w_{wo} \cdot h_{wo} \cdot \eta_{M,wo} \cdot \eta_{K,wo} \cdot \eta_{F,wo} \quad (19.77)$$

$$I_{R,li} = (\eta_{\beta'_{litter}})^{A_{li}} \cdot \Gamma'_{\max,li} \cdot w_{li} \cdot h_{li} \cdot \eta_{M,li} \cdot \eta_{K,li} \cdot \eta_{F,li} \quad (19.78)$$

In the above equations, w_{sh}, w_{he}, w_{wo} and w_{li} are the loadings of the corresponding shrub, herb, woody and litter strata, respectively. These quantities were defined in previous sections, as were the corresponding low heat fuel contents (h_{sh}, h_{he}, h_{wo} and h_{li}) and flammability indices ($\eta_{F,sh}$, $\eta_{F,he}$, $\eta_{F,wo}$ and $\eta_{F,li}$). Mineral damping coefficient (η_K; dimensionless) is set to the same value (corresponding to the conventional value for silica-free ash content of 1%) for all strata:

$$\eta_{K,sh} = \eta_{K,he} = \eta_{K,wo} = \eta_{K,li} = 0.42 \quad (19.79)$$

In the following subsections, we describe the calculation of the remaining variables for each stratum: reaction efficiency ($\eta_{\beta'}$), Rothermel's A parameter, maximum reaction velocity ($\Gamma'_{\max}$) and moisture damping coefficient (η_M).

19.4.1.2 Reaction efficiency ($\eta_{\beta'}$)

Reaction efficiency (between 0 and 1) represents the damping effect of inefficiently packed fuels in the reaction intensity. Because shrubs rarely burn without lower surface fuels, the reaction efficiency of the surface layer ($\eta_{\beta'_{allsurf}}$) includes shrubs, herbs and woody fuels. Low surface fuels may carry flames without involving shrubs, so are assumed to burn with a single reaction efficiency ($\eta_{\beta'_{lowsurf}}$) determined by the combined characteristics of herb and woody fuel strata. Both are calculated similarly:

$$\eta_{\beta'_{allsurf}} = \beta'_{allsurf} \cdot e^{1-\beta'_{allsurf}} \quad (19.80)$$

$$\eta_{\beta'_{lowsurf}} = \beta'_{lowsurf} \cdot e^{1-\beta'_{lowsurf}} \quad (19.81)$$

where $\beta'_{allsurf}$ and $\beta'_{lowsurf}$ are the relative packing ratios corresponding to all surface fuels and low surface fuels, respectively. Relative packing ratios (β'; dimensionless) are defined as the ratio of optimum depth (δ_{opt}) to effective depth (δ_{eff}):

$$\beta'_{allsurf} \quad = \delta_{opt,allsurf}/\delta_{eff,allsurf} \tag{19.82}$$
$$\beta'_{lowsurf} \quad = \delta_{opt,lowsurf}/\delta_{eff,lowsurf} \tag{19.83}$$

Optimum depth is the depth (in ft) at which fuels are optimally packed for maximum reaction intensity:

$$\delta_{opt,allsurf} \quad = PV_{allsurf} + OptAirVol_{allsurf} \tag{19.84}$$
$$\delta_{opt,lowsurf} \quad = PV_{lowsurf} + OptAirVol_{lowsurf} \tag{19.85}$$

where $PV_{allsurf}$ and $PV_{lowsurf}$ are the volume of particles (in $ft^3 \cdot ft^{-2}$) for all surface fuels and low surface fuels, respectively, given by:

$$PV_{allsurf} \quad = PV_{sh} + PV_{he} + PV_{wo} \tag{19.86}$$
$$PV_{lowsurf} \quad \quad = PV_{he} + PV_{wo} \tag{19.87}$$

$OptAirVol_{allsurf}$ and $OptAirVol_{allsurf}$ are the volume of air space (in $ft^3 \cdot ft^{-2}$) between fuel particles that would result in maximum reaction intensity:

$$OptAirVol_{allsurf} \quad = 45 \cdot (RV_{sh} + RV_{he} + RV_{wo}) \tag{19.88}$$
$$OptAirVol_{lowsurf} \quad \quad = 45 \cdot (RV_{he} + RV_{wo}) \tag{19.89}$$

On the other hand, effective depths of all surface fuels and low surface fuels (in ft) are calculated as their depth, weighted by the reactive volume (and percentage cover in FCCS):

$$\delta_{eff,allsurf} \quad = \frac{(RV_{sh} \cdot \delta_{sh}) + (RV_{he} \cdot \delta_{he}) + (RV_{wo} \cdot \delta_{wo})}{RV_{sh} + RV_{he} + RV_{wo}} \tag{19.90}$$
$$\delta_{eff,lowsurf} \quad \quad = \frac{(RV_{he} \cdot \delta_{he}) + (RV_{wo} \cdot \delta_{wo})}{RV_{he} + RV_{wo}} \tag{19.91}$$

Reaction efficiency of the litter stratum is determined separately from the other strata. It is defined as the average of reaction efficiency across litter types, calculated using loadings as weights:

$$\eta_{\beta'_{litter}} = \frac{\sum_k \eta_{\beta'_k} \cdot w_{li,k}}{\sum_k \cdot w_{li,k}} \tag{19.92}$$

where k indicates litter type. The reaction efficiencies of litter types are [Prichard et al. (2013); Table 2]:

$$\eta_{\beta'_{shortneedlepine}} = \eta_{\beta'_{otherconifer}} = 0.18 \tag{19.93}$$

$$\eta_{\beta'_{longneedlepine}} = 0.27 \tag{19.94}$$

$$\eta_{\beta'_{hardwood}} = 0.11 \tag{19.95}$$

19.4.1.3   Rothermel's A

A dimensionless coefficient that modifies reaction's efficiency (eq. (19.81)) to account for lower sensitivity of reaction efficiency to relative packing ratio in flash fuels:

$$A_{wo} = A_{li} = 1.0 \tag{19.96}$$

$$A_{sh} = 133 \cdot \sigma_{sh}^{-0.7913} \tag{19.97}$$

$$A_{he} = 133 \cdot \sigma_{he}^{-0.7913} \tag{19.98}$$

where σ_{sh} and σ_{he} have to be expressed in $ft^2 \cdot ft^{-3}$; Values 133 and -0.7913 are empirical constants (Rothermel, 1972).

19.4.1.4   Maximum reaction velocity $(\Gamma'_{\max})$

The reaction velocity (in min^{-1}) that would exist at optimum fuelbed depth with no fuel moisture or mineral content.

$$\Gamma'_{\max,sh} = 9.495 \cdot \frac{\sigma_{sh}}{\sigma_{wo}} \tag{19.99}$$

$$\Gamma'_{\max,he} = 9.495 \cdot \frac{\sigma_{he}}{\sigma_{wo}} \tag{19.100}$$

$$\Gamma'_{\max,wo} = 9.495 \tag{19.101}$$

$$\Gamma'_{\max,li} = 15 \tag{19.102}$$

where $\sigma_{wo} = 488 ft^2 \cdot ft^{-3} = 1601.05 m^2 \cdot m^{-3}$ is the surface-to-area-volume ratio typical of small woody fuels. In Prichard et al. (2013) σ_{sh} is defined as the average of shrub foliar surface-to-area-volume ratio and σ_{wo}, but in our case $\sigma_{(SP_i)}$ for each species includes both leaves and small branches. Eq. (19.102) represent a significant departure from Rothermel (1972) maximum reaction velocity, and are also different from Sandberg et al. (2007).

19.4.1.5 Moisture damping coefficient (η_M)

Moisture damping reduces reaction velocity and hence reaction intensity (eq. (19.74)). It is calculated for each stratum using the following regression equations:

$$\eta_{M,live,sh} = \left[1 - 2.59 \cdot \left(\frac{M_{live,sh}}{X_{live,sh}}\right)\right] + \left[5.11 \cdot \left(\frac{M_{live,sh}}{X_{live,sh}}\right)^2\right] - \left[3.52 \cdot \left(\frac{M_{live,sh}}{X_{live,sh}}\right)^3\right] \tag{19.103}$$

$$\eta_{M,dead,sh} = \left[1 - 2.59 \cdot \left(\frac{M_{dead,sh}}{X_{dead,sh}}\right)\right] + \left[5.11 \cdot \left(\frac{M_{dead,sh}}{X_{dead,sh}}\right)^2\right] - \left[3.52 \cdot \left(\frac{M_{dead,sh}}{X_{dead,sh}}\right)^3\right] \tag{19.104}$$

$$\eta_{M,live,he} = \left[1 - 2.59 \cdot \left(\frac{M_{live,he}}{X_{live,he}}\right)\right] + \left[5.11 \cdot \left(\frac{M_{live,he}}{X_{live,he}}\right)^2\right] - \left[3.52 \cdot \left(\frac{M_{live,he}}{X_{live,he}}\right)^3\right] \tag{19.105}$$

$$\eta_{M,dead,he} = \left[1 - 2.59 \cdot \left(\frac{M_{dead,he}}{X_{dead,he}}\right)\right] + \left[5.11 \cdot \left(\frac{M_{dead,he}}{X_{dead,he}}\right)^2\right] - \left[3.52 \cdot \left(\frac{M_{dead,he}}{X_{dead,he}}\right)^3\right] \tag{19.106}$$

$$\eta_{M,wo} = \left[1 - 2.59 \cdot \left(\frac{M_{wo}}{X_{wo}}\right)\right] + \left[5.11 \cdot \left(\frac{M_{wo}}{X_{wo}}\right)^2\right] - \left[3.52 \cdot \left(\frac{M_{wo}}{X_{wo}}\right)^3\right] \tag{19.107}$$

$$\eta_{M,li} = \left[1 - 2.59 \cdot \left(\frac{M_{li}}{X_{li}}\right)\right] + \left[5.11 \cdot \left(\frac{M_{li}}{X_{li}}\right)^2\right] - \left[3.52 \cdot \left(\frac{M_{li}}{X_{li}}\right)^3\right] \tag{19.108}$$

where moisture contents of extinctions were arbitrarily set to $X_{dead,sh} = X_{dead,he}X_{wo} = X_{li} = 25$, $X_{live,sh} = 180$ and $X_{live,he} = 120$ in Sandberg et al. (2007). As it can be seen in the equations above, in the case of shrub and herb strata, moisture damping of live and dead fuels are differentiated. Average values are found after accounting for the proportion of live and dead material:

$$\eta_{M,sh} = \eta_{M,live,sh} \cdot (1 - P_{dead,sh}) + \eta_{M,dead,sh} \cdot P_{dead,sh} \tag{19.109}$$

$$\eta_{M,he} = \eta_{M,live,he} \cdot (1 - P_{dead,he}) + \eta_{M,dead,he} \cdot P_{dead,he} \tag{19.110}$$

19.4.1.6 Propagating flux ratio (ξ)

The propagating flux ratio (dimensionless) is the proportion of the reaction intensity (eq. (19.74)) that contributes to the forward rate of spread, estimated using an empirical regression:

$$\xi_{surf} = 0.03 + 2.5 \cdot \min\left[0.06, \frac{RV_{sh} + RV_{he} + RV_{wo} + RV_{li}}{\delta_{surfheatsink}}\right] \tag{19.111}$$

$$\xi_{litter} = 0.03 + 2.5 \cdot \min\left[0.06, \frac{RV_{li}}{\delta_{li}}\right] \tag{19.112}$$

where $\delta_{surfheatsink}$ is the depth of surface heat sink (in ft), which in Prichard et al. (2013) is calculated as the sum of strata depths weighted by their relative

cover. In our case we weighted stratum depths as in the calculation of effective depth ($\delta_{eff,allsurf}$), but considering all four strata:

$$\delta_{surfheatsink} = \frac{(RV_{sh} \cdot \delta_{sh}) + (RV_{he} \cdot \delta_{he}) + (RV_{wo} \cdot \delta_{wo}) + (RV_{li} \cdot \delta_{li})}{RV_{sh} + RV_{he} + RV_{wo} + RV_{li}}$$

(19.113)

19.4.2   Heat sink (q)

Like reaction intensity, the heat sink term (in $Btu \cdot ft^{-3}$) of the rate of spread equation is calculated in FCCS for each fuel stratum and then summed:

$$q_{surf} \quad = q_{sh} + q_{he} + q_{wo} + q_{li} \qquad (19.114)$$

$$q_{litter} \qquad\qquad = q_{li} \qquad\qquad\qquad (19.115)$$

where the heat sink for each stratum is:

$$q_{sh} \quad = \eta_{\beta'_{surf}} \cdot \frac{RV_{sh} \cdot \rho_{p,sh} \cdot Qig_{sh}}{\min(\delta_{sh}, 1ft)} \qquad (19.116)$$

$$q_{he} \quad = \eta_{\beta'_{lowsurf}} \cdot \frac{RV_{he} \cdot \rho_{p,he} \cdot Qig_{he}}{\min(\delta_{he}, 1ft)} \qquad (19.117)$$

$$q_{wo} \quad = \eta_{\beta'_{lowsurf}} \cdot \frac{RV_{wo} \cdot \rho_{p,wo} \cdot Qig_{wo}}{\min(\delta_{wo}, 1ft)} \qquad (19.118)$$

$$q_{li} \qquad = \eta_{\beta'_{li}} \cdot \frac{RV_{li} \cdot \rho_{p,li} \cdot Qig_{li}}{\min(\delta_{li}, 1ft)} \qquad (19.119)$$

Where $\rho_{p,sh}$, $\rho_{p,he}$, $\rho_{p,wo}$ and $\rho_{p,li}$ are the particle densities (in $lb \cdot ft^{-3}$) of each fuel stratum; and RV_{sh}, RV_{he}, RV_{wo}, and RV_{li} are the reactive volumes of each fuel stratum. Unlike in Sandberg et al. (2007), the calculated heat sink is corrected by the reaction-efficiency term ($\eta_{\beta'_{surf}}$, $\eta_{\beta'_{lowsurf}}$ or $\eta_{\beta'_{li}}$), and the effective depth of each stratum included is limited to 1ft, based on the assumption that it is not necessary to preheat more than one 1ft of depth within a stratum to achieve ignition.

Heat of pre-ignition (Qig; in $Btu \cdot lb^{-1}$) is the amount of heat required to ignite $1lb$ of fuel. It is calculated by stratum as a weighted average of live and dead fuels in shrubs and herbs.

$$Qig_{sh} \quad = Qig_{live,sh} \cdot (1 - P_{dead,sh}) + Qig_{dead,sh} \cdot P_{dead,sh} \qquad (19.120)$$

$$Qig_{he} \quad = Qig_{live,he} \cdot (1 - P_{dead,he}) + Qig_{dead,he} \cdot P_{dead,he} \qquad (19.121)$$

Whereas $Qig_{live,sh}$ and $Qig_{live,he}$ are corrected by fuel moisture, $Qig_{dead,sh}$, $Qig_{dead,he}$ and the other strata (Qig_{wo} and Qig_{li}) are assumed a constant value:

$$Qig_{live,sh} \quad = 250 + (V \cdot (M_{live,sh}/100)) \tag{19.122}$$
$$Qig_{live,he} \quad = 250 + (V \cdot (M_{live,he}/100)) \tag{19.123}$$
$$Qig_{dead,sh} \quad = Qig_{dead,he} = Qig_{wo} = Qig_{li} = 250 \tag{19.124}$$

where $250 Btu/lb$ is the heat of preignition of dry cellulose and $V = 1116 Btu/lb$ is the latent heat of vaporization.

19.4.3 Wind and slope coefficients (ϕ_W and ϕ_S)

Wind and slope coefficients modify the heat source term of the rate of spread equation. Owing to differences in fuel characteristics and boundary conditions between the litter stratum and other surface fuel strata, in FCCS wind and slope coefficients are calculated separately for the litter stratum. The wind and slope coefficients terms in the rate fo spread equation are a weighted average of litter and surface wind and slope coefficients using the relative contribution to reaction intensity as weights:

$$\phi_W \quad = (1 - I_{R,litter}/I_{R,surf}) \cdot \phi_{W,surf} + (I_{R,litter}/I_{R,surf}) \cdot \phi_{W,litter} \tag{19.125}$$
$$\phi_S \quad = (1 - I_{R,litter}/I_{R,surf}) \cdot \phi_{S,surf} + (I_{R,litter}/I_{R,surf}) \cdot \phi_{S,litter} \tag{19.126}$$

Wind coefficients are calculated using:

$$\phi_{W,surf} \quad = 8.8 \cdot \beta'^{-E}_{surf} \cdot (U/BMU)^B \tag{19.127}$$
$$\phi_{W,litter} \quad = 8.8 \cdot \beta^{-E}_{litter} \cdot (U/BMU)^B \tag{19.128}$$

where U is the input midflame windspeed (in $ft \cdot min^{-1}$), $BMU = 352 ft \cdot min^{-1}$ is the benchmark midflame windspeed, β'_{surf} is the relative packing ratio (eq. 19.83), B is the exponential response of wind coefficient to windspeed ($B = 1.2$ in Sandberg et al. (2007)), and E is the exponential term representing the mild effect of large fuels in reducing the accelerating effect of wind on fire spread by attenuating wind flow, given by:

$$E = 0.55 - 0.2 \cdot \frac{FAI_{sh} + FAI_{he}}{FAI_{sh} + FAI_{he} + FAI_{wo}} \tag{19.129}$$

E is assumed to be the same for both all surface fuels and litter fuels.

Slope coefficients are calculated using the empirical equation of Rothermel (1972), applied to all surface fuels and litter fuels:

$$\phi_{S,surf} = 5.275 \cdot (S/100)^2 \cdot (\beta_{sh} + \beta_{he} + \beta_{wo})^{-0.3} \tag{19.130}$$

$$\phi_{S,litter} = 5.275 \cdot (S/100)^2 \cdot \beta_{li}^{-0.3} \tag{19.131}$$

where S is the slope (in percent) and β is the packing ratio (not relative!) of fuels.

19.4.4 Fireline intensity (I_B) and flame length (FL)

Byram's fireline intensity (I_B) is the rate of heat release per unit of fire edge (in $Btu \cdot ft^{-1} \cdot min^{-1}$), and in FCCS is calculated as (Albini, 1976):

$$I_B = I_{R,surf} \cdot (R \cdot t_R) \tag{19.132}$$

where $I_{R,surf}$ is the surface reaction intensity, R is the rate of spread and t_R is the flame residence time, which is defined as the time (in min) fuels contribute to propagating flux and is estimated as Albini (1976):

$$t_R = 192 \cdot \frac{(I_{R,sh} \cdot RT_{sh}) + (I_{R,he} \cdot RT_{he}) + (I_{R,wo} \cdot RT_{wo}) + (I_{R,li} \cdot RT_{li})}{I_{R,surf}} \tag{19.133}$$

where RT is the reaction thickness, the approximate thickness (in ft) of a fuel element shell that contributes to reaction intensity. In FCCS, reaction thickness is estimated as $RT = 0.0028 ft$ for thermally thick fuel elements (Sandberg et al., 2007). When the diameter of a fuel element is less than twice the reaction thickness, the entire fuel element contributes to reaction intensity. Reaction thickness values for each stratum are given by:

$$RT_{sh} = \min(0.0028, 2/\sigma_{sh}) \tag{19.134}$$

$$RT_{he} = \min(0.0028, 2/\sigma_{he}) \tag{19.135}$$

$$RT_{wo} = \min(0.0028, 2/\sigma_{wo}) \tag{19.136}$$

$$RT_{li} = \min(0.0028, 2/\sigma_{li}) \tag{19.137}$$

Flame length is defined as the distance (in ft) between the flame tip and the midpoint of the flame depth at the base of the flame, and is calculated (Byram, 1959):

$$FL = 0.45 \cdot (I_B/60)^{0.46} \tag{19.138}$$

where 60.0 is a factor to convert from $Btu \cdot ft^{-1} \cdot min^{-1}$ to $Btu \cdot ft^{-1} \cdot s^{-1}$.

19.5 Crown fire behavior

Crown fire behavior is difficult to model and actual rates of spread are not possible to predict. Here we mainly follow the approach given in FCCS (Prichard et al., 2013), although in our case the canopy is not subdivided into layers (overstory, midstory and understory).

19.5.1 Crown fire rate of spread (R_{crown})

The rate of spread of crown fires is estimated by using a modification of Rothermel's equation:

$$R_{crown} = \frac{I_{R,crown} \cdot \xi_{crown} \cdot WAF}{q_{crown}} = \frac{(I_{R,surf} + I_{R,ca}) \cdot \xi_{crown} \cdot WAF}{q_{surf} + q_{ca}} \tag{19.139}$$

where $I_{R,surf}$ is the surface reaction intensity, $I_{R,ca}$ is the canopy reaction intensity, ξ_{crown} is the propagating flux ratio in the canopy, q_{surf} is the surface heat sink and q_{ca} is the canopy heat sink. Note that reaction intensities and heat sinks of canopy and surface fuels are added for the application of Rothermel's equation. Other modifications include the exclusion of slope effects and the consideration of wind effects through a wind adjustment factor (WAF).

Crown propagating flux ratio (ξ_{crown}; in $Btu \cdot ft^{-3}$) represents the proportion of the crown reaction intensity that contributes to crown fire's forward rate of spread:

$$\xi_{crown} = 1 - e^{\left(-\frac{FAI_{ca}}{4 \cdot \delta_{ca}}\right)} \tag{19.140}$$

where FAI_{ca} is the fuel area index of the canopy, and δ_{ca} is the canopy depth (in ft). Wind adjustment factor (WAF) is defined as:

$$WAF = \frac{U/\sqrt{U^2 + VS^2}}{BMU/\sqrt{BMU^2 + VS^2}} \tag{19.141}$$

where U is the input (midflame) windspeed (in $ft \cdot min^{-1}$), $BMU = 352ft \cdot min^{-1}$ is the benchmark windspeed and $VS = 900ft \cdot min^{-1}$ is the vertical stack velocity.

The following two subsections detail the calculation of canopy reaction intensity $(I_{R,ca})$ and canopy heat sink (q_{ca}).

19.5.2   Canopy reaction intensity $(I_{R,ca})$

Reaction intensity of canopy fuels (in $Btu \cdot ft^{-2} \cdot min^{-1}$) is estimated as:

$$I_{R,ca} = (\eta_{\beta'_{ca}})^{A_{ca}} \cdot \Gamma'_{max,ca} \cdot w_{ca} \cdot h_{ca} \cdot \eta_{M,ca} \cdot \eta_{K,ca} \cdot \eta_{F,ca} \tag{19.142}$$

where $A_{ca} = 133 \cdot \sigma_{ca}^{-0.7913}$ is Rothermel's A coefficient, $\Gamma'_{max,ca} = 15 min^{-1}$ is the maximum reaction velocity of the canopy, w_{ca} is the loading of canopy fuels (in $lb \cdot ft^{-2}$), h_{ca} is the heat content of the canopy fuels (in $Btu \cdot lb^{-1}$), $\eta_{K,ca} = 0.42$ is the mineral damping coefficient and $\eta_{F,ca}$ is the flammability index of the canopy stratum. Moisture damping coefficient for the canopy $(\eta_{M,ca})$ is estimated as done for shrub and herb strata:

$$\eta_{M,live,ca} = \left[1 - 2.59 \cdot \left(\frac{M_{live,ca}}{X_{live,ca}}\right)\right] + \left[5.11 \cdot \left(\frac{M_{live,ca}}{X_{live,ca}}\right)^2\right] - \left[3.52 \cdot \left(\frac{M_{live,ca}}{X_{live,ca}}\right)^3\right] \tag{19.143}$$

$$\eta_{M,dead,ca} = \left[1 - 2.59 \cdot \left(\frac{M_{dead,ca}}{X_{dead,ca}}\right)\right] + \left[5.11 \cdot \left(\frac{M_{dead,ca}}{X_{dead,ca}}\right)^2\right] - \left[3.52 \cdot \left(\frac{M_{dead,ca}}{X_{dead,ca}}\right)^3\right] \tag{19.144}$$

$$\eta_{M,ca} = \eta_{M,live,ca} \cdot (1 - P_{dead,ca}) + \eta_{M,dead,ca} \cdot P_{dead,ca} \tag{19.145}$$

where moisture contents of extinctions were arbitrarily set to $X_{dead,ca} = 25$ and $X_{live,ca} = 180$.

The reaction efficiency in the canopy $(\eta_{\beta'_{canopy}})$ represents the damping effect of inefficiently packed fuels in the canopy:

$$\eta_{\beta'_{canopy}} = \beta'_{canopy} \cdot e^{1-\beta'_{canopy}} \tag{19.146}$$

where β'_{canopy} is the relative packing ratio in the canopy:

$$\beta'_{canopy} = \delta_{opt,canopy}/\delta_{eff,canopy} \tag{19.147}$$

where the effective depth is $\delta_{eff,canopy} = \delta_{ca}$ (in ft) and the optimum canopy depth is calculated using:

$$\delta_{opt,canopy} = 0.4 \cdot FAI_{ca} + \beta_{ca} \cdot (\delta_{ca} \cdot C_{ca}/100) \tag{19.148}$$

where C_{ca} is the percent cover of the canopy, FAI_{ca} is the fuel area index of the canopy, β_{ca} is the packing ratio of canopy fuels and δ_{ca} is the canopy depth (in ft).

19.5.3 Canopy heat sink (q_{ca})

Canopy heat sink (in $Btu \cdot ft^{-3}$) is estimated using:

$$q_{ca} = \frac{0.5 \cdot FAI_{ca} \cdot RT_{ca} \cdot \rho_{p,ca} \cdot Qig_{ca}}{(C_{ca}/100) \cdot \delta_{ca}} \tag{19.149}$$

where C_{ca} is the percent cover of the canopy, FAI_{ca} is the fuel area index of the canopy, $RT_{ca} = \min(0.0028, 2/\sigma_{ca})$ is the reaction thickness of the canopy stratum (in ft), $\rho_{p,ca}$ is the particle density of the canopy (in $lb \cdot ft^{-3}$), δ_{ca} is the canopy depth (in ft) and Qig_{ca} is the heat of pre-ignition of the canopy stratum (in $Btu \cdot lb^{-1}$), which is calculated as a weighted average of live and dead fuels:

$$\begin{align}
Qig_{live,ca} &= 250 + (V \cdot (M_{live,ca}/100)) \tag{19.150}\\
Qig_{dead,ca} &= 250 \tag{19.151}\\
Qig_{ca} &= Qig_{live,ca} \cdot (1 - P_{dead,ca}) + Qig_{dead,ca} \cdot P_{dead,ca} \tag{19.152}
\end{align}$$

where $250 Btu/lb$ is the heat of preignition of dry cellulose and $V = 1116 Btu/lb$ is the latent heat of vaporization of water.

19.5.4 Fireline intensity $(I_{B,crown})$ and flame length (FL_{crown})

Byram's fireline intensity for crown fires is estimated using:

$$I_{B,crown} = I_{R,crown} \cdot (R_{crown} \cdot t_{R,crown}) \tag{19.153}$$

where $I_{R,crown}$ is the crown reaction intensity (i.e. the sum of canopy and surface reaction intensities), R_{crown} is the rate of crown fire spread and $t_{R,crown}$ is the flame residence time, estimated as:

$$t_R = 192 \cdot RT_{ca} \tag{19.154}$$

where $RT_{ca} = \min(0.0028, 2/\sigma_{ca}$ is the reaction thickness of the canopy. As for surface fires, flame length is calculated using:

$$FL_{crown} = 0.45 \cdot (I_{B,crown}/60)^{0.46} \tag{19.155}$$

where 60.0 is a factor to convert from $Btu \cdot ft^{-1} \cdot min^{-1}$ to $Btu \cdot ft^{-1} \cdot s^{-1}$.

19.6 Fire potentials

19.6.1 Surface fire behavior potentials

The **surface fire behavior potential** (SFP; between 0 and 9) is an index defined as the maximum of spread potential (SP) and flame length (FL) potential indices (both between 0 and 9):

$$SFP = \max(SP, FP) \tag{19.156}$$

Spread potential is derived from R (in $ft \cdot min^{-1}$), and *flame length potential* is derived from FL (in ft), both quantities being calculated at benchmark environmental conditions:

$$SP = \min\left[9, R^{1/2}\right] \tag{19.157}$$

$$FP = \min\left[9, FL^{1/2}\right] \tag{19.158}$$

19.6.2 Crown fire behavior potentials

The *crown fire summary potential* (CPF) combines three subpotentials into a single index value between 0 and 9. It places more emphasis on crown fire initiation (IC) and rate of spread (RC) than to crown-to-crown transmissivity (TC):

$$CFP = 0.4286 \cdot (IC + (TC/3) + RC) \tag{19.159}$$

where 0.4286 is used to limit CPF between 0 and 9.

The *crown fire initiation potential* (IC) represents the likelihood of a surface fire torching into single or multiple trees. IC is based on the work by Van Wagner. If $FAI_{ca} = 0$ then $IC = 0$. Otherwise it is calculated as:

$$IC = \min\left[9, 4 \cdot \left(\frac{I_B/60}{I_c}\right)^{0.2}\right] \tag{19.160}$$

where I_B is the surface fireline intensity (60 is used to convert it to $Btu \cdot ft^{-1} \cdot s^{-1}$) and I' is Van Wagner's critical fireline intensity (Scott and Reinhardt, 2002):

$$I_c = 0.288894658 \cdot \left[0.01 \cdot (H_{gap}/100) \cdot (460 + 25.9 \cdot M_{live,ca})\right]^{1.5} \tag{19.161}$$

where $M_{live,ca}$ is the moisture content of the canopy (in percent of dry weight), 0.288894658 is used to convert from $kJ \cdot m^{-1} \cdot s^{-1}$ to $Btu \cdot ft^{-1} \cdot s^{-1}$ and H_{gap} is the canopy gap (in cm) determined from the analysis of the bulk density profile.

The *crown-to-crown transmittivity potential* (TC) is set to zero if $FAI_{ca} < TFAI/(3 \cdot \pi)$, where $TFAI$ is a threshold for FAI calculated as:

$$TFAI = A_q \cdot e^{-0.0019 \cdot U} \tag{19.162}$$

where $A_q = 3.2868$ if $\sigma_{ca} > 2000 ft^2 \cdot ft^{-3}$ and $A_q = 2.6296$ otherwise. If $FAI_{ca} > TFAI/(3 \cdot \pi)$, then TC is calculated as:

$$TC = \min [9, 10 \cdot TC_q] \tag{19.163}$$

where TC_q is the efficiency of crown-to-crown heat transfer, as a proportion of maximum efficiency at 100 % canopy cover:

$$TC_q = \frac{(\max(0.0, C_{ca} \cdot WAF - 40))^{0.3}}{(100 \cdot WAF - 40)^{0.3}} \tag{19.164}$$

In this last equation 40 represents the threshold of canopy cover necessary to initiate dependent crown spread, and 0.3 is a coefficient describing the assumed effect of crown cover on transmittivity at benchmark windspeed. The canopy adjustment ratio WAF is added to modulate transmittivity depending on windspeed.

Finally, the *crown fire rate of spread potential* (RC) is defined as:

$$RC = \min \left[9, 2.5 \cdot R_{crown}^{1/e}\right] \tag{19.165}$$

where R_{crown} is the rate of spread (in $ft \cdot min^{-1}$) of the crown fire.

19.7 Unit conversion of outputs

The following factors are used to express fire behavior outputs to metric units:

- *Fire spread rates*: $1 ft \cdot min^{-1} = 0.3048 m \cdot min^{-1}$
- *Flame length*: $1 ft = 0.3048 m$
- *Reaction intensity*: $1 Btu \cdot ft^{-2} \cdot min^{-1} = 11.3484 kJ \cdot m^{-2} \cdot min^{-1}$
- *Heat sink*: $1 Btu \cdot ft^{-3} = 37.2589458 kJ \cdot m^{-3}$
- *Fireline intensity*: $1 Btu \cdot ft^{-1} \cdot min^{-1} = 0.0576911555 kW \cdot m^{-1}$

Appendix A

Model parametrization

Package **medfate** provides routines to estimate them from a minimum set of input parameters. The whole process of estimation of those parameters is done automatically in functions `spwbInput()` and `forest2spwbInput()`, with the user controlling the process through the species parameter table input (e.g., `SpParamsMED`) an object `control` (see default values in `defaultControl()`). In the following we detail the calculations and present individual functions that perform partial calculations.

A.1   Plant Hydraulics

A.1.1   Vulnerability curves

Leaf and xylem vulnerability curves are often described using Ψ_{50}, the water potential at which hydraulic conductance is half of maximum. As noted above, parameter d in eq. (11.1) is the water potential Ψ at which $k_x(\Psi)/k_{x,max} = e^{-1} = 0.367$ (and the same for eq. (11.2)). Hence, the two definitions do not match. Using the definition of Ψ_{50} in eq. (11.1) we have:

$$0.5 = e^{-((\Psi_{50}/d)^c)} \tag{A.1}$$

from which we obtain that the value for parameter d should be:

$$d = \frac{\Psi_{50}}{(-ln(0.5))^{1/c}} = \frac{\Psi_{50}}{0.69314^{1/c}} \tag{A.2}$$

Hence, this operation should be used when specifying this parameter from Ψ_{50}. Vulnerability curves for root xylem are less common than for stem xylem. If

these values are missing, functions `spwbInput()` and `forest2spwbInput()` will use for c the same value as in stems, and for d half the value of that of stems (Sperry et al., 2016a). If the values for leaves are missing, initialization functions will use for c the same value as in stems, and for d 66% of the value for stems.

Rhizosphere conductance is regulated in the model using the van Genuchten function given in eq. (11.5), and parameters n and α for each soil layer were already available from soil initialization (i.e. function `soil()`):

```
s = soil(defaultSoilParams(3))
s$VG_n
```

```
## [1] 1.267359 1.303861 1.303861
```

```
s$VG_alpha
```

```
## [1] 147.32468  89.16112  89.16112
```

Aboveground and belowground stem maximum conductance values at the plant level ($k_{s,max}$ and $k_{r,max}$) will not be normally available and the same for the rhizosphere ($k_{rh,max}$).

A.1.2   Leaf maximum conductance

Leaf maximum conductance ($k_{l,max}$, in $mmol \cdot m^{-2} \cdot s^{-1} \cdot MPa^{-1}$) is an input parameter that should be provided for each species. When missing, leaf maximum hydraulic conductance is assumed $k_{l,max} = 6$ for conifers and $k_{l,max} = 8$ for angiosperms (Sack and Holbrook, 2006).

A.1.3   Stem xylem maximum conductance

Estimation of maximum stem conductance ($k_{s,max}$, in $mmol \cdot m^{-2} \cdot s^{-1} \cdot MPa^{-1}$) is done by function `hydraulics_maximumStemHydraulicConductance()` and follows the work by Savage et al. (2010), Olson et al. (2014) and Christoffersen et al. (2016). Calculations are based on tree height and two species-specific parameters: maximum sapwood reference conductivity ($K_{s,max,ref}$) and the ratio of leaf area to sapwood area (A_l/A_s; `Al2As` in `SpParamsMED`), i.e. the inverse of the Huber value H_v.

The reference value for maximum sapwood conductivity $K_{s,max,ref}$ is assumed to have been measured on a *terminal branch* of a plant of known height H_{ref}. If our target plant is very different in height, the conduits of terminal branches will have different radius and hence conductivity. We correct the reference conductivity to the target plant height using the following empirical relationship, developed by Olson et al. (2014) between tree height and diameter of conduits for angiosperms and the equation described by Christoffersen et al. (2016):

$$2 \cdot r_{int,H} = 10^{1.257+(0.24 \cdot log_{10}(H))} \tag{A.3}$$

$$2 \cdot r_{int,ref} = 10^{1.257+(0.24 \cdot log_{10}(H_{ref}))} \tag{A.4}$$

$$K_{s,max,cor} = K_{s,max,ref} \cdot (r_{int,H}/r_{int,ref})^2 \tag{A.5}$$

Where $r_{int,H}$ is the radius of conduits for a terminal branch of a tree of height H and $r_{int,ref}$ is the corresponding radius for a tree of height H_{ref} (H and H_{ref} are measured in m). The form of the empirical relationship by Olson et al. (2014) is:
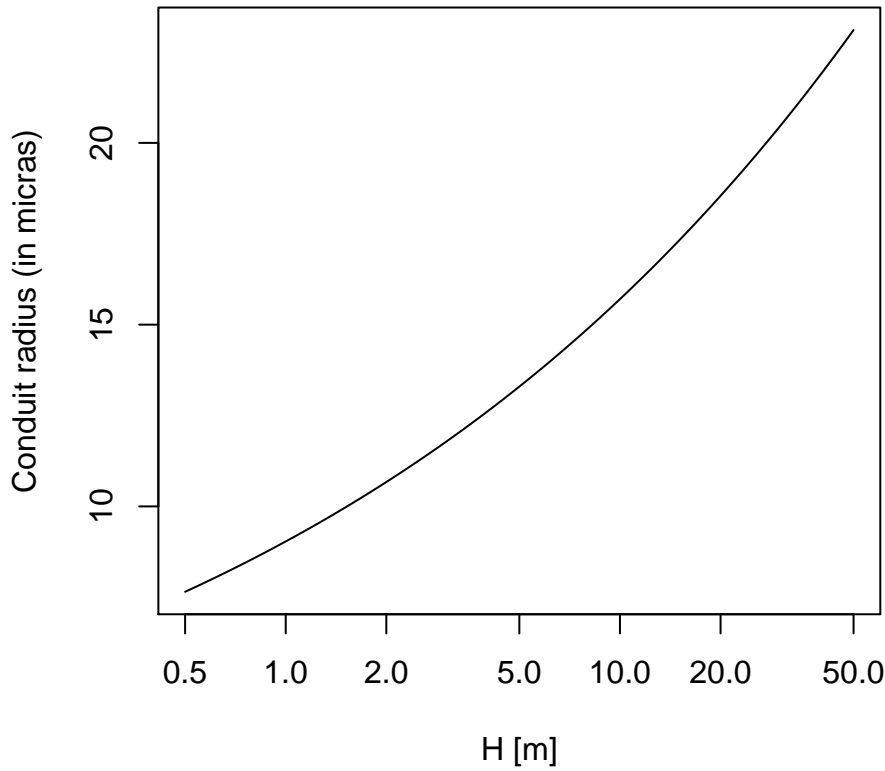
Let's consider an example for a *Quercus ilex* target tree of 4m height and where species-specific conductivity $K_{s,max,ref} = 0.77$ is the apical value for trees of $H_{ref} = 6.6$ m (in medfate, values of H_{ref} are taken from median height values; see parameter Hmed in SpParamsMED). The corrected conductivity for a tree of height 4 m will be a bit lower than that of the reference height:

```
xylem_kmax = 0.77
H = 400 # in cm
Href = 660 # in cm
f = hydraulics_referenceConductivityHeightFactor(Href, H);
f
```

```
## [1] 0.7863352
```

```
xylem_kmax_cor = xylem_kmax * f
xylem_kmax_cor
```

```
## [1] 0.6054781
```

Once the reference conductivity is corrected, the maximum stem conductance without accounting for conduit taper is:

$$k_{s,max,notaper} = \frac{1000}{0.018} \frac{K_{s,max,cor} \cdot A_s}{H \cdot A_l} \tag{A.6}$$

where H is the tree height (here in m), A_s is the sapwood area, A_l is the leaf area and $1000/0.018$ is a factor used to go from kg to mmol. The ratio $A_l/A_s = 1/H_v$ is a fixed species parameter in soil water balance calculations (see parameter `Al2As`), but becomes variable when simulating plant growth. Let's assume that *Quercus ilex* the leaf to sapwood area ratio is $A_l/A_s = 2512$. The maximum (leaf-specific) stem conductance without taper ($k_{s,max,notaper}$) for the tree of 4 m height is then:

```
Al2As = 2512
```

```
kstemmax = hydraulics_maximumStemHydraulicConductance(xylem_kmax,
             Href, Al2As, H, angiosperm = TRUE,taper = FALSE)
kstemmax
```

```
## [1] 3.347698
```

In order to consider taper of xylem conduits we calculate the whole-tree conductance per unit leaf area ($k_{s,max,taper}$) as described in Christoffersen et al. (2016):

$$k_{s,max,taper} = \frac{1000}{0.018} \cdot \frac{K_{s,max,pet} \cdot A_s}{H \cdot A_l} \cdot \chi_{tap:notap,ag}(H) \tag{A.7}$$

where $K_{s,max,pet}$ is the conductivity at the petiole level and $\chi_{tap:notap,ag}(H)$ is the taper factor accounting for the decrease in the xylem conduits diameter with the height, from the petiole to base of the trunk, which mitigates the negative effects of height on the hydraulic safety. The conductivity at the petiole level is obtained from $K_{s,max,ref}$ using again:

$$K_{s,max,pet} = K_{s,max,ref} \cdot (r_{int,pet}/r_{int,ref})^2 \tag{A.8}$$

where $r_{int,pet}$ is the radius of the petiole in the model of Savage et al. (2010). Christoffersen et al. (2016) use $r_{int,pet} = 10 \ \mu m$ but we define it as the radius of apical conduits in a tree of 1 m height:

```
hydraulics_terminalConduitRadius(100.0)
```

```
## [1] 9.035871
```

$\chi_{tap:notap,ag}(H)$ is calculated as described in the Appendix 1 section of Christoffersen et al. (2016) (see also Savage et al. (2010)). The following figure shows the value of $\chi_{tap:notap,ag}$ for different heights:
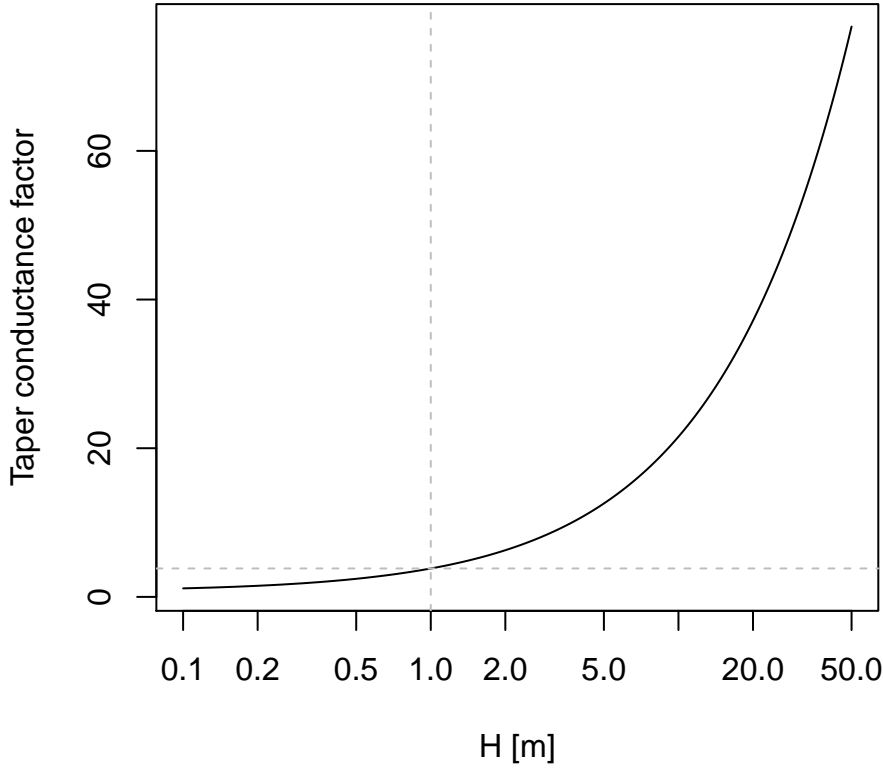
Note that, since $\chi_{tap:notap,ag}(1) = 3.82$ (indicated using grey dashed lines in the last figure), the equation of maximum conductance with taper would give a higher conductance than the equation without taper for a tree of 1 m height, which is supposed to have a conductance equal to conductivity. To solve this issue we define the taper factor as $\chi_{tap:notap,ag}(H)/\chi_{tap:notap,ag}(1)$:

$$k_{s,max,taper} = \frac{1000}{0.018} \cdot \frac{K_{s,max,pet} \cdot A_s}{H \cdot A_l} \cdot \frac{\chi_{tap:notap,ag}(H)}{\chi_{tap:notap,ag}(1)} \qquad (A.9)$$

The maximum stem conductance with taper ($k_{s,max,taper}$) of a *Q. ilex* tree of 4 m height, calculated with this second equation, is:

```
kstemmax_tap = hydraulics_maximumStemHydraulicConductance(xylem_kmax,
                    Href, Al2As, H, angiosperm = TRUE, taper = TRUE)
kstemmax_tap
```

```
## [1] 4.764396
```

The next two plots show the variation of $k_{s,max}$ for *Q. ilex* depending on the tree height and with/without considering taper of conduits. The plot on the right (both axes in log) show the slope of the dependency of conductance with height in both cases:
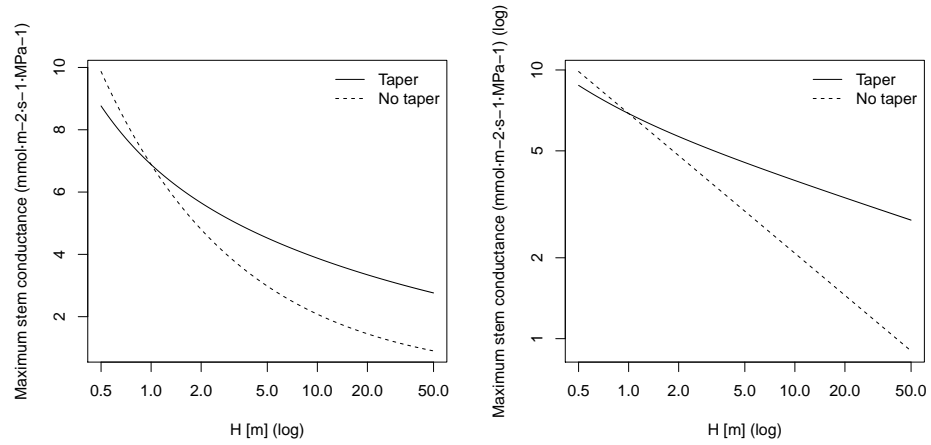
A.1.4 Root xylem maximum hydraulic conductance

To obtain maximum root xylem conductance ($k_{r,max}$, in $mmol \cdot m^{-2} \cdot s^{-1} \cdot MPa^{-1}$), one option taken by Christoffersen et al. (2016) is to assume that minimum stem resistance (inverse of maximum conductance) represents a fixed proportion of the minimum total tree (stem+root) resistance. A value 0.625 (i.e. 62.5%) suggested by these authors leads to maximum total tree conductance for our *Q. ilex* tree being:

```
ktot = kstemmax*0.625
ktot
```

```
## [1] 2.092311
```

and the maximum root xylem conductance would be therefore:

```
krootmax = 1/((1/ktot)-(1/kstemmax))
krootmax
```

```
## [1] 5.579497
```

Now, we need to divide total maximum conductance of the root system xylem among soil layers we need weights inversely proportional to the length of transport distances (Sperry et al., 2016a). Vertical transport lengths can be calculated from soil depths and radial spread can be calculated assuming cylinders with volume proportional to the proportions of fine root biomass. Let's assume a soil with three layers:

```
d = s$dVec
d
```

```
## [1]  300  700 1000
```

The proportion of fine roots in each layer, assuming a linear dose response model, will be:

```
Z50 = 200
Z95 = 1500
v1 = root_ldrDistribution(Z50,Z95, d)
v1
```

```
##           [,1]      [,2]        [,3]
## [1,] 0.6661036 0.2784153 0.05548106
```

Having this information, the calculation of root length (i.e. the sum of vertical and radial lengths) to each layer (L_j) is done using function `root_rootLength()`:

```
rl = root_rootLengths(v1, d)
rl
```

```
## [1] 2150.000 1496.481 1816.149
```

where lengths are in mm. The proportion of total root xylem conductance corresponding to each layer (w_j) is given by `root_xylemConductanceProportions()`:

```
w1 = root_xylemConductanceProportions(v1, d)
w1
```

```
## [1] 0.2762029 0.3968217 0.3269754
```

Xylem conductance proportions can be quite different than the fine root biomass proportions. This is because radial lengths are largest for the first top layers and vertical lengths are largest for the bottom layers. The maximum root xylem conductances of each layer will be the product of maximum total conductance of root xylem and weights:

```
w1*krootmax
```

```
## [1] 1.541073 2.214065 1.824358
```

In **medfate** we calculate maximum root xylem conductance using a reference root xylem conductivity value $(K_{r,max,ref})$:

$$k_{r,max} = \frac{1000}{0.018} \cdot \sum_{j} \frac{w_j \cdot K_{r,max,ref} \cdot A_s}{L_j \cdot A_l} \tag{A.10}$$

where w_j are root xylem conductance proportion of layer j and L_j is the root length (in m) to layer j. Note that here we use weights w_j assuming they represent proportions of total sapwood area that come from each layer (i.e. the longer the path the larger the proportion of sapwood area). This calculation is made available by function `hydraulics_maximumRootHydraulicConductance()`. When $K_{r,max,ref}$ is missing, then we assume that $K_{r,max,ref} = K_{x,max,ref}$. Let's consider the same *Q. ilex* tree of 4m height as before. If we specify root xylem specific conductivity as $K_{r,max,ref} = K_{s,max,ref} = 0.77$ we have:

```
rootxylem_kmax = 0.77
krootmax = hydraulics_maximumRootHydraulicConductance(rootxylem_kmax, Al2As,
                                                      v1, d)
krootmax
```

```
## [1] 9.769308
```

The maximum root xylem conductances of each layer would be:

```
krootmaxvec = w1*krootmax
krootmaxvec
```

```
## [1] 2.698311 3.876673 3.194324
```

and the fraction of total xylem resistance due to stem would be:

```
(1/kstemmax)/((1/kstemmax)+(1/krootmax))
```

```
## [1] 0.7447818
```

In contrast with the approach of Christoffersen et al. (2016), in this approach the root maximum conductance depends root length and distribution, and is not a fixed fraction of stem maximum conductance. Assuming constant root length, then the proportion of total resistance due to the stem will increase with tree height (Magnani et al., 2000):
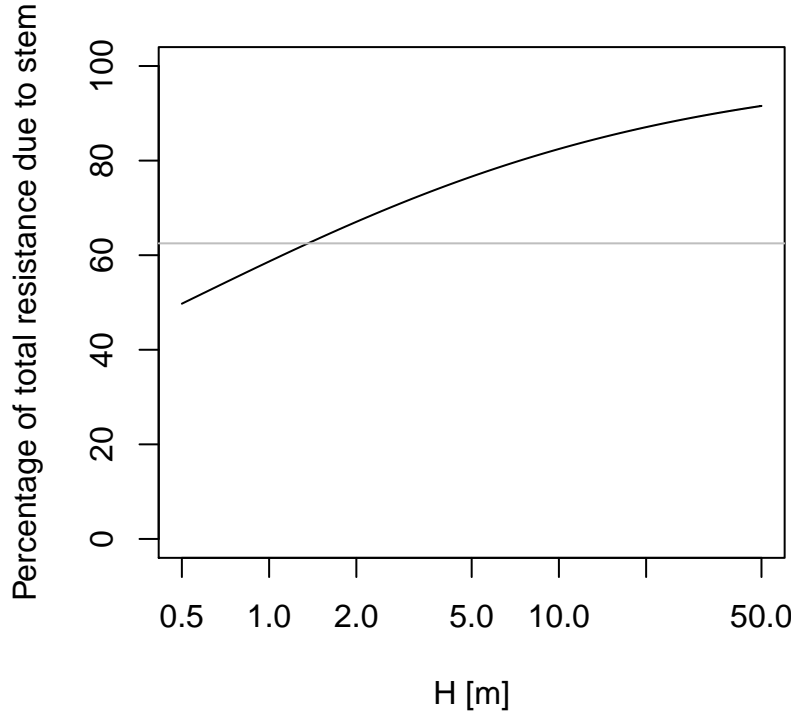
where the horizontal gray line indicates the value of 62.5%. Of course rooting depth also increases with tree age, but young trees have higher root-to-shoot ratios than older ones. Hence, a root maximum conductance that is not fixed but increases with age seems a priori more realistic. Moreover, Christoffersen et al. (2016) justify the value of 62.5% from a study which quantified total aboveground and belowground resistance in tropical trees (Fisher et al., 2006) under near-saturated (wet season) conditions, but values of belowground resistance reported in this study for wet conditions and trees of 30 m height are around 13%, which equals to 87% fraction of aboveground resistance. On the other hand, while rooting depths are limited by soil depth, lateral root length increases with age and, hence, the model could be made more realistic if this is taken into account and the curve above would probably saturate at lower percentages.

A.1.5 Rhizosphere maximum hydraulic conductance

Maximum rhizosphere conductance ($k_{rh,max}$, in $mmol \cdot m^{-2} \cdot s^{-1} \cdot MPa^{-1}$) is difficult to measure directly, as it depends on the rhizosphere (i.e. fine root) surface in each soil layer, and will probably always be a parameter to be calibrated. Instead of trying to estimate rhizosphere surface from root architecture (Sperry et al., 1998), we follow Sperry et al. (2016b) and determine the maximum rhizosphere conductance in each layer from an inputed 'average percentage

rhizosphere resistance'. The percentage of continuum resistance corresponding
to the rhizosphere is calculated from the vulnerability curves of stem, root and
rhizosphere at the same water potential. The average resistance is found by
evaluating the percentage for water potential values between 0 and Ψ_{crit}. The
following figure illustrates how the supply function, for different soil water po-
tentials, is affected by increasing values of the average percentage of rhizosphere
resistance:
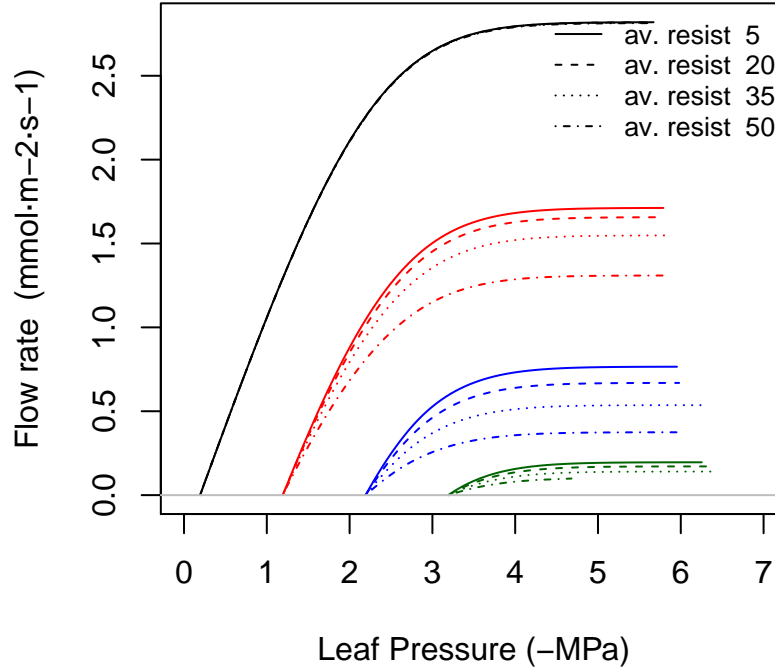
Sperry et al. (2016b) found average percentages of rhizosphere resistance around
67%, but these exceptionally-high values were probably a consequence of using
an unsegmented supply function (i.e. single vulnerability curve for roots, stem
and leaves). If we specify a 15% of average resistance in the rhizosphere (see pa-
rameter `averageFracRhizosphereResistance` in function `defaultControl()`),
the maximum rhizosphere conductance values for the three layers are found call-
ing:

```
krmax = rep(0,3)
krmax[1]= hydraulics_findRhizosphereMaximumConductance(15,
                     s$VG_n[1],s$VG_alpha[1],
                     krootmax, rootc,rootd,
                     kstemmax, stemc, stemd,
                     kleafmax, leafc, leafd)
krmax[2] = hydraulics_findRhizosphereMaximumConductance(15,
                      s$VG_n[2],s$VG_alpha[2],
                      krootmax, rootc,rootd,
```

```
                        kstemmax, stemc, stemd,
                        kleafmax, leafc, leafd)
krmax[3] = hydraulics_findRhizosphereMaximumConductance(15,
                        s$VG_n[3],s$VG_alpha[3],
                        krootmax, rootc,rootd,
                        kstemmax, stemc, stemd,
                        kleafmax, leafc, leafd)
krmax
```

```
## [1] 276438796  97039144  97039144
```

The values are the same because the texture of the three layers is the same in this case. If we take into account root distribution, actual maximum rhizosphere conductance values are:

```
krmax*v1
```

```
##            [,1]      [,2]     [,3]
## [1,] 184136883 27017184 5383835
```

A.1.6 Pressure-volume curves

Parameters of the pressure-volume curve (i.e. $\pi_{0,stem}$ and ϵ_{stem}) for leaf and stem symplastic tissue are required for each species. When parameters for stem tissue are missing, **medfate** estimates them from wood density following Christoffersen et al. (2016):

$$\pi_{0,stem} = 0.52 - 4.16 \cdot \rho_{wood} \tag{A.11}$$

$$\epsilon_{stem} = \sqrt{1.02 \cdot e^{8.5 \cdot \rho_{wood}} - 2.89} \tag{A.12}$$

A.1.7 Plant water storage capacity

The water storage capacity of sapwood tissue per leaf area unit ($V_{sapwood}$; in $m^3 \cdot m^{-2}$) can be estimated as the product of stem height (H in m) and Huber value (H_v; ratio of sapwood area to leaf area in $m^2 \cdot m^{-2}$) times a factor to account for the non-cylindrical shape (http://www.fao.org/forestry/17109/en/):

$$V_{sapwood} = 0.48 \cdot H \cdot H_v \cdot \Theta_{sapwood} \tag{A.13}$$

$\Theta_{sapwood}$ is sapwood porosity (cm^3 of water per cm^3 of sapwood tissue), which can be estimated from wood density (ρ_{wood}; in $g \cdot cm^{-3}$):

$$\Theta_{sapwood} = 1 - (\rho_{wood}/1.54) \qquad (A.14)$$

where the density of wood substance can be assumed to be fixed and equal to 1.54 $g \cdot cm^{-3}$ (Dunlap, 1914). For example, wood densities ranging from 0.443 to 1.000 $g \cdot cm^{-3}$ result in sapwood porosity values between 0.35 and 0.71.

Water storage capacity of leaf tissue per leaf area unit (V_{leaf}; in $m^3 \cdot m^{-2}$) can be estimated as the product of specific leaf area (SLA; in $m^2 \cdot kg^{-1}$) and leaf density (ρ_{leaf}; in $g \cdot cm^{-3}$):

$$V_{leaf} = \frac{10^{-3}}{SLA \cdot \rho_{leaf}} \cdot \Theta_{leaf} \qquad (A.15)$$

Θ_{leaf} is leaf porosity (cm^3 of water per cm^3 of leaf tissue), which can be estimated from leaf density:

$$\Theta_{leaf} = 1 - (\rho_{leaf}/1.54) \qquad (A.16)$$

where the density of wood substance can be assumed to be fixed and equal to 1.54 $g \cdot cm^{-3}$ (Dunlap 1914).

For example, let's calculate the stem and leaf water capacity for a Q. ilex tree of 15 m height:

```
wd = 1.0
Al2As = 2512
H = 1500 # 15 m
hydraulics_stemWaterCapacity(Al2As, H, wd)
```

```
## [1] 0.001005046
```

```
ld = 0.7
SLA = 5.870
hydraulics_leafWaterCapacity(SLA, ld)
```

```
## [1] 0.0001327463
```

A.2   Stomatal regulation and photosynthesis

A.2.1   Stomatal conductance

Maximum stomatal conductance (g_{swmax}) is an input parameter for each species. When species-specific values are missing, the following relation with maximum leaf hydraulic conductance ($k_{l,max}$) is used (Mencuccini, 2003):

$$g_{swmax} = e^{4.797 + 0.633 \cdot \log(k_{l,max})} \tag{A.17}$$

Species values for g_{swmin} were taken from Duursma et al. (2018). Following the same authors, a value of $g_{swmin} = 0.0045 \ molH_2O \cdot s^{-1} \cdot m^{-2}$ is taken as default, when species-specific values are missing.

A.2.2 Photosynthesis

Rubisco's maximum carboxylation rate at 25ºC ($V_{max,298}$, in $\mu molCO_2 \cdot s^{-1} \cdot m^{-2}$) is a required input parameter for each species (`Vmax298`), and if its value is missing a default value of 100 $\mu molCO_2 \cdot s^{-1} \cdot m^{-2}$ is used. The maximum rate of electron transport at the same temperature ($J_{max,298}$) can be provided by the user (`Jmax298`) but, if not, it is estimated from $V_{max,298}$ using Walker et al. (2014):

$$J_{max,298} = e^{1.197 + 0.847 \cdot \log(V_{max,298})} \tag{A.18}$$

Appendix B

Symbols

The following tables list all symbols used in this document, along with their units and definition. When symbols are input for **medfate** model functions, the R name of those parameters in the package (either in data frame `SpParamsMED`, soil input data frame, or the output of functions such as `spwbInput()`) is also indicated.

B.1 Soils

Symbol	Units	R param	Description
d_s	mm	`widths`	Soil layer width in soil layer s
$P_{clay,s}$	$\%$	`clay`	Percent of clay in soil layer s
$P_{sand,s}$	$\%$	`sand`	Percent of sand in soil layer s
OM	$\%$	`om`	Percentage of organic mater per dry weight
BD_s	$g \cdot cm^{-3}$	`bd`	Bulk density in soil layer s
$P_{rocks,s}$	$\%$	`rfc`	Percentage of rock fragment content in soil layer s
θ_s	$m^3 \cdot m^{-3}$		Volumetric moisture in soil layer s
Ψ_s	MPa		Water potential in soil layer s
Ψ_{fc}	MPa		Water potential at field capacity
A, B			Parameters of the Saxton pedotransfer functions
θ_{sat}	$m^3 \cdot m^{-3}$	`VG_theta_sat`	Volumetric moisture at saturation
θ_{fc}	$m^3 \cdot m^{-3}$		Volumetric moisture at field capacity (-0.033 MPa)

Symbol	Units	R param	Description
θ_{wp}	$m^3 \cdot m^{-3}$		Volumetric moisture at wilting point (-1.5 MPa)
θ_{res}	$m^3 \cdot m^{-3}$	VG_theta_res	Residual volumetric moisture
n		VG_n	Parameter of the Van Genuchten (1980) model
α		VG_alpha	Parameter of the Van Genuchten (1980) model
$P_{macro,s}$	$\%$	macro	Percentage of macroporosity corresponding to each soil layers.
γ_{soil}	$mm \cdot day^{-1}$	Gsoil	The maximum daily evaporation from soil
κ_{soil}		Ksoil	Extinction parameter to regulate the amount of water evaporated from each soil layer
WT	mm		Water table depth
V_s	mm		Water content in soil layer s
$V_{fc,soil}$	mm		Water retention capacity of the whole soil
W_s	[0-1]	W	Proportion of volumetric moisture in relation to field capacity in soil layer s
S_{snow}	mm	SWE	Snow water equivalent of the snow pack storage over the soil surface

B.2 Vegetation

Symbol	Units	R param	Description
SP_i		Species	Species identity of cohort i
H_i	cm	Height	Average tree or shrub height of cohort i
$H_{b,i}$	cm		Crown base height (i.e. the height corresponding to the first living branch) of cohort i
CR_i		CR	Crown ratio (i.e. ratio between crown length and plant height) of cohort i
N_i	$ind \mathring{u} ha^{-1}$	N	Density of tree individuals of cohort i
DBH_i	cm	DBH	Diameter at breast height of trees in cohort i

Symbol	Units	R param	Description
$Cover_i$	%	Cover	Percent cover of shrubs in cohort i
FB_i	$kg \cdot m^{-2}$		Foliar biomass of cohort i
ϕ_i	[0-1]		Fraction of maximum leaf area currently expanded for cohort i
LAI_i^{live}	$m^2 \cdot m^{-2}$	LAI_live	(Maximum) leaf area index (one-side leaf area per surface area of the stand) of cohort i
LAI_i^{dead}	$m^2 \cdot m^{-2}$	LAI_dead	Dead leaf area index (one-side dead leaf area per surface area of the stand) of cohort i
LAI_i^{ϕ}	$m^2 \cdot m^{-2}$	LAI_expanded	Current expanded leaf area index (one-side expanded leaf area per surface area of the stand) of cohort i
LAI_i^{all}	$m^2 \cdot m^{-2}$		Total leaf area index (live or dead) of cohort i
LAI_{stand}^{live}	$m^2 \cdot m^{-2}$		Maximum leaf area index of living leaves of the stand
LAI_{stand}^{dead}	$m^2 \cdot m^{-2}$		Leaf area index of dead leaves of the stand
LAI_{stand}^{ϕ}	$m^2 \cdot m^{-2}$		Current expanded leaf area index of live leaves of the stand
LAI_{stand}	$m^2 \cdot m^{-2}$		Total leaf area index (live or dead) of the stand
LA_i	m^2		Leaf area of an individual of cohort i
$v_{i,s}$	[0-1]	V[i,s]	The proportion of fine roots of cohort i in soil layer s
$Z_{50,i}$	mm	Z50	Depth above which 50% of the fine root mass of cohort i is located
$Z_{95,i}$	mm	Z95	Depth above which 95% of the fine root mass of cohort i is located

B.3 Meteorology

Symbol	Units	R param	Description
T_{mean}	°C	MeanTemperature	Mean temperature
T_{min}	°C	MinTemperature	Minimum temperature
T_{max}	°C	MaxTemperature	Maximum temperature
RH_{min}	%	MinRelativeHumidity	Minimum relative humidity
RH_{max}	%	MaxRelativeHumidity	Maximum relative humidity

Symbol	Units	R param	Description
P	$L \cdot m^{-2} = mm$	Precipitation	Precipitation
PET	$L \cdot m^{-2} = mm$	PET	Potential evapotranspiration, preferably calculated using Penman's equation
Rad	$MJ \cdot m^{-2}$	Radiation	Solar radiation after accounting for clouds
u	$m \cdot s^{-1}$	WindSpeed	Wind speed
GDD	$^{\circ}$C	GDD	Growth degree days.

B.4   Anatomy

Symbol	Units	R param	Description
H_v	$m^2 \cdot m^{-2}$	1/Al2As	Huber value (ratio of sapwood area to leaf area)
d	cm	LeafWidth	Leaf width
SLA	$m^2 \cdot kg^{-1}$	SLA	Specific leaf area
ρ_{leaf}	$g \cdot cm^{-3}$	LeafDens	Leaf tissue density
ρ_{wood}	$g \cdot cm^{-3}$	WoodDens	Wood tissue density
$\Theta_{sapwood}$	$m^3 \cdot m^{-3}$		Sapwood porosity (volume of empty spaces over total volume)
Θ_{leaf}	$m^3 \cdot m^{-3}$		Leaf porosity (volume of empty spaces over total volume)

B.5   Light extinction

Symbol	Units	R param	Description
$k_{PAR,i}$		k	PAR extinction coefficient for cohort i
$k_{SWR,i}$			SWR extinction coefficient for cohort i
L_{ground}^{PAR}	[0-1]	LgroundPAR	Fraction of PAR reaching the ground
L_{ground}^{SWR}	[0-1]	LgroundSWR	Fraction of SWR reaching the ground

B.6   Hydrology and water balance

Symbol	Units	R param	Description
Ps	mm	`Snow`	Precipitation as snow
Pr	mm	`Rain`	Precipitation as rainfall
Sm	mm	`Snowmelt`	Snowmelt
Pr_{net}	mm	`NetRain`	Net rainfall
In	mm	`Interception`	Interception loss
Ru	mm	`Runoff`	Water exported from the stand as runoff
Ro	mm	`Runon`	Water imported to the stand as runon
Dd	mm	`DeepDrainage`	Water exported from the stand as deep drainage
P_G	mm		Amount of rainfall needed to saturate the canopy for a given event
S_{canopy}	mm	`Cm`	Canopy water storage capacity
(E/R)			Ratio between evaporation rate and rainfall rate
C_{canopy}	[0-1]		Canopy cover
PE_{soil}	mm		Evaporation demand from the soil
SE_{soil}	mm		Evaporation supply from the soil
Es	mm	`SoilEvaporation`	Evaporation from the soil surface

B.7 Plant hydraulics

Symbol	Units	R param	Description
$K_{s,max,ref}$	$kg \cdot s^{-1} \cdot m^{-1} \cdot MPa^{-1}$	`Kmax_stemxylem`	Maximum stem sapwood reference conductivity per leaf area unit
$K_{r,max,ref}$	$kg \cdot s^{-1} \cdot m^{-1} \cdot MPa^{-1}$	`Kmax_rootxylem`	Maximum root sapwood reference conductivity per leaf area unit
$k_{s,max}$	$mmol \cdot s^{-1} \cdot m^{-2} \cdot MPa^{-1}$		Maximum whole-stem conductance (per leaf area unit)
$k_{r,max}$	$mmol \cdot s^{-1} \cdot m^{-2} \cdot MPa^{-1}$		Maximum root conductance (per leaf area unit)
$k_{rh,max}$	$mmol \cdot s^{-1} \cdot m^{-2} \cdot MPa^{-1}$		Maximum rhizosphere conductance (per leaf area unit)
$k_{l,max}$	$mmol \cdot s^{-1} \cdot m^{-2} \cdot MPa^{-1}$	`VCleaf_kmax`	Maximum leaf conductance (per leaf area unit)

Symbol	Units	R param	Description
c_l, d_l	(unitless), MPa	VCleaf_c, VCleaf_d	Parameters of the vulnerability curve for leaves
c_r, d_r	(unitless), MPa	VCroot_c, VCroot_d	Parameters of the vulnerability curve for root xylem
c_s, d_s	(unitless), MPa	VCstem_c, VCstem_d	Parameters of the vulnerability curve for stem xylem
n, α			Texture-specific parameters of the van Genuchten equation
Ψ	MPa		Water potential in a given water compartment
Ψ_P	MPa		Turgor water potential in a given water compartment
Ψ_S	MPa		Osmotic (solute) water potential in a given water compartment
Ψ_{cav}	MPa		Minimum water potential experienced by xylem in previous steps (cavitation)
Ψ_{canopy}	MPa		Canopy water potential
Ψ_{leaf}	MPa		Leaf water potential
$\Psi_{rootcrown}$	MPa		Water potential at the root crown
Ψ_{stem}	MPa		Water potential at the end (highest part) of the stem
PLC	[0-1]		Proportion of conductance loss in stem xylem tissue
p_{root}	[0-1]	pRootDisc	Relative root conductance leading to hydraulic disconnection from a soil layer

B.8   Plant water compartments

Symbol	Units	R param	Description
ϵ_{leaf}	MPa	LeafEPS	Modulus of elasticity of leaves
ϵ_{stem}	MPa	StemEPS	Modulus of elasticity of symplastic xylem tissue
$\pi_{0,leaf}$	MPa	LeafPI0	Osmotic potential at full turgor of leaves
$\pi_{0,stem}$	MPa	StemPI0	Osmotic potential at full turgor of symplastic xylem tissue
RWC	[0-1]		Relative water content
RWC_{sym}	[0-1]		Relative water content in the symplasm fraction of a tissue

Symbol	Units	R param	Description
RWC_{apo}	[0-1]		Relative water content in the apoplasm fraction of a tissue
$V_{segment}$	$m^3 \cdot m^{-2}$		Water capacity of a segment (leaf or stem)
V_{leaf}	$m^3 \cdot m^{-2}$		Leaf water capacity per leaf area unit
$V_{sapwood}$	$m^3 \cdot m^{-2}$		Sapwood water capacity per leaf area unit

B.9 Stomatal regulation and photosynthesis

Symbol	Units	R param	Description
g_{swmin}	$molH_2O \cdot s^{-1} \cdot m^{-2}$	Gwmin	Minimum stomatal conductance to water vapour
g_{swmax}	$molH_2O \cdot s^{-1} \cdot m^{-2}$	Gwmax	Maximum stomatal conductance to water vapour
$J_{max,298}$	$\mu molelectron \cdot m^{-2} \cdot s^{-1}$	Jmax298	Maximum rate of electron transport at 298K
$V_{max,298}$	$\mu molCO_2 \cdot s^{-1} \cdot m^{-2}$	Vmax298	Rubisco's maximum carboxylation rate at 298K

Bibliography

Albini, F. A. (1976). Estimating wildfire behavior and effects. *For. Serv. Gen. Tech. Rep. INT-30*, 4235(789273912):44 ST – Guidelines and sample protocol for sampli.

Anten, N. P. R. and Bastiaans, L. (2016). The use of canopy models to analyze light competition among plants. In Hikosaka, K., Niinemets, Ü., and Anten, N. P. R., editors, *Canopy photosynthesis: from basics to application*, pages 379–398. Springer.

Bartlett, M. K., Scoffoni, C., and Sack, L. (2012). The determinants of leaf turgor loss point and prediction of drought tolerance of species and biomes: a global meta-analysis. *Ecology letters*, 15(5):393–405.

Bernacchi, C. J., Singsaas, E. L., Pimentel, C., Portis, A. R., and Long, S. P. (2001). Improved temperature response functions for models of Rubisco-limited photosynthesis. *Plant, Cell and Environment*, 24(2):253–259.

Best, M., Pryor, M., and Clarck, D. (2011). The Joint UK Land Environment Simulator (JULES), Model description – Part 1: Energy and water fluxes. *Geoscientific Model Development Discussions*, 4(1):677–699.

Birk, E. M. and Simpson, R. W. (1980). Steady state and the continuous input model of litter accumulation and decompostion in Australian eucalypt forests. *Ecology*, 61(3):481–485.

Boughton, W. (1989). A review of the USDA SCS curve number method. *Australian Journal of Soil Research*, 27:511–523.

Byram, G. (1959). Combustion of forest fuels. In Davis, K., editor, *Forest fire: control and use*, chapter Chapter 3, pages 61–89. McGraw-Hill, New York.

Campbell, G. S. and Norman, J. M. (1998). *An introduction to environmental biophysics.* Springer-Verlag, New York, 2nd editio edition.

Carsel, R. F. and Parrish, R. S. (1988). Developing joint probability distributions of soil water retention characteristics. *Water Resources Research*, 24(5):755–769.

Christoffersen, B. O., Gloor, M., Fauset, S., Fyllas, N. M., Galbraith, D. R., Baker, T. R., Rowland, L., Fisher, R. A., Binks, O. J., Sevanto, S. A., Xu, C., Jansen, S., Choat, B., Mencuccini, M., McDowell, N. G., and Meir, P. (2016). Linking hydraulic traits to tropical forest function in a size-structured and trait-driven model (TFS v.1-Hydro). *Geoscientific Model Development Discussions*, 0(June):1–60.

Collatz, G. J., Ball, J. T., Grivet, C., and Berry, J. A. (1991). Physiological and environmental regulation of stomatal conductance, photosynthesis and transpiration: a model that includes a laminar boundary layer. *Agricultural and Forest Meteorology*, 54(2-4):107–136.

Collins, D. B. G. and Bras, R. L. (2007). Plant rooting strategies in water-limited ecosystems. *Water Resources Research*, 43(6):W06407.

De Cáceres, M., Martin-StPaul, N., Turco, M., Cabon, A., and Granda, V. (2018). Estimating daily meteorological data and downscaling climate models over landscapes. *Environmental Modelling & Software*, 108(August):186–196.

De Cáceres, M., Martínez-Vilalta, J., Coll, L., Llorens, P., Casals, P., Poyatos, R., Pausas, J. G., and Brotons, L. (2015). Coupling a water balance model with forest inventory data to predict drought stress: the role of forest structural changes vs. climate changes. *Agricultural and Forest Meteorology*, 213:77–90.

De Pury, D. G. G. and Farquhar, G. D. (1997). Simple scaling of photosynthesis from leaves to canopies without the errors of big-leaf models. *Plant, Cell and Environment*, 20(5):537–557.

Deguchi, A., Hattori, S., and Park, H.-T. (2006). The influence of seasonal changes in canopy structure on interception loss: Application of the revised Gash model. *Journal of Hydrology*, 318(1-4):80–102.

Dietze, M. C., Sala, A., Carbone, M. S., Czimczik, C. I., Mantooth, J. A., Richardson, A. D., and Vargas, R. (2014). Nonstructural Carbon in Woody Plants. *Annual Review of Plant Biology*, 65(1):667–687.

Dunlap, F. (1914). Density of wood substance and porosity of wood. *Journal of Agricultural Research*, II(6):423–428.

Duursma, R. A., Blackman, C. J., Lopéz, R., Martin-StPaul, N. K., Cochard, H., and Medlyn, B. E. (2018). On the minimum leaf conductance: its role in models of plant water use, and ecological and environmental controls. *New Phytologist*, (September).

Fatichi, S., Leuzinger, S., and Körner, C. (2014). Moving beyond photosynthesis: From carbon source to sink-driven vegetation modeling. *New Phytologist*, 201(4):1086–1095.

Federer, C. (1982). Transpirational supply and demand: plant, soil, and atmospheric effects evaluated by simulation. *Water Resources Research*, 18(2):355–362.

Fisher, R. A., Williams, M., Do Vale, L. R., Da Costa, A. L., and Meir, P. (2006). Evidence from Amazonian forests is consistent with a model of isohydric control of leaf water potential. *Plant, Cell and Environment*, 29(2):151–165.

Friend, A. D., Stevens, A. K., Knox, R. G., and Cannell, M. G. R. (1997). A process-based, terrestrial biosphere model of ecosystem dynamics (Hybrid v3.0). *Ecological Modelling*, 95:249–287.

Gash, J., Lloyd, C., and Lachaud, G. (1995). Estimating sparse forest rainfall interception with an analytical model. *Journal of Hydrology*, 170(79-86).

Genuchten, M. V. (1980). A closed-form equation for predicting the hydraulic conductivity of unsaturated soils. *Soil science society of America journal*, 44:892–898.

Granier, A., Bréda, N., Biron, P., and Villette, S. (1999). A lumped water balance model to evaluate duration and intensity of drought constraints in forest stands. *Ecological Modelling*, 116:269–283.

Granier, A., Reichstein, M., Bréda, N., Janssens, I., Falge, E., Ciais, P., Grünwald, T., Aubinet, M., Berbigier, P., Bernhofer, C., Buchmann, N., Facini, O., Grassi, G., Heinesch, B., Ilvesniemi, H., Keronen, P., Knohl, A., Köstner, B., Lagergren, F., Lindroth, A., Longdoz, B., Loustau, D., Mateus, J., Montagnani, L., Nys, C., Moors, E., Papale, D., Peiffer, M., Pilegaard, K., Pita, G., Pumpanen, J., Rambal, S., Rebmann, C., Rodrigues, A., Seufert, G., Tenhunen, J., Vesala, T., and Wang, Q. (2007). Evidence for soil water control on carbon and water dynamics in European forests during the extremely dry year: 2003. *Agricultural and Forest Meteorology*, 143(1-2):123–145.

Guillemot, J., Martin-Stpaul, N. K., Dufrêne, E., François, C., Soudani, K., Ourcival, J. M., and Delpierre, N. (2015). The dynamic of the annual carbon allocation to wood in European tree species is consistent with a combined source-sink limitation of growth: Implications for modelling. *Biogeosciences*, 12(9):2773–2790.

Hasenauer, H. and Monserud, R. A. (1996). A crown ratio model for Austrian Forests. *Forest Ecology and Management*, 84(1-3):49–60.

Hikosaka, K., Kumagai, T., and Ito, A. (2016). Modeling Canopy Photosynthesis. pages 239–268.

Hölttä, T., Cochard, H., Nikinmaa, E., and Mencuccini, M. (2009). Capacitive effect of cavitation in xylem conduits: Results from a dynamic model. *Plant, Cell and Environment*, 32(1):10–21.

Kergoat, L. (1998). A model for hydrological equilibrium of leaf area index on a global scale. *Journal of Hydrology*, 212-213:268–286.

Körner, C. (2015). Paradigm shift in plant growth control. *Current Opinion in Plant Biology*, 25:107–114.

Krajicek, J., Brinkman, K., and Gingrich, S. (1961). Crown competition-a measure of density. *Forest Science*, 7(1):35–42.

Landsberg, J. and Waring, R. (1997). A generalised model of forest productivity using simplified concepts of radiation-use efficiency, carbon balance and partitioning. *Forest Ecology and Management*, 95(3):209–228.

Leij, F. J., Alves, W. J., Genuchten, M. V., and Williams, J. R. (1996). *The UNSODA Unsaturated Soil Hydraulic Database User's Manual Version 1.0.* Number August.

Leuning, R. (2002). Temperature dependence of two parameters in a photosynthesis model. *Plant, Cell and Environment*, 25(9):1205–1210.

Lindner, M., Sievänen, R., and Pretzsch, H. (1997). Improving the simulation of stand structure in a forest gap model. *Forest Ecology and Management*, 95(2):183–195.

Magnani, F., Mencuccini, M., and Grace, J. (2000). Age-related decline in stand productivity: The role of structural acclimation under hydraulic constraints. *Plant, Cell and Environment*, 23(3):251–263.

Martin-StPaul, N., Delzon, S., and Cochard, H. (2017). Plant resistance to drought depends on timely stomatal closure. *Ecology Letters*, 20(11):1437–1447.

McMurtrie, R. E., Rook, D. A., and Kelliher, F. M. (1990). Modelling the yield of Pinus radiata on a site limited by water and nitrogen. *Forest Ecology and Management*, 30(1-4):381–413.

Medlyn, B. E., Loustau, D., and Delzon, S. (2002). Temperature response of parameters of a biochemically based model of photosynthesis. I. Seasonal changes in mature maritime pine (Pinus pinaster Ait.). *Plant, Cell and Environment*, 25(9):1155–1165.

Mencuccini, M. (2003). The ecological significance of long-distance water transport : short-term regulation , long-term acclimation and the hydraulic costs of stature across plant life forms. *Plant, Cell & Environment*, 26:163–182.

Mencuccini, M. and Grace, J. (1995). Climate influences the leaf area/sapwood area ratio in Scots pine. *Tree Physiology*, 15(1):1–10.

Miralles, D. G., Gash, J. H., Holmes, T. R. H., de Jeu, R. A. M., and Dolman, A. J. (2010). Global canopy interception from satellite observations. *Journal of Geophysical Research*, 115(D16):D16122.

Mitsopoulos, I. D. and Dimitrakopoulos, A. P. (2007). Allometric equations for crown fuel biomass of Aleppo pine (Pinus halepensis Mill.) in Greece. *International Journal of Wildland Fire*, 16(5):642–647.

Mouillot, F., Rambal, S., and Joffre, R. (2002). Simulating climate change impacts on fire frequency and vegetation dynamics in a Mediterranean-type ecosystem. *Global Change Biology*, 8(5):423–437.

Mouillot, F., Rambal, S., and Lavorel, S. (2001). A generic process-based SImulator for meditERRanean landscApes (SIERRA): design and validation exercises. *Forest Ecology and Management*, 147(1):75–97.

Olson, M. E., Anfodillo, T., Rosell, J. A., Petit, G., Crivellaro, A., Isnard, S., León-Gómez, C., Alvarado-Cárdenas, L. O., and Castorena, M. (2014). Universal hydraulics of the flowering plants: Vessel diameter scales with stem length across angiosperm lineages, habits and climates. *Ecology Letters*, 17(8):988–997.

Prentice, I. C., Sykes, M. T., and Cramer, W. (1993). A simulation model for the transient effects of climate change on forest landscapes. *Ecological Modelling*, 65(1-2):51–70.

Prichard, S. J., Sandberg, D. V., Ottmar, R. D., Eberhardt, E., Andreu, A., Eagle, P., and Swedin, K. (2013). Classification System Version 3.0: Technical Documentation. Technical report.

Rasche, L., Fahse, L., Zingg, A., and Bugmann, H. (2012). Enhancing gap model accuracy by modeling dynamic height growth and dynamic maximum tree height. *Ecological Modelling*, 232:133–143.

Reinhardt, E., Lutes, D., and Scott, J. (2006). FuelCalc: A method for estimating fuel characteristics. Technical report.

Richardson, A. D., Carbone, M. S., Keenan, T. F., Czimczik, C. I., Hollinger, D. Y., Murakami, P., Schaberg, P. G., and Xu, X. (2013). Seasonal dynamics and age of stemwood nonstructural carbohydrates in temperate forest trees. *New Phytologist*, 197(3):850–861.

Ritchie, J. (1972). Model for predicting evaporation from a row crop with incomplete cover. *Water resources research*, 8:1204–1213.

Rothermel, R. (1972). A mathematical model for predicting fire spread in wildland fuels. *USDA Forest Service Research Paper INT USA*.

Ruffault, J., Martin-StPaul, N. K., Duffet, C., Goge, F., and Mouillot, F. (2014). Projecting future drought in Mediterranean forests: bias correction of climate models matters! *Theoretical and Applied Climatology*, 117(1-2):113–122.

Ruffault, J., Martin-StPaul, N. K., Rambal, S., and Mouillot, F. (2013). Differential regional responses in drought length, intensity and timing to recent climate changes in a Mediterranean forested ecosystem. *Climatic Change*, 117(1-2):103–117.

Sack, L. and Holbrook, N. M. (2006). Leaf Hydraulics. *Annual Review of Plant Biology*, 57(1):361–381.

Sandberg, D. V., Riccardi, C. L., and Schaaf, M. D. (2007). Reformulation of Rothermel's wildland fire behaviour model for heterogeneous fuelbeds. *Canadian Journal of Forest Research*, 37:2438–2455.

Sando, R. W. and Wick, C. H. (1972). A method of evaluating crown fuels in forest stands. Research Paper NC-84. *USDA Forest Service Research Paper NC-84*, (NC-84):10 pp.

Savage, V. M., Bentley, L. P., Enquist, B. J., Sperry, J. S., Smith, D. D., Reich, P. B., and von Allmen, E. I. (2010). Hydraulic trade-offs and space filling enable better predictions of vascular structure and function in plants. *Proceedings of the National Academy of Sciences of the United States of America*, 107(52):22722–7.

Saxton, K., Rawls, W. J., Romberger, J., and Papendick, R. (1986). Estimating generalized soil-water characteristics from texture. *Soil Science Society of America Journal*, 50:1031–1036.

Saxton, K. E. and Rawls, W. J. (2006). Soil water characteristic estimates by texture and organic matter for hydrologic solutions. *Soil Science Society of America Journal*, 70(5):1569.

Schaaf, M. D., Sandberg, D. V., Schreuder, M. D., and Riccardi, C. L. (2007). A conceptual framework for ranking crown fire potential in wildland fuelbeds. *Canadian Journal of Forest Research*, 37:2464–2478.

Schenk, H. J. and Jackson, R. B. (2002). Rooting depths, lateral root spreads and below-ground/above-ground allometries of plants in water-limited ecosystems. *Journal of Ecology*, 90(3):480–494.

Scott, J. H. and Reinhardt, E. D. (2002). Estimating canopy fuels in conifer forests. *Fire Management Today*, 62(4):45–50.

Shinozaki, K., Yoda, K., Hozumi, K., and Kira, T. (1964). A quantitative analysis of plant form - the pipe model theory. I. Basic analysis. *Japanese Journal of Ecology*, 14:97–105.

Sitch, S., Smith, B., Prentice, I. C., Arneth, a., Bondeau, a., Cramer, W., Kaplan, J. O., Levis, S., Lucht, W., Sykes, M. T., Thonicke, K., and Venevsky, S. (2003). Evaluation of ecosystem dynamics, plant geography and terrestrial carbon cycling in the LPJ dynamic global vegetation model. *Global Change Biology*, 9(2):161–185.

Sperry, J. S., Adler, F. R., Campbell, G. S., and Comstock, J. P. (1998). Limitation of plant water use by rhizosphere and xylem conductance: results from a model. *Plant, Cell & Environment*, 21:347–359.

Sperry, J. S. and Love, D. M. (2015). What plant hydraulics can tell us about responses to climate-change droughts. *New Phytologist*, 207(1):14–27.

Sperry, J. S., Venturas, M. D., Anderegg, W. R. L., Mencuccini, M., Mackay, D. S., Wang, Y., and Love, D. M. (2016a). Predicting stomatal responses to the environment from the optimization of photosynthetic gain and hydraulic cost. *Plant Cell and Environment*, 40(6):816–830.

Sperry, J. S., Wang, Y., Wolfe, B. T., Mackay, D. S., Anderegg, W. R. L., Mcdowell, N. G., and Pockman, W. T. (2016b). Pragmatic hydraulic theory predicts stomatal responses to climatic water deficits. *New Phytologist*, 212:577–589.

Spitters, C. J. T., Toussaint, H., and Goudriaan, J. (1986). Separating the diffuse and direct components of global radiation and its implications for modeling canopy photosynthesis. I. Components of incoming radiation. *Agricultural and Forest Meteorology*, 38:231–242.

Stolf, R., Thurler, Á., Oliveira, O., Bacchi, S., and Reichardt, K. (2011). Method to estimate soil macroporosity and microporosity based on sand content and bulk density. *Revista Brasileira de Ciencias do Solo*, 35(1):447–459.

Tóth, B., Weynants, M., Nemes, A., Makó, A., Bilas, G., and Tóth, G. (2015). New generation of hydraulic pedotransfer functions for Europe. *European Journal of Soil Science*, 66(1):226–238.

Tyree, M. T. and Yang, S. (1990). Water-storage capacity of Thuja, Tsuga and Acer stems measured by dehydration isotherms - The contribution of capillary water and cavitation. *Planta*, 182(3):420–426.

Van Lier, Q. D. J., Neto, D. D., and Metselaar, K. (2009). Modeling of transpiration reduction in van genuchten-mualem type soils. *Water Resources Research*, 45(2):1–9.

Walker, A. P., Beckerman, A. P., Gu, L., Kattge, J., Cernusak, L. A., Domingues, T. F., Scales, J. C., Wohlfahrt, G., Wullschleger, S. D., and Woodward, F. I. (2014). The relationship of leaf photosynthetic traits - Vcmax and Jmax - to leaf nitrogen, leaf phosphorus, and specific leaf area: A meta-analysis and modeling study. *Ecology and Evolution*, 4(16):3218–3235.

Watanabe, T. and Mizutani, K. (1996). Model study on micrometeorological aspects of rainfall interception over an evergreen broad-leaved. *Agricultural and Forest Meteorology*, 80:195–214.